Central Florida Water Initiative

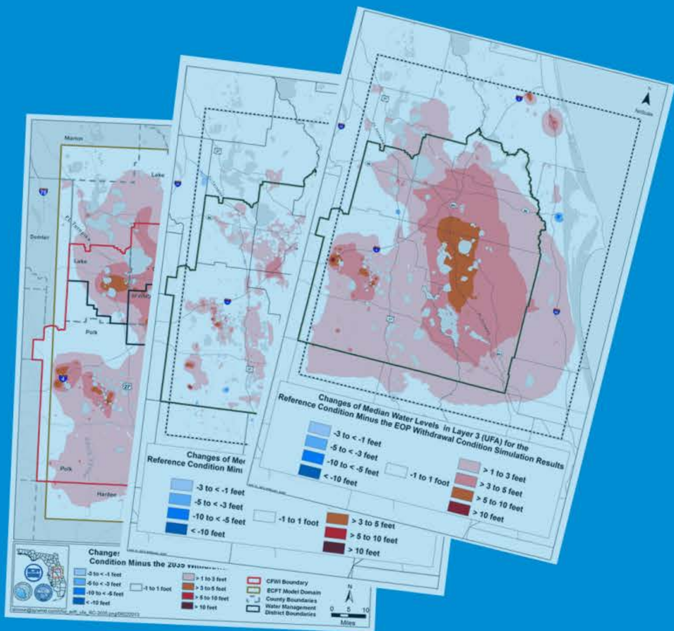

East-Central Florida Transient (ECFT) Model Documentation

In Support of the 2014 Draft CFWI Regional Water Supply Plan

August 29, 2014

Prepared by the CFWI Hydrologic Analysis Team (HAT)

Contents

Tables

Figures

Acronyms and Abbreviations

AFSIRS	Agricultural Field-Scale Irrigation Requirements Simulation
BMF	Benchmark Farms
C/I	Commercial/Industrial
cfs	cubic feet per second
CFWI	Central Florida Water Initiative
DEM	digital elevation model
DMIT	Data, Monitoring and Investigations Team
DSS	Domestic Self-Supply
ECFT model	East-Central Florida Transient model
EMT	Environmental Measures Team
EOP	End-of-Permit
ET	evapotranspiration
FAS	Floridan aquifer system
FASS	Florida Agricultural Statistics Service
FDACS	Florida Department of Agriculture and Consumer Services
FDEP	Florida Department of Environmental Protection
FLUCCS	Florida Land Use Cover Classification System
GAT	Groundwater Availability Team
GHB	General Head Boundary Package
gpd	gallons per day
HAT	Hydrologic Analysis Team
HAT-ECFT model	East-Central Florida Transient model prepared used by the Hydrologic Analysis Team
IAS	intermediate aquifer system
IFAS	University of Florida Institute of Food and Agricultural Sciences
Kc	crop water use coefficient
LRA	Landscape/Recreation/Aesthetic
MFL	minimum flows and levels
MFLRT	Minimum Flows and Levels/Reservations Team
MGD	million gallons per day
MOC	Management Oversight Committee

MODFLOW-2005	Modular Groundwater Flow Model
MSR	mean-square residual
NOAA	National Oceanic and Atmospheric Administration
OMR	overall mean residual
PET	potential evapotranspiration
PWS	Public Water Supply
RIB	rapid infiltration basin
RMS	root mean square
RMSR	root-mean-square-residual
RWSP	Regional Water Supply Plan
RWSPT	Regional Water Supply Planning Team
SAS	surficial aquifer system
SFR2	Streamflow-Routing Package
SFWMD	South Florida Water Management District
SJRWMD	St. Johns River Water Management District
SWFWMD	Southwest Florida Water Management District
TOC	Technical Oversight Committee
UFA	Upper Floridan aquifer
USGS	United States Geological Survey
USGS-ECFT model	East-Central Florida Transient model prepared by the United States Geological Survey
UZF1	MODFLOW Unsaturated Zone Package
WMD	water management district
WUCA	Water Use Caution Area
WUP	water use permit

1
Introduction

Central Florida relies on limited supplies of traditional groundwater to meet the increasing water needs of public, agricultural, industrial, and commercial users. To support these users, the Central Florida Water Initiative (CFWI) undertook a robust and cooperative effort to identify the extent of this groundwater system, support regional water supply planning, and understand groundwater resource limitations for sustainable water supplies. A primary tool for the groundwater assessment was the East-Central Florida Transient (ECFT) groundwater flow model. This report describes the development, construction, and use of the model to support the CFWI.

CFWI PROJECT OVERVIEW

Location

The CFWI Planning Area is located in central Florida and consists of all of Orange, Osceola, Polk, and Seminole counties and southern Lake County (**Figure 1**), covering approximately 5,300 square miles. The CFWI Planning Area was based on the county boundaries for the four wholly included counties and the utility service areas for Lake County.

CFWI Partners and Project Teams

Due to the extent and complexities of the planning area, the CFWI required a collaborative effort by three water management districts (WMDs) with other public agencies and stakeholders. The participants in CFWI include the South Florida Water Management District (SFWMD), the St. Johns River Water Management District (SJRWMD), the Southwest Florida Water Management District (SWFWMD), the Florida Department of Agriculture and Consumer Services (FDACS), the Florida Department of Environmental Protection (FDEP), Public Water Supply utilities, and other interested parties.

The many aspects of water supply planning for Central Florida were divided among several project teams. The groundwater flow modeling described in this document was performed by the Hydrologic Analysis Team (HAT) of the CFWI using the 2005 version of the Modular Groundwater Flow Model (MODFLOW-2005; Harbaugh, 2005). Other technical teams in the CFWI were the Minimum Flows and Levels/Reservations Team (MFLRT), Environmental Measures Team (EMT), Data, Monitoring and Investigations Team (DMIT), the Groundwater Availability Team (GAT), and the Regional Water Supply Planning Team (RWSPT). The technical teams were provided guidance from the Steering Committee through the Management Oversight Committee (MOC) and the Technical Oversight Committee (TOC). A more full-ranging description of the activities and products of the CFWI is provided in the Regional Water Supply Plan (RWSP) (CFWI 2014).

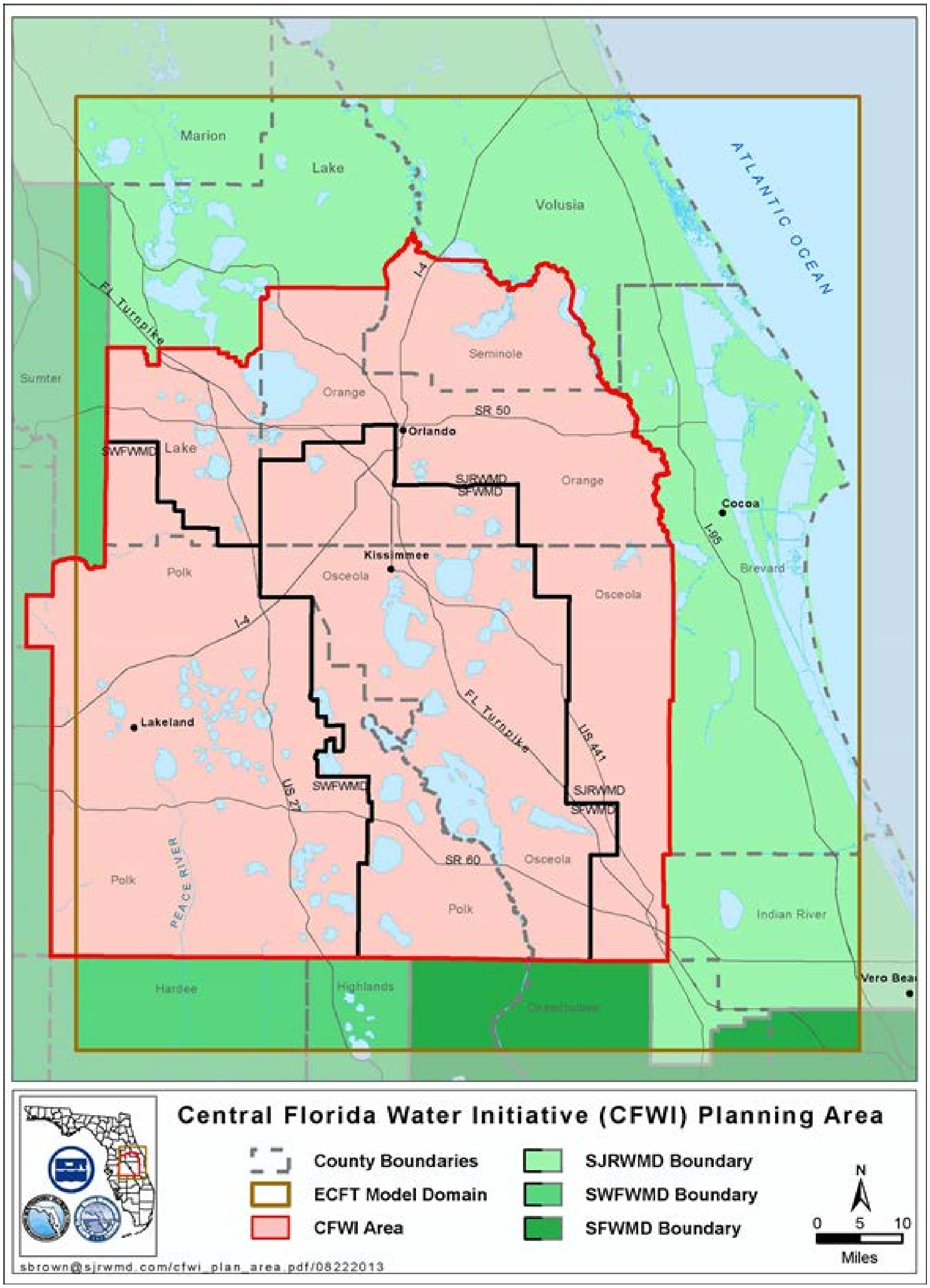

Figure 1. Map of the Central Florida Water Initiative (CFWI) Planning Area.

Need for the CFWI

As the population of central Florida has grown, so has the pace of residential, agricultural, industrial, and commercial development. With that growth, the need for water has also increased. This trend is projected to continue, which will lead to the need for more water. However, hydrogeological, hydrological and ecological studies, water supply permitting, and public policy have concluded that the use of traditional groundwater[1] is nearing its sustainable limit. This means meeting future needs may require the use of alternative, non-traditional water supplies.

The benchmarks used to assess the sustainable limit of groundwater supplies are unacceptably stressed ecological conditions of wetlands and lakes, reduced groundwater levels designed to limit saltwater intrusion, and reduced river and spring flows directly attributable to reduced aquifer water levels (drawdowns) from modeled historic or projected groundwater withdrawals with comparisons to observed conditions. The ECFT model was used to calculate changes in drawdowns and spring flows by comparing the simulation results of various regional water supply scenarios. Assessments of the relationships between drawdowns and changes to wetland and lake conditions and spring flows were performed by the MFLRT, EMT, and GAT.

Objectives of the CFWI Hydrologic Analysis Team

The objectives[2] of the HAT are to provide the necessary modeling tools and data analysis and work collaboratively with other CFWI teams to:

1. Evaluate the current and future availability of groundwater
2. Assess future water supply and management strategies
3. Develop processes to assess the long-term effectiveness of management strategies
4. Support collaborative water supply planning
5. Support future regulatory actions

ECFT MODEL OVERVIEW

The ECFT is the most recent version of a regional groundwater flow model covering central Florida. The direct predecessor to the ECFT model used for the CFWI was the ECFT model prepared by the United States Geological Survey (USGS-ECFT) and is described by Sepúlveda, et al. (2012). The HAT assessed and improved upon the USGS-ECFT for the purposes of the CFWI.

[1] Traditional groundwater supplies refer to water from the surficial aquifer system (SAS), intermediate aquifer system (IAS), and Floridan aquifer system (FAS) that has been used to meet the needs of the area and requires minimal treatment to meet the water quality requirements for the expected use.

[2] Central Florida Water Initiative Guiding Document (http://cfwiwater.com/pdfs/2013/08-16/CFWI_Guiding_Document_updates.pdf)

The updated HAT-ECFT model covers central Florida as shown in **Figure 1** and encompasses nearly 10,300 square miles. The model domain includes all of Seminole, Orange, and Osceola counties; most of Lake, Volusia, Brevard, and Polk counties; and small parts of Marion, St. Lucie, Okeechobee, Highlands, Hardee, and Sumter counties. For the purposes of the model, the area was divided into 472 rows oriented east-west and 388 columns oriented north-south. The resulting dimensions of each cell are 1,250 feet by 1,250 feet, or approximately 36 acres.

The model includes seven layers to represent the hydrogeologic units from land surface to the base of the Floridan aquifer system. The thicknesses of the layers vary based on the position within the model grid and the hydrogeologic unit that a particular layer represents. The base of the Floridan aquifer system is greater than 2,500 feet below sea level in the CFWI area. The correlation between the area's geology and hydrogeology and the model layers is shown in **Figure 2**.

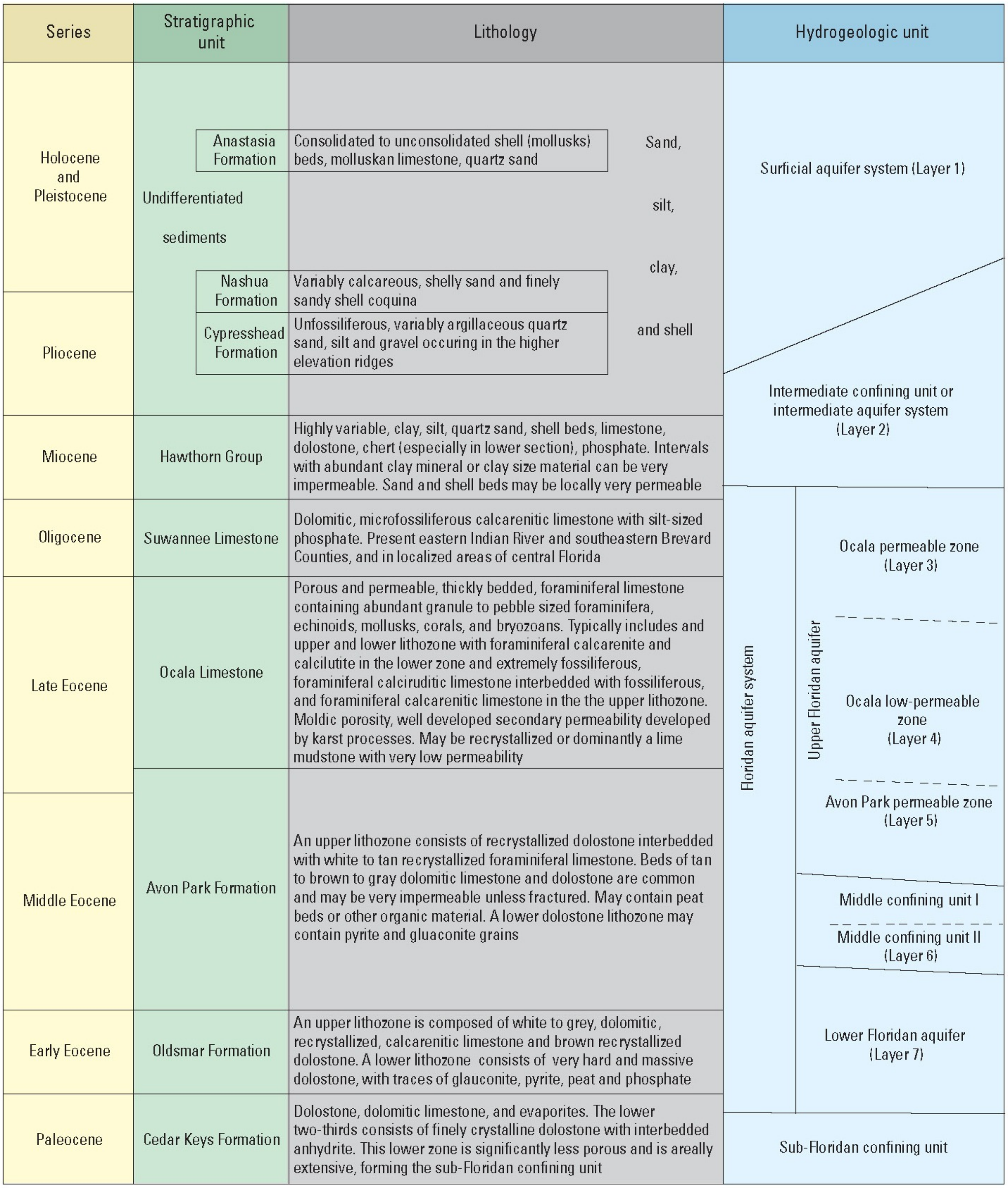

Figure 2. Relation between stratigraphic and hydrogeologic units and ECFT model layers (identified in the hydrogeologic unit column) for the CFWI Planning Area (from Sepúlveda, et al., 2012).

Assessment of the USGS-ECFT

The USGS delivered the USGS-ECFT groundwater flow model to the HAT in 2012. The HAT reviewed the logic of the model construction, distribution of input parameters, and model performance and determined that several items needed to be updated for its use in the CFWI process. The recalibration process and results are described in **Chapter 2**.

Application of the ECFT Model to the CFWI Process

For the CFWI process, the ECFT model served as a common tool to simulate groundwater conditions to evaluate the effects of water use changes on the overall status of the area's water resources. To do this, model outputs of water levels and flows were delivered to the MFLRT and the EMT for them to assess water resource conditions of water bodies under minimum flow and level (MFL) restrictions and the statistical risk of changes to the status of non-MFL wetlands in the CFWI area. The GAT assembled the assessment results of the MFLRT and EMT to evaluate availability of traditional groundwater. The GAT also requested the HAT to perform several simulations to provide additional insight to develop a range of traditional groundwater availability and sensitivity of the results to changes in withdrawal locations or management practices. The results from these teams were delivered to the RWSPT to assist in preparation of the RWSP.

The following five scenarios were developed to simulate conditions for use in the CFWI process using the HAT-ECFT model:

- The Reference Condition represents the base simulation of near-current conditions for comparison to future conditions. The Reference Condition considers 2005 water demands, recent ecologic conditions, and hydrologic conditions for 1995 to 2006.
- The 2015, 2025, and 2035 Withdrawal Scenarios represent simulations of future groundwater withdrawals to meet the expected demand conditions of the indicated year.
- The End-of-Permit (EOP) scenario is the simulation of water use permit allocations at the end of their respective permit period. Since permits expire from 2012 through 2041, the EOP simulation does not represent a point in time, but the condition of water resources if the permitted allocations were simultaneously pumped within the logic used to develop the scenarios.

2

Recalibration of the USGS-ECFT Groundwater Model

RECALIBRATION PROCESS

The HAT reviewed the USGS-ECFT model developed for the CFWI groundwater availability analysis and determined that an updated and recalibrated model (HAT-ECFT) would provide a better tool for the assessment. Through this process, the following model input data sets were identified for improvement:

1. The General Head Boundary water level values used for the Upper and Lower Floridan aquifer systems (Layers 3, 5, and 7)
2. Leakance (vertical hydraulic conductivity) values for Layer 6, which represents the Middle semi-confining unit between the Upper and Lower Floridan aquifers,
3. Specific storage
4. Spring pool elevations (a factor used to calculate spring discharge),
5. Groundwater withdrawal amounts for various categories of water use

The HAT identified that additional data were available to improve these inputs and thus improve the performance of the model.

The recalibration effort was conducted using the original process and methods developed during the collaborative effort between the WMDs and the USGS. The HAT set a goal of meeting or exceeding the USGS-ECFT model calibration goals at the groundwater level observation locations and improved transient response of the model through the 12-year simulation period. The goals established by the USGS were based on comparing modeled and measured water levels in 700 observation wells (see Appendix A) and comparing modeled and measured spring flows at 22 springs. Model performance statistics were calculated by first finding the differences between the measured and modeled values (referred to as the residuals) and then assessing the result against the metric by either direct comparison or by calculating statistics on the residuals.

The calibration goals provided by the USGS and also used by the HAT for the water levels at the observation wells were:

- More than 50 percent of wells with a residual less than or equal to 2.5 feet in absolute value
- More than 80 percent of wells with a residual less than or equal to 5 feet in absolute value

- A root-mean-square-residual (RMSR) for all wells of less than 5 feet for each of the 12 simulated years
- A maximum overall mean residual (OMR) of less than 1 foot in absolute value for each of the 12 simulated years.

Figure 3 shows an example of target locations where water level data from observation wells for Layer 3 and Layer 4 were compared to the simulated results to test model performance.

The HAT also developed the following calibration goals for the spring flows:

- RMSR of spring flow residuals for large springs[3] be less than 10 percent of the average of the measured spring flows.
- RMSR of spring flow residuals for small springs[4] be less than 20 percent of the average of the measured spring flows.

RESULTS OF RECALIBRATION

The results of the recalibration improved the performance of the model. **Table 1** shows the performance statistics for the USGS-ECFT model and the HAT-ECFT model for the wells; **Table 2** shows the statistics for the spring flows. In general, the recalibration effort provided a modest improvement at the observation locations in the groundwater system. The main benefit was improvement in the transient response of many of the simulated water levels. **Figure 4** illustrates the improvement of the transient response achieved through model recalibration at observation well ROMP 60 (circled in **Figure 3**).

[3] Springs with average measured flows greater than or equal to 10 cubic feet per second (cfs) were considered to be large springs.
[4] Springs with average measured flows less than 10 cfs were considered to be small springs.

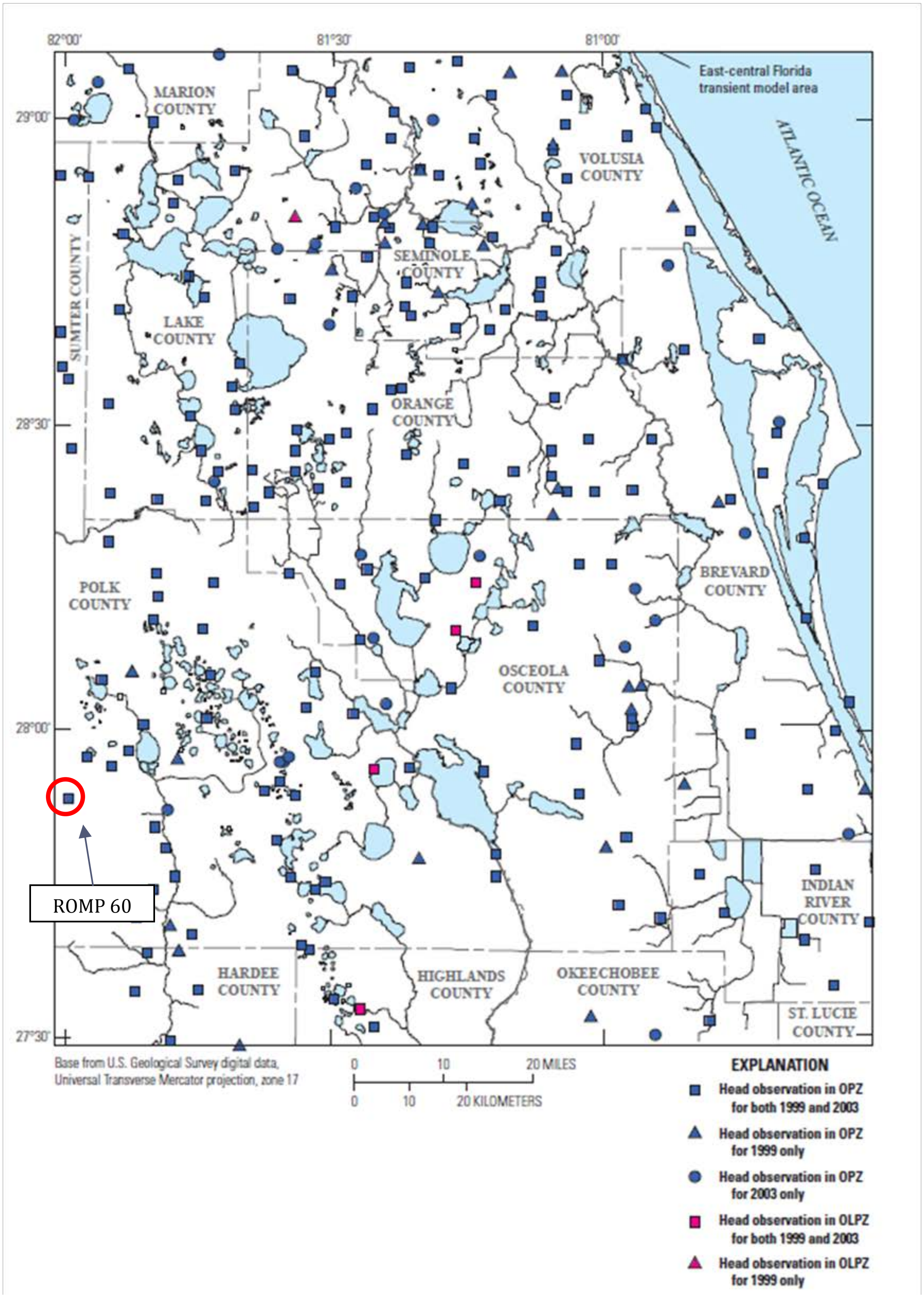

Figure 3. Example of locations of model calibration targets for Layer 3 and Layer 4 where observed water levels were compared to simulated results (from Sepúlveda et al., 2012).

Table 1. Performance statistics for observation wells for the USGS-ECFT and HAT-ECFT models.

Portion of Model		USGS-ECFT Results Number of Wells	OMR	Average MSR	Average RMSR	Wells <2.5 feet		Wells <5 feet	
Full Domain		700	2.15	11.67	2.77	481	69%	642	92%
Layer	1	289	2.19	12.19	2.66	201	70%	269	93%
Layer	2	63	2.98	16.95	3.47	34	55%	51	82%
Layer	3	260	1.83	9.26	2.59	190	73%	243	93%
Layer	4	6	2.18	15.24	3.61	3	50%	5	83%
Layer	5	54	2.34	12.63	3.15	33	61%	49	91%
Layer	6	6	2.52	17.31	3.21	5	83%	5	83%
Layer	7	22	2.31	12.76	2.93	15	68%	20	91%
		HAT-ECFT Results							
Full Domain		700	2.10	11.02	2.62	500	71%	643	92%
Layer	1	289	2.13	12.64	2.62	206	71%	268	93%
Layer	2	62	2.95	15.85	3.44	31	50%	49	79%
Layer	3	261	1.85	8.18	2.42	202	77%	246	94%
Layer	4	6	2.42	12.52	3.02	3	50%	6	100%
Layer	5	54	2.11	10.94	2.73	38	70%	50	93%
Layer	6	6	2.22	15.30	2.69	5	83%	5	83%
Layer	7	22	2.10	8.40	2.45	15	68%	19	86%

OMR – overall mean residual
MSR – mean-square residual
RMSR – root-mean-square residual
Well < 2.5 feet – Wells that met the criteria of having their simulated water level within 2.5 feet of the observed value
Well < 5 feet – Wells that met the criteria of having their simulated water level within 5 feet of the observed value

Table 2. Performance statistics for spring flows for the HAT-ECFT model.

Spring Name	Observations During Calibration Period	Average Observed flow (cfs)	MSR	RMSR	Percent Error
Alexander Spring near Astor	79	104.5	54.0	7.4	7%
Apopka (Gourdneck) Spring near Montverde	104	27.3	13.0	3.6	**13%**
Blue Spring near Orange City (Volusia Co)	93	155.6	228.9	15.1	10%
Blue Springs near Yalaha (Lake Co)	55	2.7	0.1	0.3	8%
Bugg Spring at Okahumpka	143	11.0	4.5	2.1	**19%**
Camp La-No-Che Springs near Paisley	6	0.9	0.0	0.1	11%
Clifton Springs near Oviedo	20	1.4	0.1	0.3	14%
Droty Springs near Sorrento	6	0.6	0.1	0.3	13%
Gemini Springs near Debary	64	9.9	1.7	1.3	13%
Green Spring near Osteen	54	1.7	0.1	0.2	19%
Holiday Springs near Yalaha	108	3.8	0.2	0.4	8%
Island Spring in Wekiva River near Sanford	24	8.1	1.0	1.0	11%
Messant Spring near Sorrento	46	16.5	1.6	1.3	8%
Miami Springs near Longwood	82	5.9	0.3	0.6	10%
Palm Springs near Longwood	82	5.7	0.7	0.8	14%
Rock Springs near Apopka	127	55.6	16.1	4.0	7%
Sanlando Springs near Longwood	69	20.1	5.5	2.3	**12%**
Seminole Spring near Sorrento	7	35.1	48.2	6.9	**20%**
Starbuck Spring near Longwood	80	13.8	3.9	2.0	**14%**
Wekiva Falls Resort (flowing 14" Standpipe)	9	18.0	4.1	2.0	**11%**
Wekiva Springs near Apopka	95	63.1	29.0	5.4	9%
Witherington Springs near Apopka	8	2.0	0.1	0.2	9%

MSR – mean-square residual
RMSR – root-mean-square residual

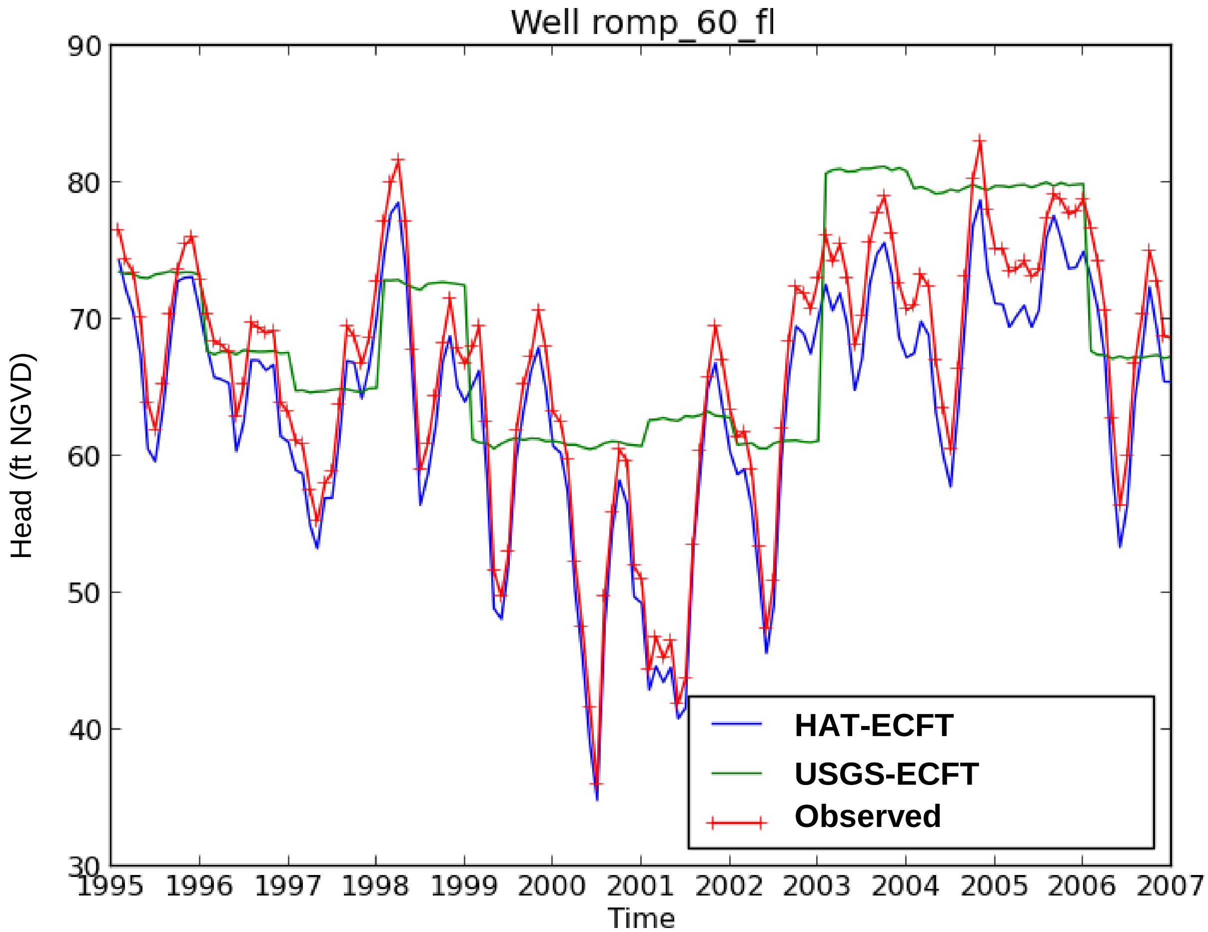

Figure 4. Hydrograph of observed and simulated water levels at the ROMP 60 Well in the Upper Floridan aquifer in Polk County for the USGS-ECFT and HAT-ECFT models.

General-Head Boundary Elevation Changes

In the USGS-ECFT model, water level assignments for the general head boundary were based on an annual average approach. This method relied on data only from wells close to the model boundary to represent the Upper Floridan aquifer (UFA).

To make the model more accurate, the HAT determined that a monthly value would improve this boundary condition. The SWFWMD, in conjunction with the HAT, developed a GIS-based method to estimate a monthly water level surface to be used as an input to the general head boundary of the recalibrated model. This process included many more wells and expanded the region for the interpolation to improve the estimation of water levels for the aquifer with a monthly time step for all 12 years of the simulation. The approach created 144 monthly water level surfaces for the UFA and then used these values to develop water levels for the aquifer and adjacent aquifers based on head differences for observed wells in each of the lower layers.

Leakance Value Changes

The initial USGS-ECFT model calibration assumed uniform leakance values (vertical hydraulic conductivity) of the Middle Semi-Confining Unit (Layer 6)[5]. However, the HAT thought it would be important to allow for adjustment of this parameter. The automated calibration process initially developed for this project was changed by the HAT to allow for adjustments in these values by including them as a variable in the automated process. The calibration method developed for this project relied on a regional approach where important model parameters, such as the horizontal and vertical hydraulic conductivities of the aquifers, were allowed to adjust in a systematic way to best match observed water levels.

In addition to Middle Semi-Confining Unit values, the vertical hydraulic conductivities of the lakes were revisited during recalibration. More information was provided by the HAT that improved the simulation of the interaction of the lakes within the model. Lake bed leakance values were altered to improve the water balances for these systems. The lakes were included in the ECFT model to provide a better boundary condition for groundwater simulation.

Storage Changes

During the recalibration process, the HAT also noted that the storage parameters for the aquifer system would best be estimated as a compilation of zones or as a continuous spatial field variable instead of as a single parameter across a model layer. As the name suggests, the storage parameters help describe the rate that water is taken from the aquifer matrix and help develop the time-varying responses of the transient model. Changes in these parameters were accomplished by enabling estimation of the spatial variation similar to the approach used with the rest of the horizontal conductivity values of the aquifer layers estimated in the automated calibration process.

Spring Pool Elevation Changes

The ECFT model includes 22 simulated springs. For the USGS-ECFT model, spring pool elevations were kept constant for all months within a calendar year by using the given year’s average elevation for each spring pool. The recalibrated HAT-ECFT model uses monthly averages based on spring pool elevations equal to the measured elevation relative to the National Geodetic Vertical Datum of 1929 (NGVD), allowing the spring pool elevations in the model to change from month to month.

[5] Sepúlveda et al. (2012) provides a detailed description of the calibration, which involves the use of parameter estimation software and several steady-state solutions to estimate conductivity values and a transient simulation to estimate storage values.

The SJRWMD website provides measured spring pool elevations for 16 of the 22 simulated springs. Gaps in the elevation data were replaced with linearly interpolated values in time from two points with data. The six springs with no elevation data listed on the SJRWMD website were left as before since these were best estimates of the digital elevation model (DEM) and Upper Floridan aquifer potentiometric values at the spring.

Irrigation Withdrawal Locations and Demands

The HAT adjusted the USGS-ECFT model by water use type as follows:

- **Agricultural** – The revisions to the USGS-ECFT model for irrigation demands were primarily directed toward withdrawal locations and demands. Previously, it was assumed that the irrigation was spread evenly across a farm field. This was modified in the SFWMD by applying the estimated demand to the permitted groundwater withdrawal facilities. Surface water withdrawals were not included in the model unless the permittee used an isolated lake. In this case, the demand would be applied to the SAS (Layer 1). Irrigation demands were calculated from the Agricultural Field-Scale Irrigation Requirements Simulation (AFSIRS) model and varied based upon climatic conditions. A review of the permit database was also conducted to determine when a newly issued permit became operational within the simulation period. For these users, pumpage values before permit issuance were assigned a value of zero.

- **Golf Course** – Established golf courses were analyzed to determine if, when, and at what volume reuse became available at the site. For golf courses where reuse water was available, the water demands estimated using the AFSIRS model for the earlier part of the simulations were reduced or set to zero depending on the amount of reuse water received. This reduction began on the estimated date that reuse irrigation started.

- **Pasture** – In the initial USGS-ECFT model, all improved pasture was assumed not to be irrigated. For the recalibrated HAT-ECFT model, this assumption was modified for pastures that were known to be irrigated.

OVERALL EFFECTS OF MODEL RECALIBRATION

Table 3 summarizes the overall water budget of the HAT-ECFT model. The percent discrepancies, evaluated as (IN-OUT)/(IN+OUT)*200, are close to zero.

Table 3. Overall water budget for the HAT-ECFT model in million gallons per day (MGD).

	In						Out										
Period	**Storage**	**Wells**	**Head Dep Bounds**	**UZF Recharge**	**Stream Leakage**	**Lake Seepage**	**Storage**	**Wells**	**Drains**	**Head Dep Bounds**	**Groundwater ET**	**Surface Leakage**	**Stream Leakage**	**Lake Seepage**	**Total In**	**Total Out**	**Discrepency (Percent)**
1995	1952	61	433	12398	5	33	1743	900	364	807	8773	2232	22	42	14882	14883	-0.01
1996	2438	63	444	11850	4	33	1799	996	376	814	8518	2263	23	41	14832	14830	0.01
1997	1883	64	439	11381	5	36	2065	937	352	841	7580	1973	22	38	13808	13808	0
1998	3127	51	467	11703	6	36	2410	1087	361	769	7737	2969	20	37	15390	15390	0
1999	2453	45	446	11842	4	36	2406	1052	343	870	7904	2190	24	39	14826	14828	-0.01
2000	2826	45	465	7666	2	41	1443	1248	322	985	5752	1231	27	37	11045	11045	0
2001	2315	53	486	11767	5	42	2656	1048	326	961	7522	2100	22	34	14668	14669	-0.01
2002	2438	65	483	14470	6	40	2999	1035	345	858	9219	2989	21	36	17502	17502	0
2003	2462	60	474	14125	5	31	1850	934	379	813	9763	3356	21	42	17157	17158	-0.01
2004	2651	80	458	12831	7	34	2201	954	366	840	8823	2816	20	39	16061	16059	0.01
2005	1853	67	424	14965	7	31	1510	771	382	827	10204	3591	20	42	17347	17347	0
2006	2561	44	433	9658	2	34	1685	1052	359	893	6915	1759	27	43	12732	12733	-0.01
1995–2006	**2413**	**58**	**454**	**12055**	**5**	**36**	**2064**	**1001**	**356**	**857**	**8226**	**2456**	**22**	**39**	**15021**	**15021**	**0**

The effects of the HAT recalibration on overall model head error are shown in **Figure 5**. The figure shows the average simulation error for all wells with water level observations in the model domain for each year of the simulation. For this statistic, average head error can be positive or negative, and the most desirable outcome is the one closest to a value of zero. The USGS-ECFT version performed better during the first three years of the simulation and this is thought to be the result of a better initial condition setting by the USGS (testing indicates that an extended multi-year run-in is required before the model is able to fully overcome the effects of any ill-fitting initial condition assignments). After the first three years, both versions of the model behave quite similarly, but the HAT-ECFT version shows slightly better average error distribution in six of the remaining nine years of simulation.

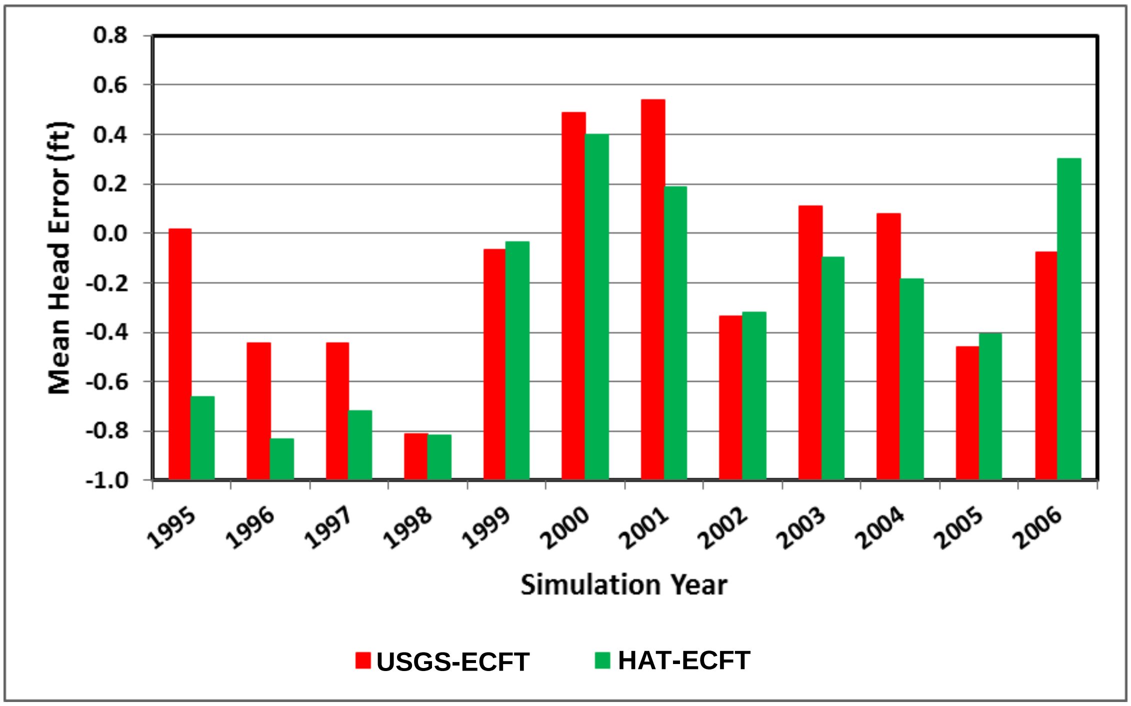

Figure 5. Model-wide overall mean head error for the USGS-ECFT and HAT-ECFT models

The effects of the recalibration on overall model head error are shown in another way in **Figure 6**. The figure shows the average root mean square (RMS) simulation error for all head observations in the model domain throughout the calibration period. This statistic is less influenced by a small number of outlier data points than the ordinary mean error statistic shown in **Figure 5**. The RMS error should be as small as possible, and the HAT-ECFT model provides slightly smaller RMS head errors throughout the calibration period for all model layers compared to the USGS-ECFT model.

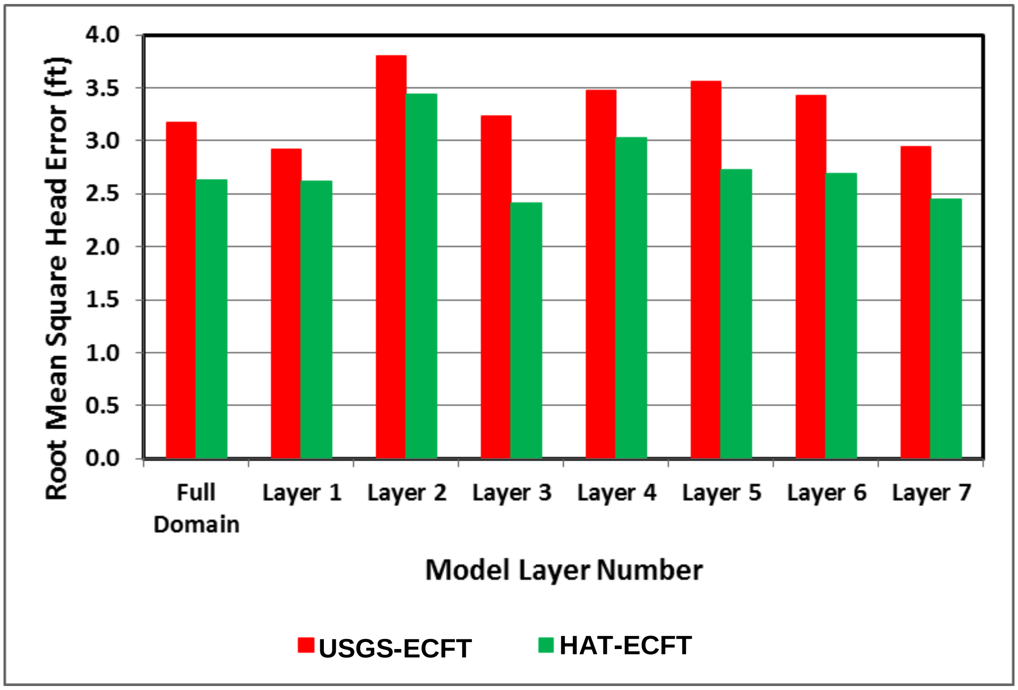

Figure 6. Model-wide root mean square head error for USGS-ECFT and recalibrated HAT-ECFT model.

The number of observations with head errors of less than 2.5 ft. and 5 ft., respectively, are shown in **Figure 7** and **Figure 8**. For these performance statistics, values closer to 100 percent are better than values further from 100 percent. Overall, the recalibrated model has slightly better performance than the USGS-ECFT model.

While the recalibration made substantial improvements to the USGS-ECFT model in certain areas, the overall effect was a relatively modest improvement in calibration performance by most measures.

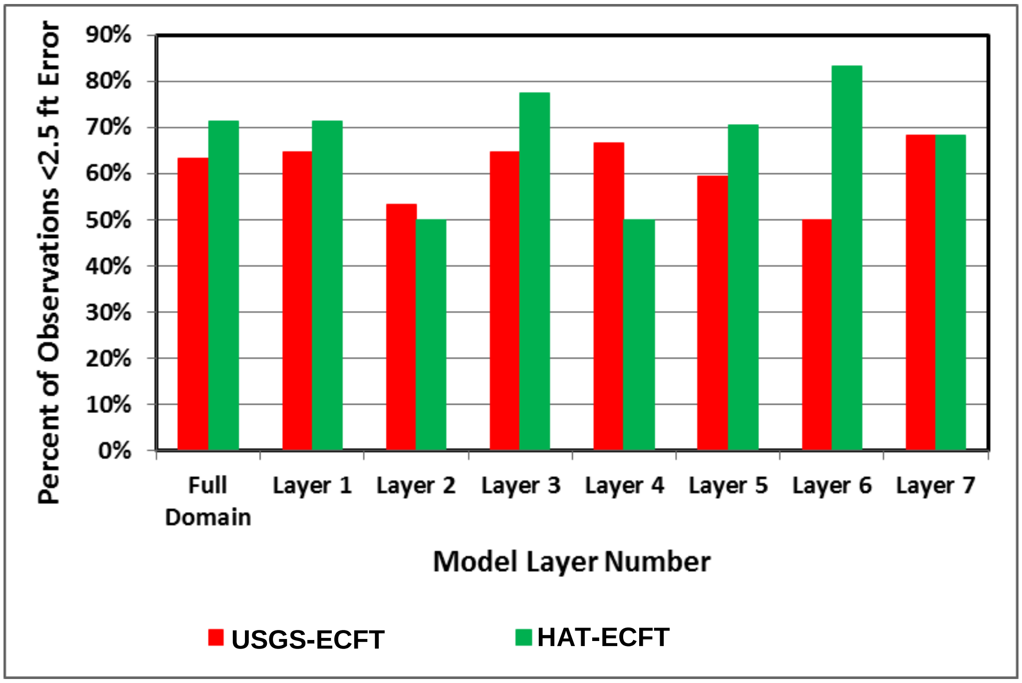

Figure 7. Model-wide percentage of observations with less than 2.5 ft. head error for the USGS-ECFT and HAT-ECFT models.

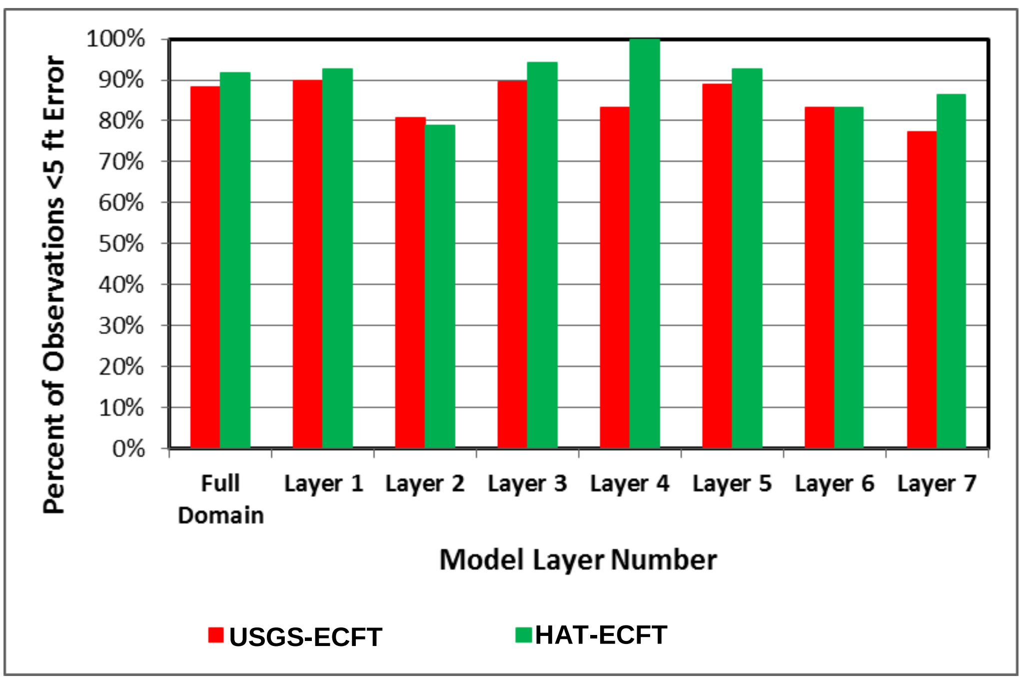

Figure 8. Model-wide percentage of observations with less than 5 ft. head error for the USGS-ECFT and HAT-ECFT models.

3
Description of Model Scenarios

Multiple groundwater flow modeling scenarios were conceived, constructed, and simulated for the CFWI process to evaluate groundwater availability for the region. This section summarizes the rationale, conceptualization, and construction of the scenarios. Scenarios were developed for the Reference Condition and future conditions that represent the withdrawals necessary to satisfy projected water demands through 2035. Additional scenarios were developed to represent 2015 and 2025 withdrawal conditions, as well as the EOP condition that addressed the potential withdrawal of all groundwater quantities currently permitted for the CFWI Planning Area. In some instances, model inputs were unchanged from the USGS-ECFT model. In these instances, the reader is directed to Sepúlveda, et al. (2012) for more detailed descriptions of those variables.

The simulations consist of 144 monthly stress periods, covering 12 years that correlate to the calibration period of January 1995 through December 2006. This duration is kept for each of the scenarios.

SCENARIO RATIONALE

The scenarios were developed to evaluate the modeled effects related to changes in groundwater withdrawals while keeping other input variables constant or consistent. The results of the modeling efforts were used by the CFWI technical teams to assess potential impacts to MFL and non-MFL water bodies and the potential for water quality degradation.

The scenarios were constructed by adjusting dependent input variables based on observed and calculated relationships with independent variables. Rainfall is a primary independent variable that is used to spatially and temporally adjust the dependent variables. The dependent input variables that were modified between scenarios based on rainfall were groundwater withdrawals, irrigation, runoff and infiltration, evapotranspiration (ET), and recharge. Land use is an independent variable that is unaffected by rainfall; however it affects runoff, infiltration, and ET and was used to modify these dependent variables for the model scenarios. While the values of dependent variables can change from stress period to stress period and from scenario to scenario, the process to calculate their spatial and temporal distributions to input into the model was consistent throughout the CFWI process.

Rainfall

The spatial and temporal distribution of historical rainfall between 1995 and 2006 was a hydrologic parameter that influences other variables in the model. It was the same for the calibration run and the future withdrawal condition scenarios and was based on observed and calculated monthly distributions at multiple rain gauge stations throughout central Florida. This period contains extreme wet (hurricanes of 2004 and 2005) and dry (droughts of 2000 and 2001) conditions. As a result, the approach provides insight to the potential changes of hydrologic conditions to meet projected needs during extreme conditions. Rainfall was unchanged from the USGS-ECFT model.

Land Use

Land use presents a distribution of pervious and impervious surfaces that are used in separating runoff and infiltration of the total of rainfall and irrigation as explained below. The distributions of land use for 1995, 2000, and 2004 were available to use for the model. Distributions of land use were unchanged from the USGS-ECFT model.

Irrigation

Two types of irrigation were used in the model: agricultural and landscape. Agricultural irrigation was based on observed or calculated water need in excess of rainfall considering soil type and crop type. Landscape irrigation was simulated as a direct groundwater withdrawal or as irrigation return flow of reuse/Public Water Supply water applied to the grass based upon estimated irrigated areas. Both landscape and agricultural irrigation were changed from the USGS-ECFT model as described in **Chapter 2**.

Withdrawals

Water supply demands and groundwater withdrawals are significantly influenced by rainfall. The distribution of monthly rainfall for 1995 through 2006 was used to adjust the projected demands to monthly withdrawals for a model scenario using a peaking factor approach. The approach is described in more detail in **Chapter 5**. The overall effect of this process was to distribute withdrawals of a representative scenario over the 12-year period. While the projected withdrawal conditions for the Reference Condition and future withdrawal scenarios are described as a single value representing a long-term average demand condition, in the model these conditions are implemented as a fluctuating time series. **Figure 9** shows the total modeled withdrawals for the CFWI area distributed over the 12-year simulation period and the long-term average value for the Reference Condition.

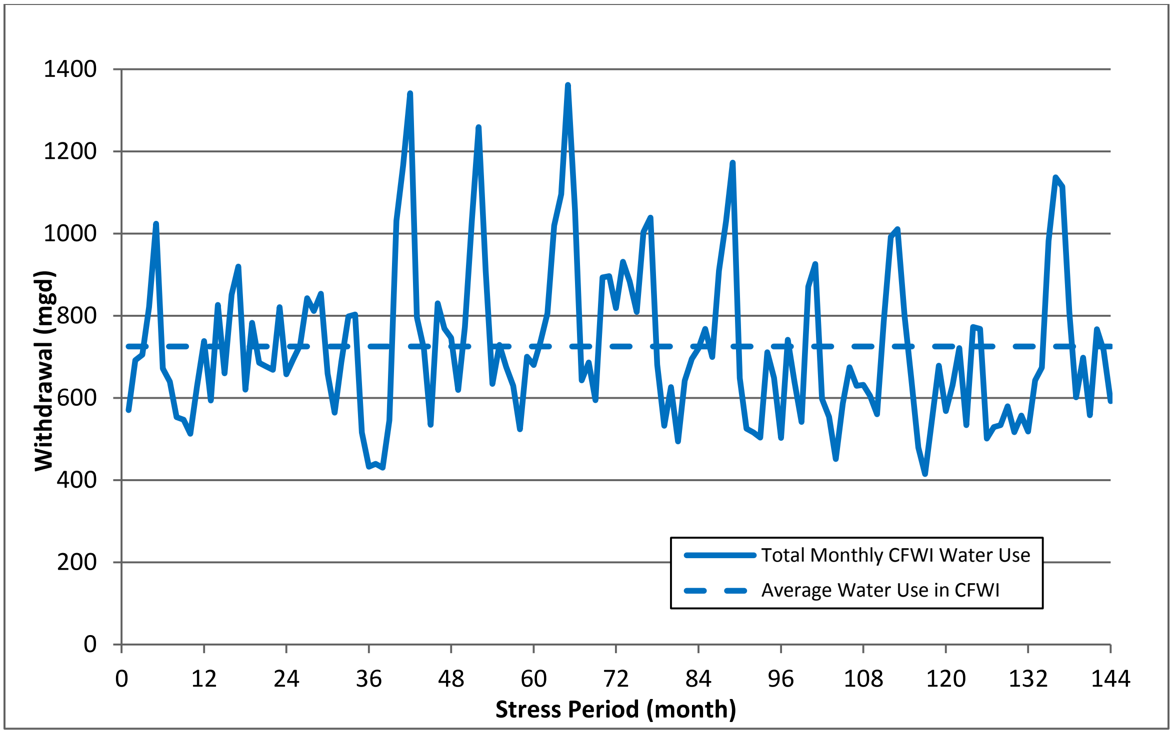

Figure 9. Distribution of total monthly modeled withdrawals and average water use for the Reference Condition over the 12-year simulation period.

Public Water Supply

The monthly distributions of Public Water Supply withdrawals for the future scenarios were based on the temporal water use patterns developed for 2006. The 2006 withdrawal patterns were used instead of those from 2005, in part, due to some above-average rainfall and related pumpage patterns resulting from an active 2005 hurricane season. **Figure 10** shows the modeled total withdrawals for the major water use types (Agriculture, Public Water Supply, Commercial/Industrial, and Domestic Self-Supply). The largest variation occurs with the agricultural irrigation demands, which are predominately driven by variations in climatic conditions (rainfall and season). Public Water Supply and Commercial/Industrial demands generally fluctuate in a narrower band because they typically have base demand conditions that are needed to supply, such as typical indoor residential uses, regardless of climatic conditions. Fluctuations of modeled withdrawals at individual locations, regardless of use type, may significantly vary from the patterns shown in the chart. For the future scenarios, it was assumed that Domestic Self-Supply (DSS) was fixed at the average demand throughout the simulation and therefore shows no changes through time.

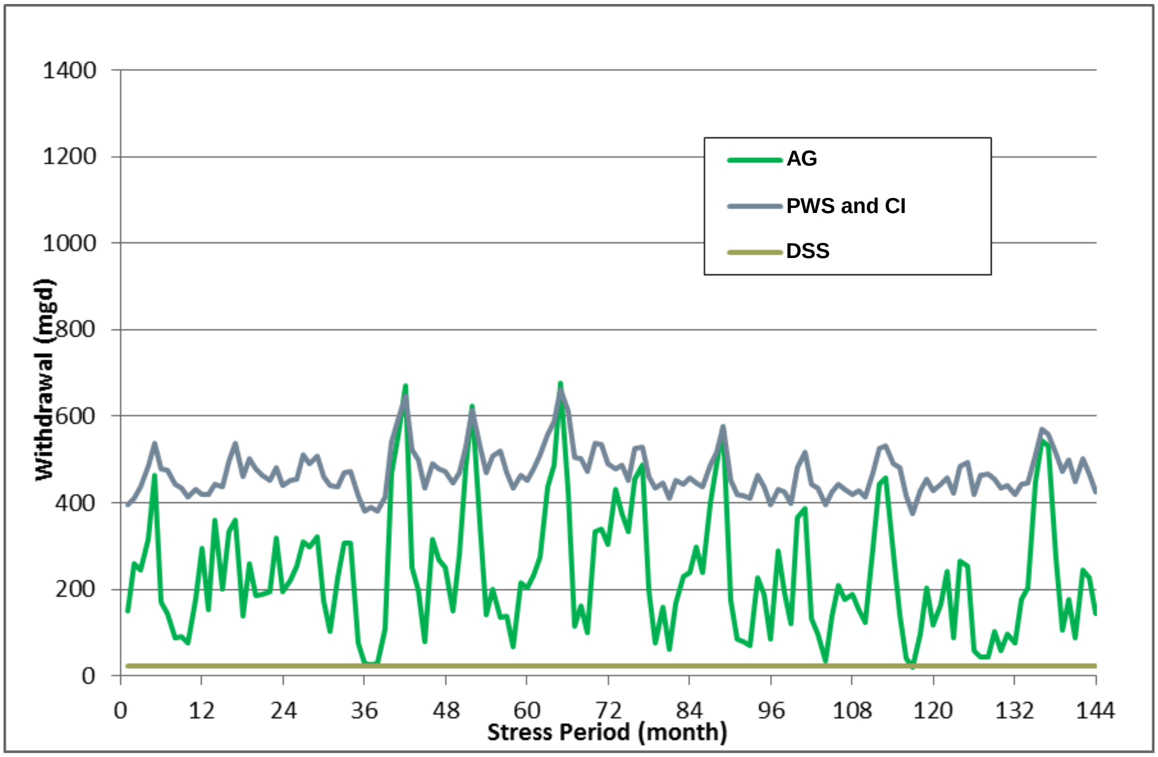

Figure 10. Distribution of monthly modeled Agricultural (AG), Public Water Supply (PWS), Commercial/Industrial (CI), and Domestic Self-Supply (DSS) withdrawals for the Reference Condition.

Monthly water production data from water supply utilities reflect changes in withdrawals to meet the demands of their systems. In dry periods of late spring and early summer, withdrawals typically increase; in wet periods of July through October, demands typically decrease. During tourist seasons around spring break, summer vacations, and Thanksgiving through early January, demands typically increase to satisfy the water needs of the influx of tourists. These demand changes are reflected in the monthly production data from the water supply facilities. The monthly data were used to calculate 144 monthly peaking factors for the period of 1995 through 2006. The peaking factors are referenced to the average water production; the peaking factor for the average production month is 1, for a month with higher production it is greater than 1, and for a month with lower production it is less than 1. For these one-year periods, the projected values were considered the average annual value for the utility and the monthly input data for withdrawals were the product of that value times the monthly peaking factors.

Agricultural Demands

Agricultural withdrawals for individual scenarios represented the quantity of water necessary to irrigate the acreage grown during the actual “scenario year”. For example, in the Reference Condition simulation, the acreage determined to be irrigated in 2005 (the “scenario year”) was held constant throughout the 12-year simulation period. The withdrawals necessary to irrigate that acreage were estimated on a monthly basis and varied throughout the simulation period according to the actual monthly rainfall that occurred. In the SWFWMD, these withdrawals were developed based on the metered/estimated monthly irrigation application rates that were used for the calibration period; whereas, in the SJRWMD and SFWMD, where these data were not as readily available, monthly withdrawals were estimated using a modified AFSIRS approach.

For future scenarios (e.g., 2035 withdrawal conditions), the Reference Condition withdrawals were first updated to include new permits issued since 2005 and exclude permitted withdrawals that were no longer active. The goal was to have a withdrawal dataset for the future scenarios that represented only currently (as of December 2012) permitted withdrawals. Projected withdrawal quantities for the future scenarios were as projected and reported for the RWSP effort and distributed proportionally to permitted withdrawals on a countywide basis. The exception was in Osceola County where a few agricultural permits with significant quantities were recently issued. In that case, county quantities were first assigned to the recently issued permits and the remainder was proportionally distributed to remaining withdrawals in the county. With respect to the location of withdrawals, quantities within the SFWMD and SWFWMD were assigned to permitted withdrawal locations; whereas, in the SJRWMD, quantities were assigned to the centroid of agricultural land parcels.

Commercial and Industrial Demands

Permitted allocations provided the basis for development of Commercial/Industrial (C/I) withdrawal uses for the future scenarios. Withdrawals for particular scenarios were developed in the same manner as was done for agricultural withdrawals.

For C/I uses within the CFWI Planning Area, demands input to the model for the future scenarios (withdrawal conditions from 2015, 2025, 2035, and EOP projected average day demands) were obtained from the CFWI Regional Water Supply Planning Team (RWSPT) Team. For uses outside the CFWI, future demands were obtained from the respective WMD’s regional water supply plan or maintained at permitted allocations.

Landscape, Recreation and Aesthetic irrigation

With respect to the future scenarios, irrigation withdrawals for landscape, recreation, and aesthetic uses in the SWFWMD were only included for existing permits. Projected demand quantities that were not tied to specific property were not included in the future scenarios. For existing permits, withdrawal quantities for these uses in the future scenarios were treated the same as they were for the EOP simulation. Elsewhere, within the CFWI, irrigation withdrawals were adjusted for each simulation based upon the projected increases/decreases provided by the RWSPT with the demands applied at the permitted facilities in SFWMD and at the land-use parcel level for the SJRWMD.

RUNOFF AND INFILTRATION

The combination of rainfall and irrigation was subjected to a process to separate water that fell onto impervious or pervious surfaces into runoff and infiltration. Runoff was routed to nearby surface water features, while infiltration water percolated through the soil for plant uptake. Infiltrated water that was not consumed by plant uptake through ET percolated deeper as available for aquifer recharge. The process to separate rainfall and irrigation to runoff and infiltration was unchanged from the USGS-ECFT model.

Irrigation Return Flow

Irrigation return flow was applied using the same methodology for all model simulations. Return flow is irrigated water that gets returned to the SAS (Model Layer 1) from inefficient irrigation practices. This occurs in agricultural areas and Public Water Supply service areas where landscape irrigation utilizes either potable or reclaimed water. The effect of this may result in some apparent mounding of water in Layer 1 in certain areas of some future scenarios depending on aquifer characteristics and the applied irrigation application rate and irrigation efficiency.

SCENARIO REPRESENTATION

The model scenarios implemented using the HAT-ECFT model for the Regional Water Supply Plan fall into one of three categories: Calibration, Reference Condition, and Future Scenarios. The scenarios were constructed so that withdrawals were the primary variable to change and to maintain as much consistency as possible in the input data and processes. As a result, differences in the simulation results were indicative of withdrawal-based effects. **Table 4** summarizes the differences in model inputs for the model calibration period and the five scenarios.

Of the six scenarios simulated, only the calibration simulation represents a progression through time. This primarily affected groundwater withdrawals with the withdrawals derived from measured or estimated monthly rates from January 1995 through December 2006. This allowed direct comparison of modeled and measured results over the 144-month simulation period to assess the agreement between the two and evaluate performance relative to calibration goals. All scenario simulations were run in transient mode using monthly stress periods for a 144-month simulation period representing January 1995 through December 2006 rainfall conditions. This was done to allow direct comparison between simulations by maintaining observed climatological conditions recorded during that period. The other simulations include the groundwater withdrawals of future periods or the EOP condition.

Table 4. Model input parameters for the HAT-ECFT model calibration and selected withdrawal condition scenarios.

Parameter		Scenario/Withdrawal Condition: Calibration	Reference Condition	2015	2025	2035	End-of-Permit (EOP)
Duration		144 Months	144 Months	144 Months	144 Months	144 Months	144 Months
Stress Period		Monthly	Monthly	Monthly	Monthly	Monthly	Monthly
Timeframe		1995 to 2006	2005	2015	2025	2035	EOP - Varies by Permit
Land Use		1995 for 1995 - 1999 2000 for 2000 - 2003 2004 for 2004 - 2006	2004	2004	2004	2004	2004
Rainfall & ET		Measured 1995-2006	Measured 1995-2006	Measured 1995-2006	Measured 1995-2006	Measured 1995-2006	Measured 1995-2006
Runoff and Infiltration Partitioning		Calculated using Green-Ampt [1]	Calculated using Green-Ampt [1,2]	Calculated using Green-Ampt [1,2]	Calculated using Green-Ampt [1,2]	Calculated using Green-Ampt [1,2]	Calculated using Green-Ampt [1,2]
Water Use Sector		1995-2006	2005 [1]	2015 Projected [1,3,5]	2025 Projected [1,3,5]	2035 Projected [1,3,5]	EOP Allocations [1,3,4]
	PWS	Measured over the period	Measured for 2005	Projected average 2015 demands	Projected average 2025 demands	Projected average 2035 demands	Permitted allocations
	AG	Measured or AFSIRS estimated over the period	Measured or AFSIRS estimated for 2005	Projected average 2015 demands	Projected average 2025 demands	Projected average 2035 demands	Permitted allocations
	C/I	Measured over the period	Average 2005	Projected average 2015 demands	Projected average 2025 demands	Projected average 2035 demands	Permitted allocations
	DSS	Estimated based on land use	Estimated based on 2004 land use	Projected average 2015 demands	Projected average 2025 demands	Projected average 2035 demands	Same as Calibration
	REC	Measured or not included	Same as Calibration	Same as Calibration	Same as Calibration	Same as Calibration	Same as Calibration
Irrigation and RIB Recharge	**IRR**	Estimated based on land use (indexed to measured pumping)	Estimated (indexed to 2005 pumping)	Estimated (indexed to 2015 pumping)	Estimated (indexed to 2025 pumping)	Estimated (indexed to 2035 pumping)	Estimated (indexed to EOP pumping)
	RIBs	Measured	Estimated average 2005 RIB loading	Estimated average 2005 RIB loading	Estimated average 2005 RIB loading	Estimated average 2005 RIB loading	Estimated average 2005 RIB loading

Notes:

[shaded] Indicates that values or processes are unchanged between scenarios

[1] Adjusted through the simulation period using rainfall amounts and patterns

[2] Adjusted based on depth to water

[3] Change within CFWI boundary unchanged otherwise

[4] EOP scaled based on 2006 use patters to preserve county by county average. Limited in dry years to permit maximum. Limited any 12 months to permit annual use. Includes new permits where identified.

Calibration Condition

Calibration represents the culmination of model parameter and input adjustments for the simulation results to match measured and calculated field conditions such as aquifer water levels, spring flows, aquifer flows, and water budget. The calibration of the HAT-ECFT model was intended to represent the hydrologic conditions of 1995 through 2006. Prior to the calibration process, calibration goals were identified that describe reasonable tolerance limits for the goodness-of-fit of the simulation results to the measured and calculated field conditions. In this case, the comparisons were spatial and temporal. Multiple adjustments to aquifer hydraulic property types and values and to water recharge-related and discharge-related inputs were made in a focused, trial-and-error process until the simulation results reasonably achieved the calibration goals. The use of a combination of observed and estimated hydrologic data inputs for model calibration has been described by Sepúlveda et al. (2012) and in Chapters 2 and 5 of this report. The resulting calibrated model was then used to simulate historic and future aquifer conditions within the limits of calibration and model construction.

The calibration simulation was based on a historical record from a period that saw significant changes in population, land use, and water use. This variation in the average magnitude, location, and type of water uses being simulated in the calibration run presents an obstacle to use of the calibration run as a basis of comparison to future conditions. In the future conditions, the estimated population and the corresponding average magnitude, location, and type of water uses are all held constant within each simulation, and the only variations in groundwater recharges and withdrawals are those attributed to changing weather conditions. In other words, the calibration condition reflects increasing demands due to growth over the 12-year simulation period, whereas the individual future scenarios reflect the same level of demands over the period.

Reference Condition

Rationale for Reference Condition Simulation and Intended Use of the Results

As described above, the difference between 1) the constant population and land use construction of the future conditions and 2) the continuously varying population and land use construction of the calibration condition, would create inconsistency and interpretive bias if the results of the future condition simulations were compared to those of the calibration simulation. To overcome this difficulty, it was necessary to create a reference condition simulation that approximated the historical condition and was constructed in the same way as the future condition scenarios.

Because the reference condition is constructed in the same way as the future simulation conditions and is subject to the same applied weather variation, all changes in hydrologic conditions from the reference condition to each future condition simulation were the direct consequence of changes in population and land use, as expressed through their resulting changes in water use. This would not be true if we assessed changes in hydrologic conditions from the calibration condition to the future condition, because some of those differences are the consequence of one simulation having a constant population and land use and the other having population and land use that vary. It is much easier to assess the significance of future changes in population and land use if they are separate from the effects of other changes. The reference condition approach achieves this and removes confusion about cause and effect that would otherwise arise if future conditions simulations were compared to the calibration condition or any other non-constant historical condition.

For the CFWI Planning Area, conditions of 2005 were selected as the Reference Condition. The scenario was developed to represent aquifer conditions that would be expected if 2005 water demands were realized over the 12-year simulation period. Dependent water input variables were adjusted based on monthly changes of rainfall using observed and calculated relationships between rainfall and specific variables. The 2005 condition was chosen for the Reference Condition because it corresponded with the time-frames used for CFWI hydro-ecological assessments of water body conditions, MFLs assessments, and the availability of water use records. More information on the assessments of water body conditions can be found in Zahina-Ramos et al. (2013) and Appendix B of the draft CFWI RWSP. The use of 2005 water demands as the Reference Condition does not imply that 2005 is considered a base year for acceptable environmental conditions. Instead, it is simply a period for which modeled environmental conditions were characterized for a common period with relatively well known hydrologic conditions.

Reference Condition

In the Reference Condition, the estimated population and the corresponding average magnitude, location, and type of water uses were held to a constant value that represents the water uses that would have taken place if the 2005 population and land use condition had been maintained consistently throughout the 12 years of weather variation that was observed from 1995 through 2006. During this simulation period, the only variations in groundwater recharges and withdrawals are those attributed to changing weather conditions. The method of estimating these variations in monthly groundwater recharges and withdrawals is presented in **Chapter 5** of this report.

Future Withdrawal Scenarios

The 2015, 2025, and 2035 Withdrawal Scenarios and End-of-Permit Condition were developed to test consistent sets of groundwater withdrawals. The scenarios were constructed and evaluated in a manner parallel to that of the Reference Condition, but use the projected withdrawals for the specified year or at the end of each current permit instead of withdrawal conditions for 2005. The results of each withdrawal condition scenario represent the modeled hydrologic system for those projected water needs subjected to the rainfall conditions of 1995 through 2006. Error! Reference source not found. provides a breakdown of withdrawals by use type for each scenario.

Table 5. Summary of demands within the CFWI Project Area by use type for the Reference Condition and the future scenarios (in MGD).

Scenario	Public Water Supply and Commercial/ Industrial	Agriculture	Domestic Self-Supply	Total
Reference Condition	454	179	20	653
2015 Withdrawal Scenario	551	210	23	784
2025 Withdrawal Scenario	656	214	23	893
2035 Withdrawal Scenario	766	226	23	1015
EOP Withdrawal Scenario	708	253	23	984

2035 Withdrawal Scenario

The 2035 Withdrawal Scenario was developed to assess modeled hydrologic conditions at the end of the 20-year planning period required for the CFWI RWSP.

Figure 11 illustrates the changes in withdrawals for all the use types comparing the Reference Condition against the 2035 Withdrawal Scenario.

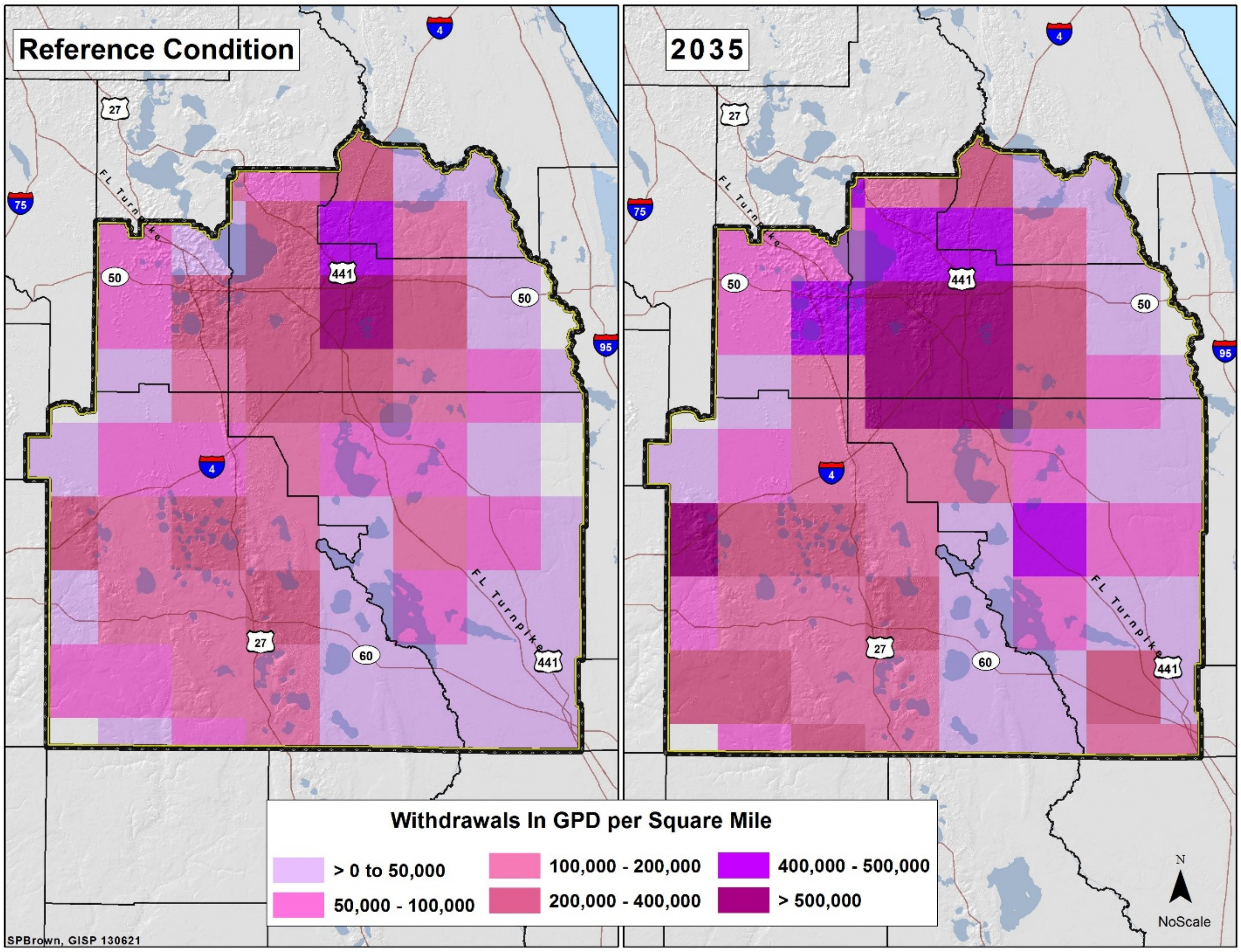

Figure 11. Comparison of the distribution of groundwater withdrawal quantities for the Reference Condition and the 2035 Withdrawal Scenario based on withdrawal totals for 100-square mile sections of the CFWI Planning Area (gpd = gallons per day).

2015 and 2025 Withdrawal Scenarios

The 2015 and 2025 Withdrawal Scenarios were constructed as intermediate points between the Reference Condition and the 2035 Future Condition. These intermediate scenarios were needed because water use needs differ throughout the CFWI area compared to uniform changes to water needs through time over the area.

End-of-Permit (EOP) Condition

The EOP Condition simulation was unlike the other future simulations because it was not based on a fixed set of consistently projected future demands at a given future projection date. Instead, it used information on currently permitted groundwater allocations, even though these allocations are valid at different dates. The EOP Condition can be thought of as representing a future condition that would occur if all current permits were renewed at current allocation levels until all permittees' water demands had grown to use their full permitted allocations.

For the EOP Condition, groundwater withdrawals were assumed to be maximized subject to the constraints of the permits. In months when a permittee's groundwater withdrawals would have exceeded permitted monthly maximum flow limits, or permitted annual and/or moving average flow limits, the groundwater withdrawals were reduced to comply with the permit requirements. This process is discussed in greater detail in **Chapter 5**.

4

Model Data Set Construction, Static Input Data Sets, and Applicable MODFLOW Packages

Input data for the CFWI application of transient groundwater flow modeling can be placed into two broad categories: static data (this chapter) and time-variant data (**Chapter 5**). Static input data may be constant, such as aquifer characteristics, or may change from stress period to stress period, like rainfall, but these changes are consistent across the various scenarios. In contrast, time-variant input data refers to model inputs that change between scenarios.

The static data sets in the ECFT model include intrinsic aquifer properties (hydraulic conductivity, specific storage, and leakance), land use, rainfall, evapotranspiration, unsaturated zone conditions, lake properties, perimeter boundary conditions, and streams/rivers/structure operations. In addition, the position of the saline groundwater interface (simulated as a no-flow boundary) was also not allowed to change between stress periods and between scenarios although other performance indicators can be used in the model to estimate if a particular simulation may potentially induce saltwater movement.

INTRINSIC AQUIFER PARAMETERS

Intrinsic aquifer parameters describe the physical and hydraulic properties of the sediments and rocks of the aquifers and water contained in the aquifers. The combination of these parameters and water level differences from stresses were used to calculate changes to groundwater flow regimes in response to the stresses. The values of the intrinsic aquifer parameters did not change between stress periods of the simulations or between the different model scenarios. These parameters are hydraulic conductivity, specific storage, and leakance and were assigned as follows:

- **Hydraulic Conductivity –** The values of hydraulic conductivity in the HAT-ECFT model were unchanged from the USGS-ECFT model. Assignments of hydraulic conductivity were described in Sepúlveda et al. (2012).

- **Specific Storage –** The values of specific storage in the HAT-ECFT model were changed for Layers 5 and 7 from the USGS-ECFT model. Resulting assignments were described in **Chapter 2** of this document.

- **Leakance –** The values of leakance in the HAT-ECFT model were unchanged from the USGS-ECFT. Assignments of leakance were described in Sepúlveda et al. (2012).

RAINFALL

The spatial and temporal distributions of rainfall over the study area from 1995 through 2006 were obtained from the National Oceanic and Atmospheric Administration (NOAA), SJRWMD, SWFWMD, and SFWMD rainfall stations. The methodology used to calculate the initial spatial distribution of NEXRAD rainfall data was presented by Hoblit et al. (2003). The spatial and temporal distribution of rainfall prepared by Sepúlveda et al. (2012) was unchanged by the HAT.

Because of known differences between data collected at specific rainfall stations and the methodology used to generate the spatial rainfall distribution for NEXRAD, multiplication factors were introduced to make the NEXRAD rainfall values representative of the measured rainfall. The general spatial distribution of rainfall data from NEXRAD was retained and adjustments were then made in an attempt to match observed rainfall data at selected rainfall stations. A complete discussion of the methodology used to develop the multiplication factors can be found in Sepúlveda et al. (2012).

Figure 12 shows the average annual spatial distribution of rainfall used in the model for the 12-year simulation period. Average rainfall rates tend to cluster within a range of 45 to 55 inches per year. The rainfall arrays for cells located in the Atlantic Ocean, Indian River Lagoon, and the barrier island were assigned a zero-value because they are inactive in the model. In addition, the areas that exceed 55 inches per year in the figure have the irrigation demands added to the rainfall arrays to account for runoff and recharge for the Green-Ampt runoff equation and the unsaturated zone MODFLOW package. This explains why localized areas have rainfall rates in excess of 100 inches per year. These high rainfall areas are identified in the figure as yellow to red in color.

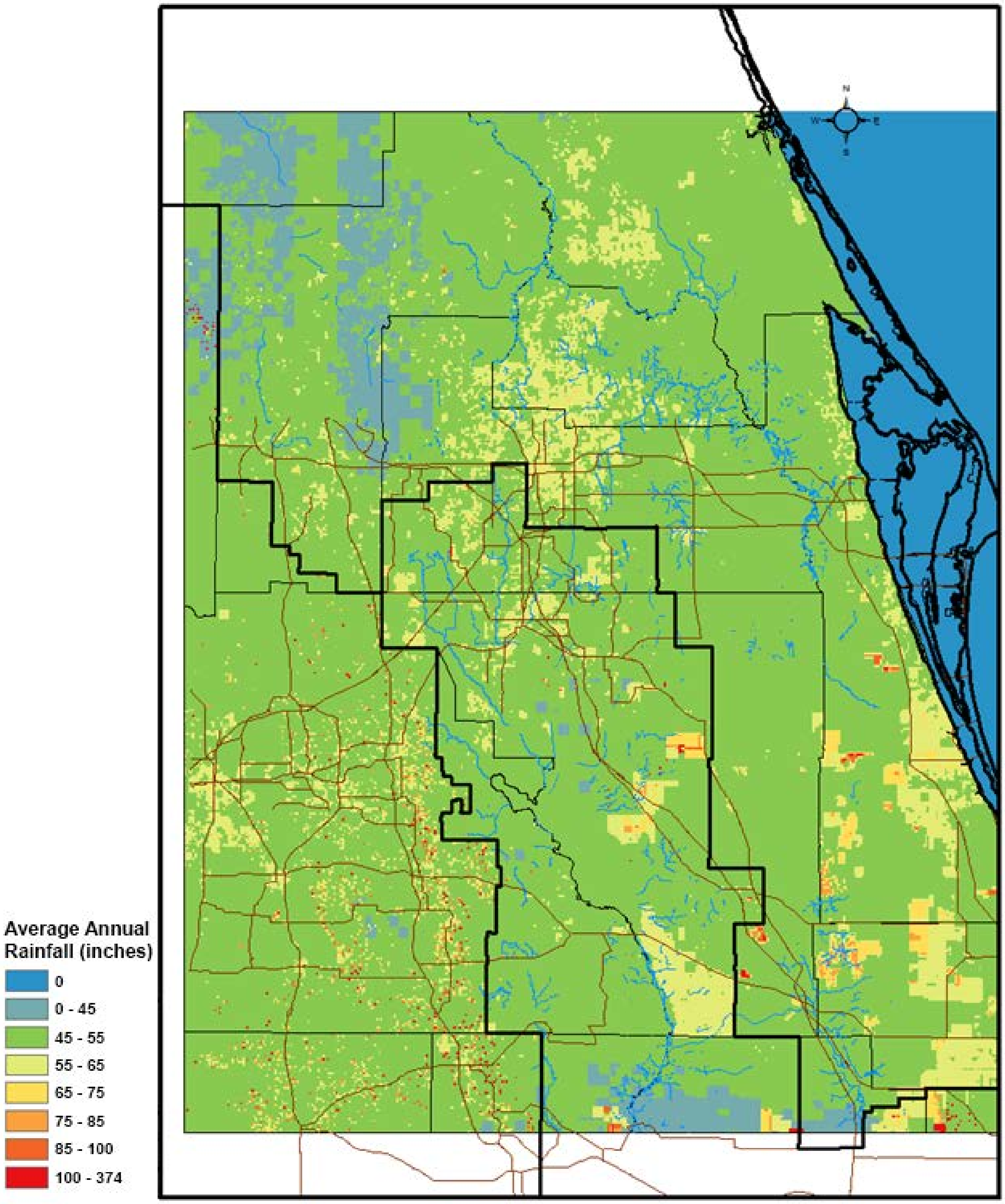

Figure 12. Average annual rainfall (1995-2006) in the HAT-ECFT model. (Note: Areas that exceed 55 inches/year in the figure have the irrigation demands added to the rainfall arrays to account for runoff and recharge for the Green-Ampt runoff equation and the unsaturated zone MODFLOW package.)

Figure 13 illustrates the comparison of rainfall data calculated with NEXRAD against the observed data at an Orlando rainfall gauge. A relatively close match was obtained at this site between what was used in the model and what was measured at this specific location. Several other rain gauges were checked in this way and provided similar comparisons, but this was not true for all locations. .

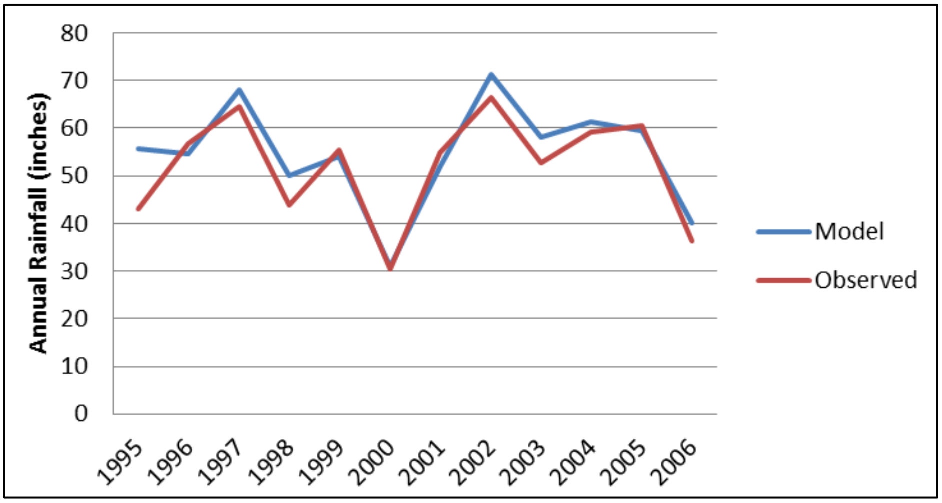

Figure 13. Simulated and measured rainfall for Orlando

To understand the rainfall volumes used in the 1995 through 2006 simulation, rainfall data was obtained for four long-term gauges (Orlando, Bartow, Deland, and Avon Park). These data were from an archive of monthly precipitation data from selected cities in Florida, generally beginning around 1900 and compiled by the Florida State University Climate Center. The data were monthly summaries and annual totals originally compiled by the National Climatic Data Center. Gaps for missing time periods at these locations were in-filled using observations from nearby areas (Winsburg, 2003).

Monthly rainfall rates as calculated by NEXRAD with the adjustments were then removed from the model grid cells consistent with the geographic location of the long-term rainfall gauges. These values were then statistically compared against the long-term rainfall gauges to determine the representativeness of the 1995 through 2006 model simulation period. The four gauges selected had data sets generally ranging from 1900 through 2012. **Table 6** provides the comparison between the 12-year model simulation period and the 112-year historical period of record.

Table 6. Comparison of long-term period of record (~1900–2012) and model (1995-2006) rainfall data (in inches per year).

	Average			Minimum			Maximum		
	POR	Model	Dif	POR	Model	Dif	POR	Model	Dif
Avon Park	52.1	51.4	-0.7	26.1	25.5	-0.6	80.1	64.6	-15.5
Bartow	54.2	55.4	1.2	34.6	38.0	3.3	83.4	69.3	-14.1
Deland	54.8	61.6	6.8	34.2	43.1	8.9	84.0	75.1	-8.9
Orlando	54.0	54.6	0.7	30.4	30.9	0.5	84.0	71.2	-12.9

Note:
POR: long-term period of record
Dif: Difference = Model - POR

In general, the average long-term rainfall rate is within 2 inches of the average rainfall for the 12-year model simulation period with the exception of the Deland area. Extreme wet years are not observed during the simulation period; however, the 2000 drought was one of the worst on record and is represented in the model. This point is illustrated in **Figure 14**, which shows the long-term rainfall data collected at the Avon Park rain gauge. The 2000 drought was the lowest recorded rainfall at this gauge. The second lowest recorded rainfall at this site occurred in 2006, at the end of the model simulation period.

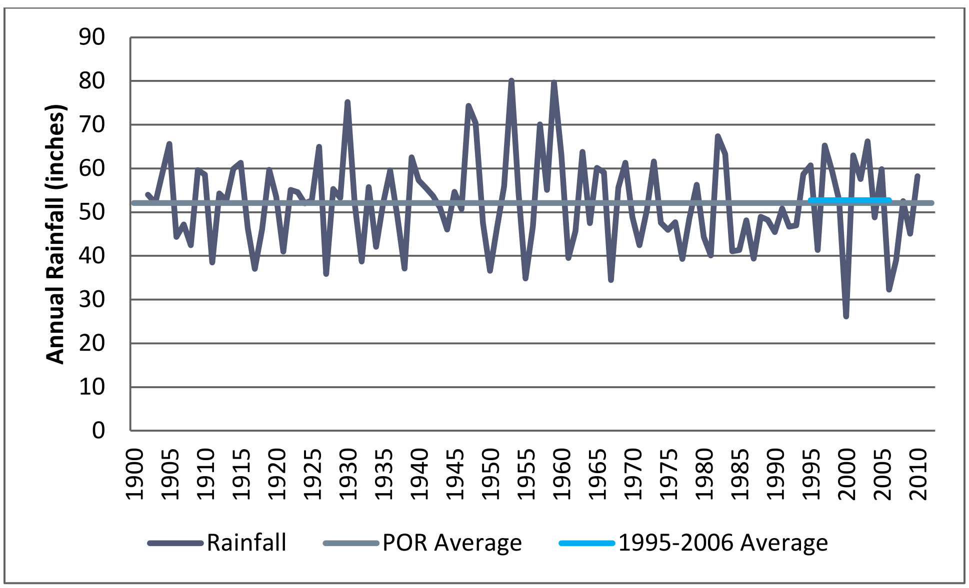

Figure 14. Long-term annual rainfall at the Avon Park rain gauge.

After the rainfall arrays had been developed, they were used to estimate surface runoff, infiltration, and irrigation demands, which were subsequently rolled up into monthly values for each month of the 12-year simulation period. These 144 monthly rainfall arrays were used for the Reference Condition and future simulations without being allowed to change.

EVAPOTRANSPIRATION

Evapotranspiration (ET) causes the largest loss in the water budget in central Florida. ET generally accounts for approximately half of the rainfall for an average year but can well exceed rainfall during dry periods and for large open water body systems in central Florida. In the model, ET over land areas is calculated from potential ET (PET) and depth to groundwater. For these areas, the ET values are PET values that decrease using the depth to water in the surficial aquifer and a linear function of a decreasing ET rate with increasing depth. The ET rate is set to zero at and below the ET extinction depth. Over open water, PET is used as ET directly in the model.

PET was calculated by Sepúlveda et al. (2012) using the Priestly-Taylor method. The source of data was from the USGS statewide coverage on a daily 2-kilometer pixel resolution derived from satellite and ground-based data from June 1995 to 2006 (Sepúlveda et al., 2012). **Figure 15** provides the average annual PET rate calculated by this method. For the model area, PET rates generally increase from north to south, ranging from 48 to 52 inches per year. The larger lake systems in the model with the higher PET rates in the figure are shown for illustrative purposes only. The distributions of PET, ET versus depth functions, and ET extinction depths were unchanged from Sepúlveda et al. (2012).

Smajstrala (1990) generated long-term daily potential ET rates for several weather stations in Florida. One of these stations is located in the CFWI Planning Area near Orlando. Several other stations have long-term periods of record including Tampa, West Palm Beach, and Daytona Beach, but are located outside the model area. The average annual long-term PET rate was determined to be approximately 53.7 inches at the Orlando station from 1952 through 1973, 50.6 inches in Daytona, 55.3 inches for West Palm Beach, and 54.1 inches at Tampa. These values agree well with the rates calculated by Sepúlveda et al. (2012), which had an average annual rate of 50.1 inches between 1995 through 2006. However, recent potential ET calculations by the Florida Automated Weather Network do show some differences as illustrated in **Figure 16**. In the late 1990s and early 2000s, the two methods agree reasonably well; however, they diverge beginning in 2003 through the end of the simulation period in 2006.

Calculation of the PET rates applies to a hypothetical, well-irrigated, and manicured crop, such as grass. To determine actual ET rates for a specific model cell, the PET was adjusted to meet the demands of the predominant crop at that location. This was generally accomplished using a monthly crop coefficient multiplication factor that reflects various stages of crop growth. Sepúlveda et al. (2012) did not specifically adjust the PET to the observed crops at a specific location; instead, they adjusted the actual ET based upon physiographic, land use, and other features. Estimates of actual ET developed for the model were based upon nine zones including marsh, forest, scrub, and ridge areas. Areas including agricultural, mining, lakes, and urban land use had to be adjusted because the PET stations where data were collected were not located in those land use types. **Figure 17** provides the average annual distribution of actual ET used in the model.

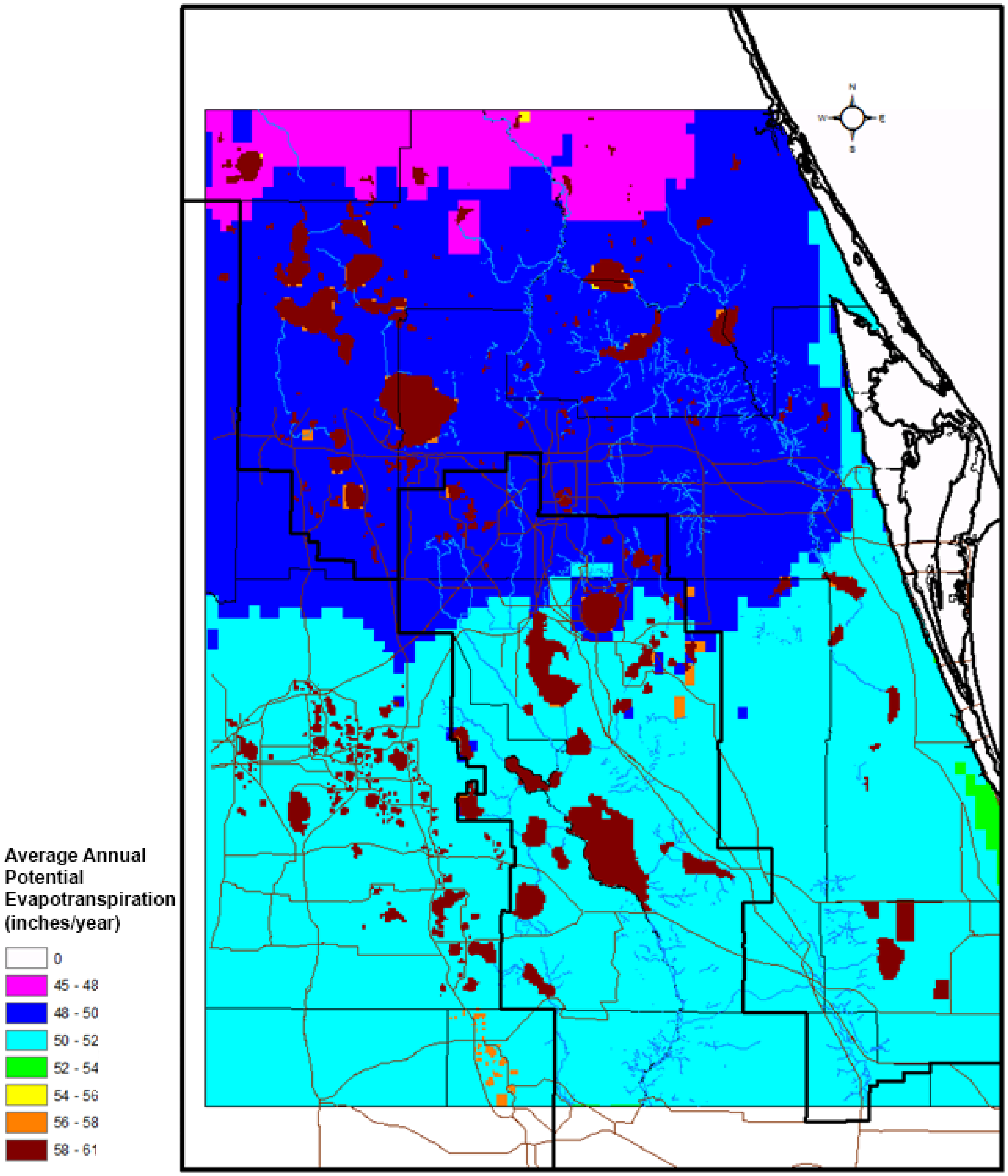

Figure 15. Average annual potential evapotranspiration (inches/year) for 1995 through 2006 (Sepulveda et al., 2012).

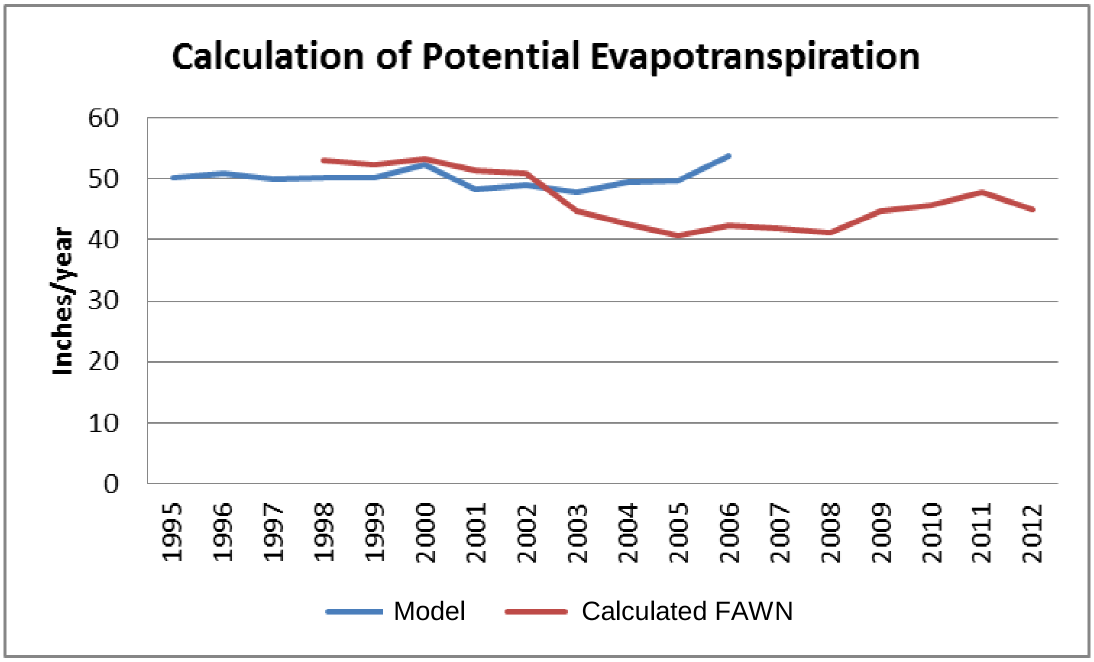

Figure 16. Average annual potential evapotranspiration in central Florida as modeled and calculated by the Florida Automated Weather Network.

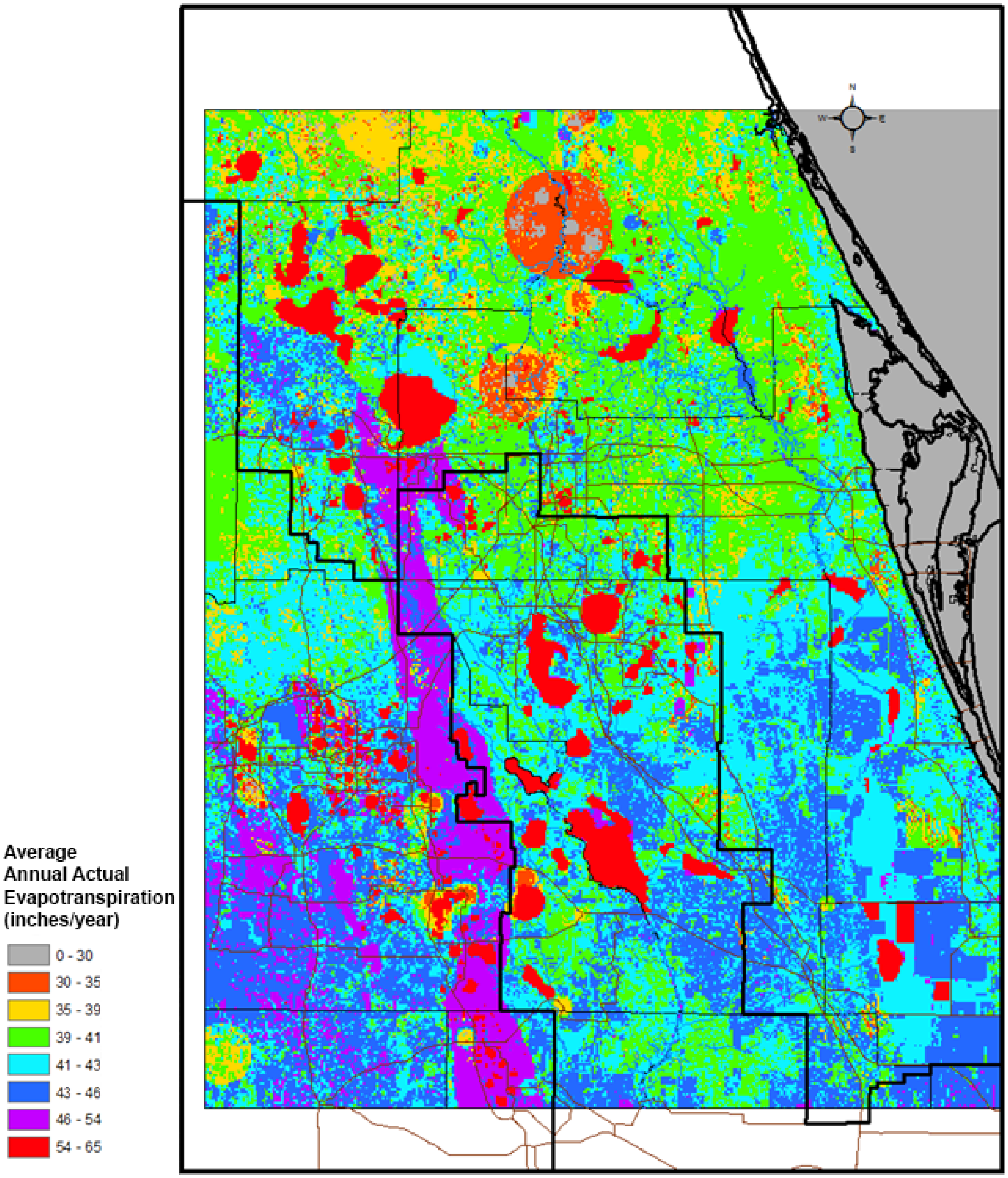

Figure 17. Average annual actual evapotranspiration rates, 1995-2006 (Sepulveda et al., 2012).

Actual ET rates were used in the unsaturated zone component of the model. These values represent the maximum amount of water that could be removed from the model by ET. Actual ET rates were calculated from the potential ET rates and further adjusted during the model calibration. Actual ET rates were further adjusted, through a pre-processing program, upward in the model during high rainfall or irrigation events at a cell-by-cell level (Sepulveda et al., 2012). For the Reference Condition and future simulations, the 2004 land use cover was used to develop monthly actual ET rates for the unsaturated zone package and does not change between simulations. Other coverages affecting the ET loss that do not change between simulations are the soil coverage and the ET extinction depths. The soil coverage is divided into four hydraulic groups based upon the rate of infiltration with a dual designation for areas having high water tables. The four groups include (A) soils with high infiltration rates, (B) soils with moderate infiltration rates, (C) soils with low infiltration rates, and (D) soils with very low infiltration rates. ET extinction depths were also developed using the soil texture and land use coverages (Sepúlveda et al., 2012) as shown in **Table 7** and not allowed to vary between simulations.

Table 7. Evapotranspiration extinction depths based on values from Shah et al. (2007).

Soil Texture Class	Extinction Depth (feet below land surface)
Sand	4.76
Loamy sand	5.58
Sandy loam	7.55
Sandy clay loam	7.55
Sandy clay	7.55
Muck	7.55
Urban	4.76
Water	4.76
Wetlands	4.76

LAND USE

Land cover and land-use areas were primarily used in the model to develop the actual ET rates for the unsaturated zone package to estimate landscape irrigation and agricultural irrigation return flows, and for land use types where it was needed to split the sum of rainfall and irrigation into infiltration and runoff using the Green-Ampt equation. The Green-Ampt equation is an external preprocessing routine to the ECFT model that splits the combination of rainfall and irrigation into infiltration and runoff depending on the land cover and properties of the surface soil. Infiltration resulting from Green-Ampt is input into the Unsaturated Zone Flow (UZF1) package of MODFLOW. Runoff resulting from Green-Ampt is input into the LAKE or STREAM packages of MODFLOW. For the Reference Condition and future simulations, the land use that was utilized was the statewide land use cover developed by four of the five Florida water management districts. Each water management district independently developed their own land use cover for their jurisdictional boundaries and then combined them into a single coverage. In general, up to a

Level 4 Florida Land Use Cover Classification System (FLUCCS) code was assigned to each polygon depending upon available data.

Distributions of land use for 1995, 2000, and 2004 were available to the USGS when developing the USGS-ECFT model. The 1995 land use was used for the stress periods of January 1995 through December 1999; 2000 land use was used for stress periods of January 2000 through December 2003; and 2004 land use was used for stress periods of January 2004 through December 2006. The distributions of land uses were not changed during the CFWI process.

Future land use maps are prepared by planning departments of local and county governments to assist in growth planning. Distributions of future land use conditions to correspond to simulations of future water use conditions (2015, 2025, 2035, and EOP) were not available from local and county governments for the CFWI process. As a result, 2004 land use was used for simulations of future water use conditions. While this is not ideal, it was the only reasonable alternative available.

In 2004, agriculture was the most extensive land use and covered 27 percent of the study area, followed by wetlands (26 percent), urban (19 percent), forest (11 percent), water (8 percent), rangeland (6 percent), roads and utilities (2 percent), and barren land (less than 1 percent). A generalized FLUCCS Level 1 breakdown of 2004 land use is presented in **Figure 18.** A map using Level 1 FLUCCS codes and generic soil types (i.e., sand) were combined to develop the final coverage for generating runoff and actual ET rates for the model. This simplified 2004 combination of soils and land use was then used to determine rates for the Reference Condition and future simulations and did not change between simulations.

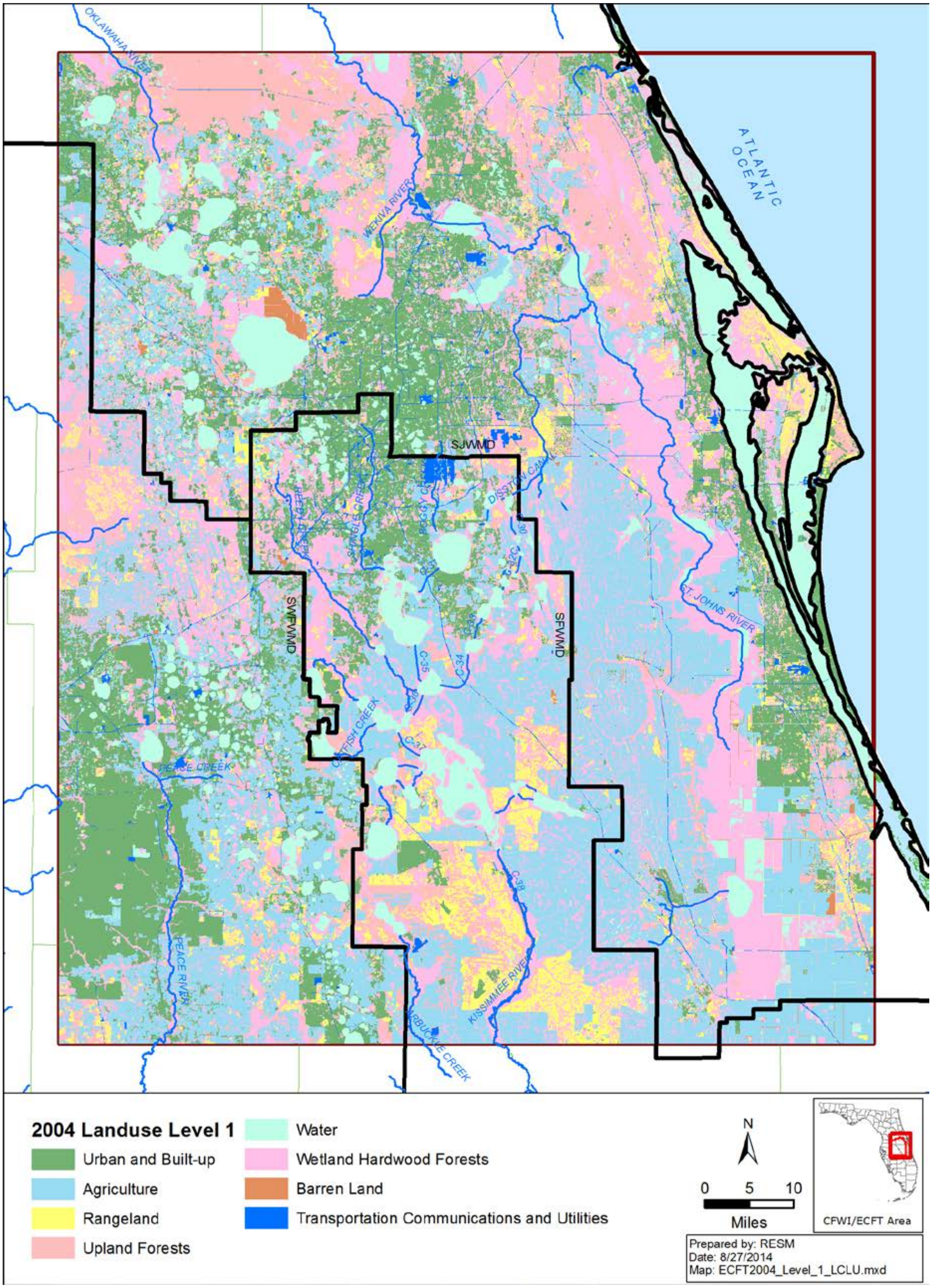

Figure 18. Level 1 2004 Land Use Map.

MODFLOW PACKAGES USED IN THE ECFT MODEL

MODFLOW Unsaturated Zone Package

The MODFLOW Unsaturated Zone (UZF1) Package is a substitution for the typical recharge and evapotranspiration packages normally used by MODFLOW before the release of the MODFLOW 2005 version of the code. Previous versions of MODFLOW required recharge to be calculated as the rate directly entering the water table and ignoring the unsaturated zone. In the UZF1 Package, an infiltration rate is applied at land surface at the top of the unsaturated zone, where present, with the infiltration rate governed by the saturated vertical hydraulic conductivity. The Evapotranspiration Package previously removed water down to a prespecified depth below the water table at a linearly decreasing rate with depth. The UZF1 Package includes the unsaturated zone so that the evapotranspiration losses are first removed from the unsaturated zone above the ET extinction depth, and if the demand is not met, then water can be removed directly from groundwater whenever the depth to groundwater is less than the extinction depth (Niswonger et al., 2006). The UZF1 Package allows for water to discharge to the land surface when the elevation of the water table exceeds land surface. Water that is discharged to the land surface, as well as applied rainfall and irrigation in excess of the recharge rate, may be routed directly to specified streams or lakes if these packages are active; otherwise, this water is removed from the model (Niswonger et al., 2006).

The UZF1 Package uses the kinematic wave approximation to Richards' equation and is solved by the method of characteristics to simulate vertical unsaturated flow. The approach assumes uniform vertical hydraulic properties in the unsaturated zone and downward gravitational movement without accounting for deep capillary fringe upward fluxes (Niswonger et al., 2006). As a result, a number of input model parameters are required and only the primary parameters are discussed in this section. The residual water content was set to 0.1 across the model, the saturated water content varies between 0.2 and 0.3, and the Brooks-Corey exponent (epsilon) was set to 3.5 across the model. **Figure 19** provides the saturated vertical hydraulic conductivity of the unsaturated zone and is similar in range to the horizontal hydraulic conductivity of the SAS.

The other three primary variables required are the actual monthly ET rates, the monthly recharge rates, and the ET extinction depth. The ET extinction depths are provided by media type by Shah et al. (2007) and shown in in **Figure 20**. The dominant extinction depth is 4.75 feet. The zero values assigned at the lakes are a result of the rainfall and ET being applied in the Lake and Stream packages, therefore they are not active in the UZF1 Package.

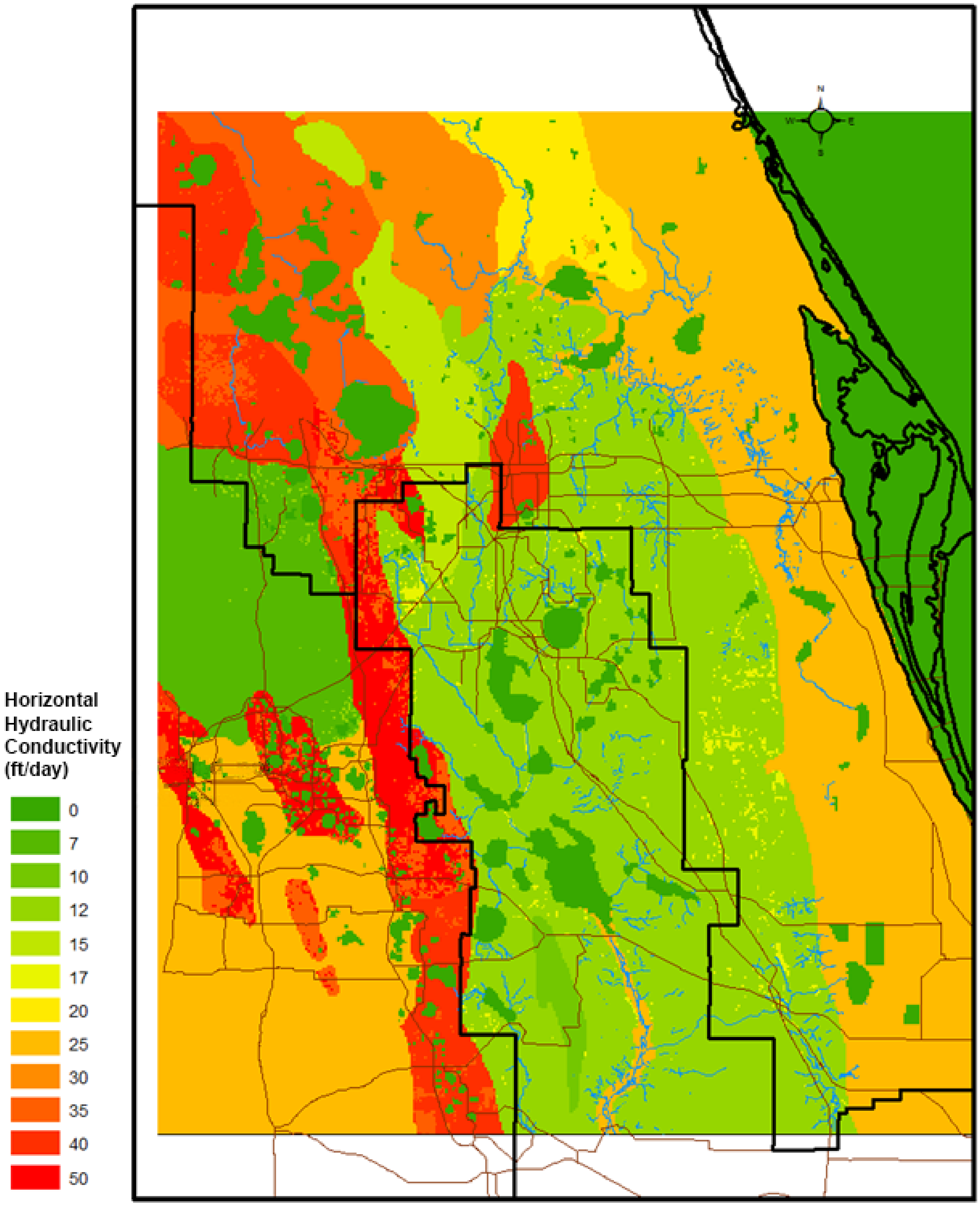

Figure 19. Horizontal hydraulic conductivity of the unsaturated zone (feet per day).

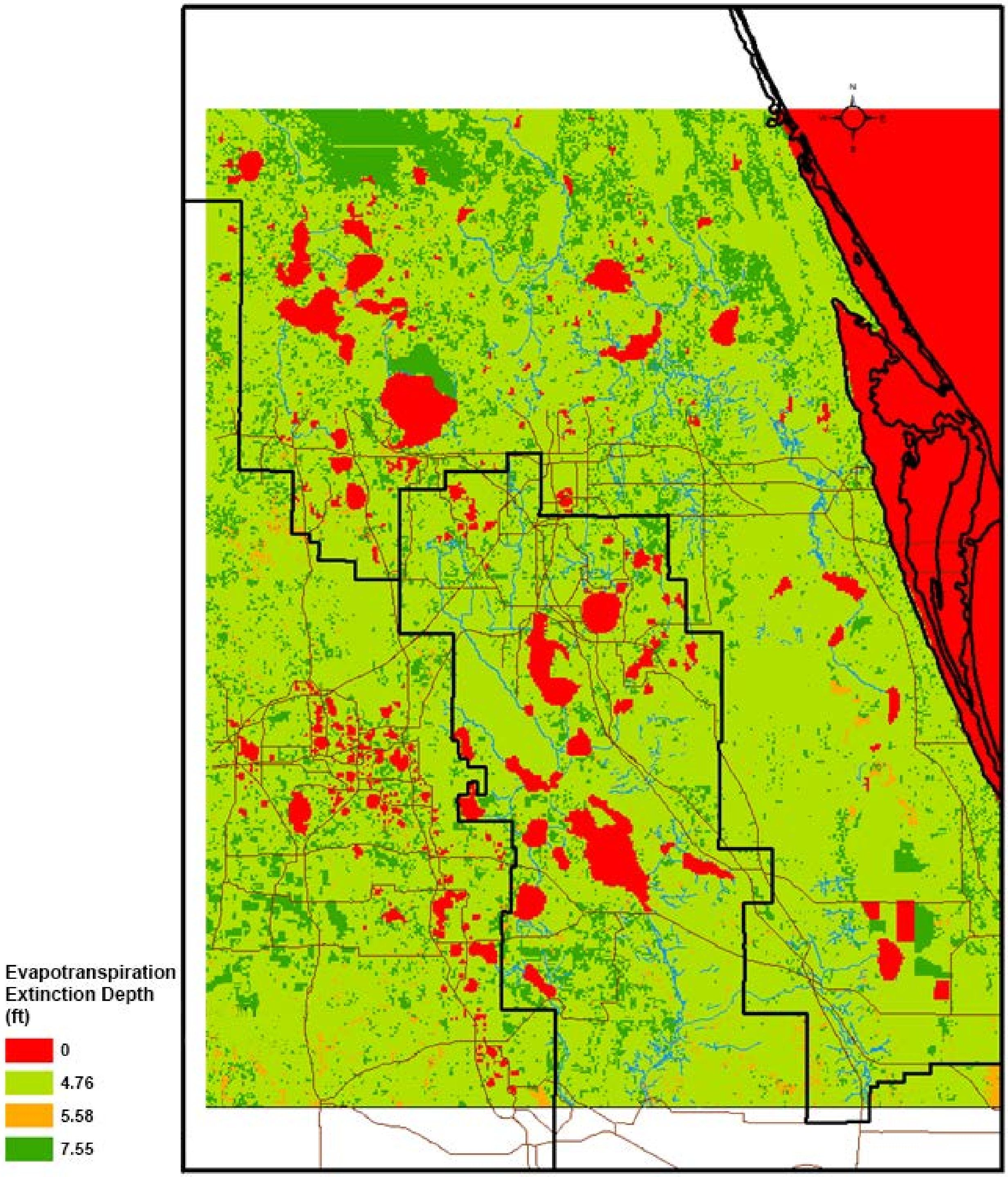

Figure 20. Evapotranspiration extinction depths (feet) from Shah et al. (2007).

MODFLOW Lake Package

The Lake Package simulates the interaction between lakes with variable water levels and groundwater (Merritt and Konikow, 2000). The package has two key functions: it serves as a boundary condition for the groundwater flow equation and it simulates the lake stage and calculates the water budget of the lakes. The terms for the lake water budget include evaporation, precipitation, stream flow, and groundwater flux with the stage calculated from this budget.

The version of the Lake Package used in CFWI modeling was LAK7 with MODFLOW 2005, version 1.8. LAK7 includes the capability to simulate vertical unsaturated flow below the lakes (Merritt and Konikow, 2000). Another minor change to this version was to make lake stage related variables to be double precision.

The input data to the Lake Package includes nine separate data sets, each consisting of one or more records. In general, these data have specifications of the physical geometry of the lakes, hydraulic properties of the lake beds, and the degree of hydraulic stress imposed on the groundwater system. It is important to note that several of these data are not usually available readily to the users. Rainfall and ET are needed to be applied to each lake cell. These values were computed by the methods discussed previously and added to each individual lake. Other parameters, including control elevations, did not vary between the base case and future simulations. The result is that potential or proposed future changes in lake operations may not be fully reflected in the present model simulations. Changes in runoff into a lake due to future changes in land use may also not be simulated. The number of lakes simulated in the HAT-ECFT model is 351 and shown in **Figure 21.**

In the HAT-ECFT model, individual lake stages were assessed for fatal flaws of the model but not fully calibrated to observed data at some locations for several reasons, including lack of data. Calibration of lake parameters was initially conducted through the Green-Ampt preprocessor for determining runoff into the lakes. As a result, the simulated lake stages were not used to evaluate impacts to individual lakes for the Reference Condition or other withdrawal scenarios. The approach used to assess impacts on the lakes was to evaluate drawdowns in the Upper Floridan aquifer that underlies the lakes. In other words, the changes in UFA stages were used as a surrogate to evaluating the lake stages themselves. Limitations include cases where the lakes and the UFA are not as well connected, which is the assumption that the methodology is based on.

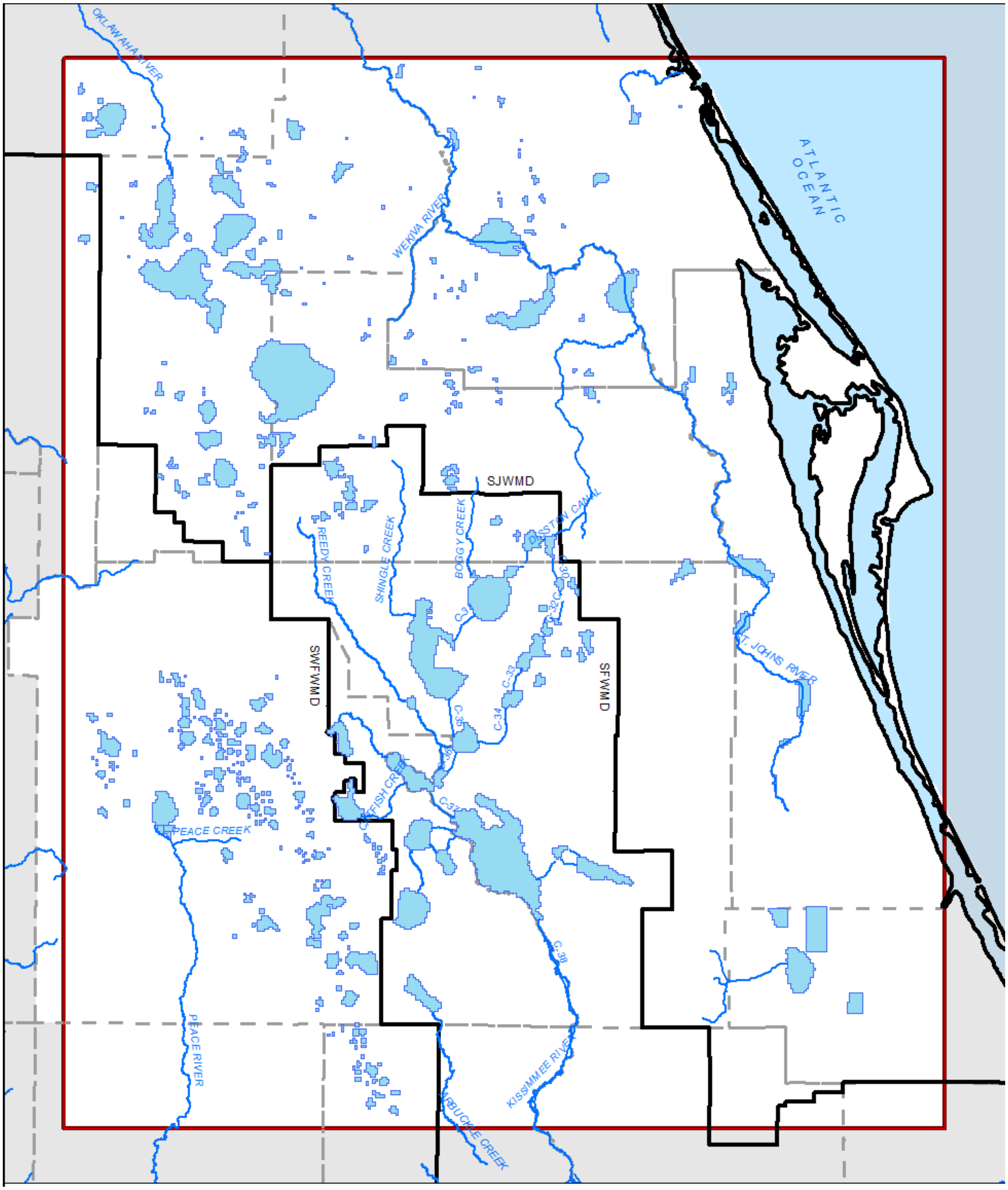

Figure 21. Lakes simulated with the Lake Package.

MODFLOW Streamflow-Routing Package

The MODFLOW Streamflow-Routing Package (SFR2) is similar to the original SFR1 version (Prudic et al., 2004) with the added capability to simulate unsaturated flow beneath a river using a similar methodology for the unsaturated zone flow as discussed for the UZF1 section. Streamflow routing is based on the continuity equation assuming steady, uniform flow such that the volumetric inflow is equal to the outflow minus all sources and sinks to the channel. Flows are routed through a network of channels where flow is always in the same direction along channels and seepage is constant for each time step (Niswonger and Prudic, 2006).

Input parameters for the SFR2 package include ET, rainfall and runoff. The parameters needed for the unsaturated zone as identified in the UZF1 section have been discussed previously and similar values are used for the SFR2 Package in the HAT-ECFT model. Additional required parameters include the stream channel width, the stream water-surface altitude slope, the streambed slope, the thickness of the streambed, the vertical hydraulic conductivity of the streambed, and the Manning's dimensionless roughness coefficient. In general, the Manning's roughness coefficient was set to 0.05, the thickness of the streambed was set to 5 feet, and the vertical hydraulic conductivity was set to 0.02 feet/day for most stream reaches. The altitude slope and streambed slope were obtained from the DEMs and the canal widths from aerial photos (Sepúlveda et al, 2012). In the model, the streams are broken up into 320 similar segments. The location of the streams reaches are shown in **Figure 22**.

Calibration of stream flows was limited to reducing, as much as possible, the differences between the total simulated and measured water volumes over the simulation period (Sepúlveda et al., 2012). Similar to other sections in this chapter, streamflow-routing parameters did not change between the Reference Condition and future simulations. Proposed future changes to structure operations and canal dimensions are not incorporated into the simulations conducted to date.

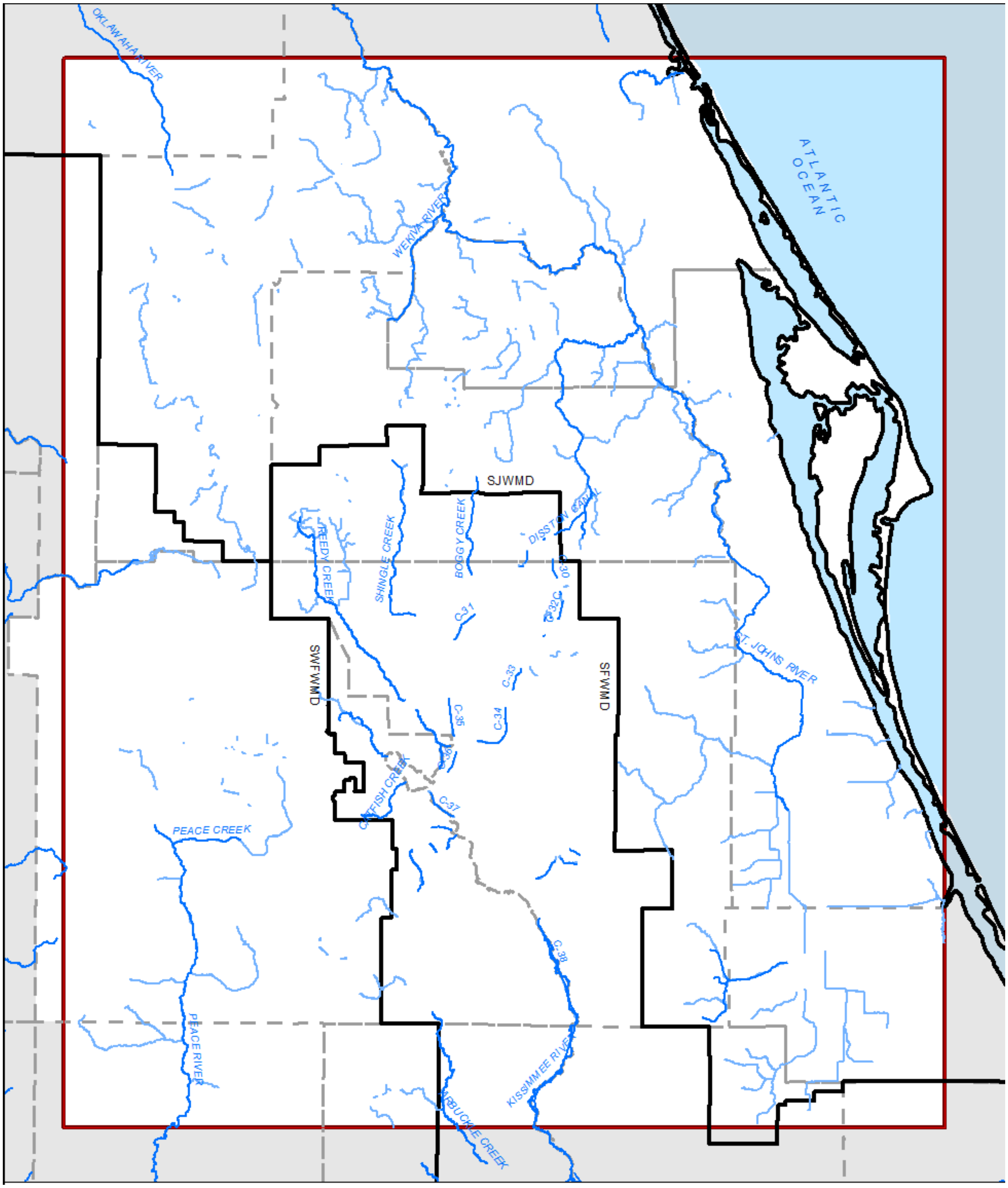

Figure 22. Location of streams used in the Streamflow-Routing Package

MODFLOW General Head Boundary Package

The lateral boundaries for the seven layers in the ECFT model were assigned as head-dependent flux boundaries and simulated using the General Head Boundary (GHB) Package in MODFLOW. Though the model simulates monthly stress periods and produces water level changes on a monthly basis, for the USGS-ECFT, specified heads used in the GHB Package varied annually over the simulation period. This caused simulated heads for model cells near the lateral boundaries to have a “stair-step” appearance (see **Figure 23** for an example). For the HAT-ECFT, it was decided to vary the specified heads in the GHB Package monthly to improve simulated water levels and more accurately represent observed changes.

The process to estimate monthly heads for the GHB Package involved constructing potentiometric surface maps for Layer 3 for each monthly stress period of the simulation. Heads in the permeable layers associated with Layers 5 and 7 were estimated based on observed differences between heads in Layer 3 and the respective layers. Water levels for the confining layers in the model (Layers 2, 4, and 6) were based on linear interpolation of boundary heads between the adjacent upper and lower aquifers.

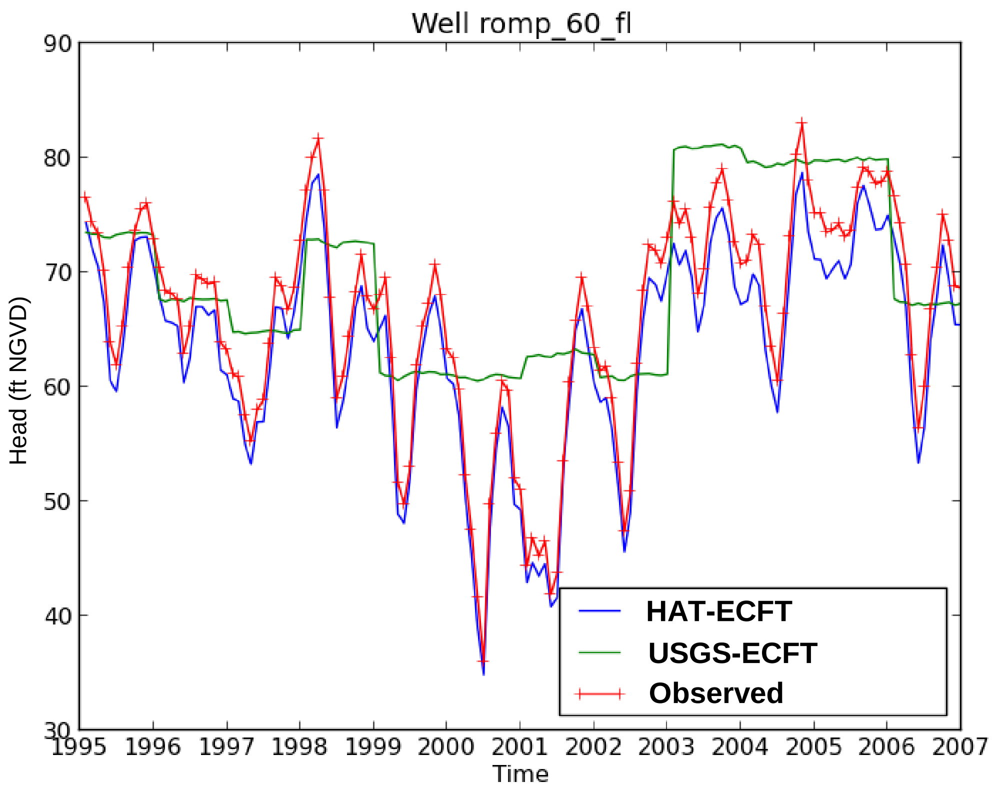

Figure 23. Layer 3 water levels for well ROMP 60 near the lateral boundary (see **Figure 3** for the location of well ROMP 60).

Estimation of Boundary Heads for Layer 3

Criteria for Including Wells to Estimate the Potentiometric Surface

A total of 292 wells were used to construct the 144 monthly potentiometric surface maps for Layer 3. Each well was assigned a model layer based on its casing and total depth in relation to the thickness of each layer defined in the model. If a well was open to multiple aquifers, the well was assigned to the model layer corresponding with the total well depth. Water level monitoring wells within the model domain were considered to establish a reasonable coverage over the area. Additional wells outside the active model domain were identified to ensure trends in the potentiometric surface beyond the model area were captured and adequately characterized. A minimum data availability of May and September for each year was established, though in some areas, where well coverage was poor, wells missing these values were used.

Data Infilling

To construct a potentiometric surface map for each month, the wells used needed a minimum of one water level value per month during the simulation period. Of the 292 Layer 3 wells used to create the surfaces, 26 had observed water levels for all months of the 12-year simulation period and an additional 91 wells had observed water levels for more than 124 months of the simulation period. The remainder of the wells used had less than 124 observed monthly water levels but more than 20 (**Figure 24**). Two types of data infilling techniques were performed for wells with missing data: 1) linear infilling when data gaps of less than four months occurred, and 2) estimating missing water levels based on observed water level fluctuations from a nearby well or wells when more than four consecutive months of data were missing. In all, 266 wells had months with linearly infilled water levels. Of the 266 wells, 110 had water levels infilled using the linear interpolation technique (**Figure 25**). In cases where there were more than four consecutive months of missing data, infilling was based on observed fluctuations from a nearby well or wells with data from the missing period (**Figure 26**). Data for the well with available data were standardized to the standard deviation as follows:

$$X_{1,SV} = \frac{\left(X_{1,m} - \bar{X}_1\right)}{SD_{X1}} \qquad \text{(Eqn. 1)}$$

Where:

$X_{1,SV}$ = standardized value of X_1 (well with available data)

$X_{1,m}$ = monthly value of X_1

$\bar{X}_1$= mean value of X_1

SD_{X1} = standard deviation of X_1

The assumption was that the well with missing data responded the same or similarly to the well with data so that the monthly standardized values would be the same. The monthly values for the infilled well data were estimated as follows:

$$X_{2,m} = \left(X_{1,SV} * SD_{X2}\right) + \bar{X}_2 \qquad \text{(Eqn. 2)}$$

Where:

$X_{2,m}$ = estimated monthly value of X_2 (well with missing data)

$\bar{X}_2$ = mean value of X_2

SD_{X2} = standard deviation of X_2

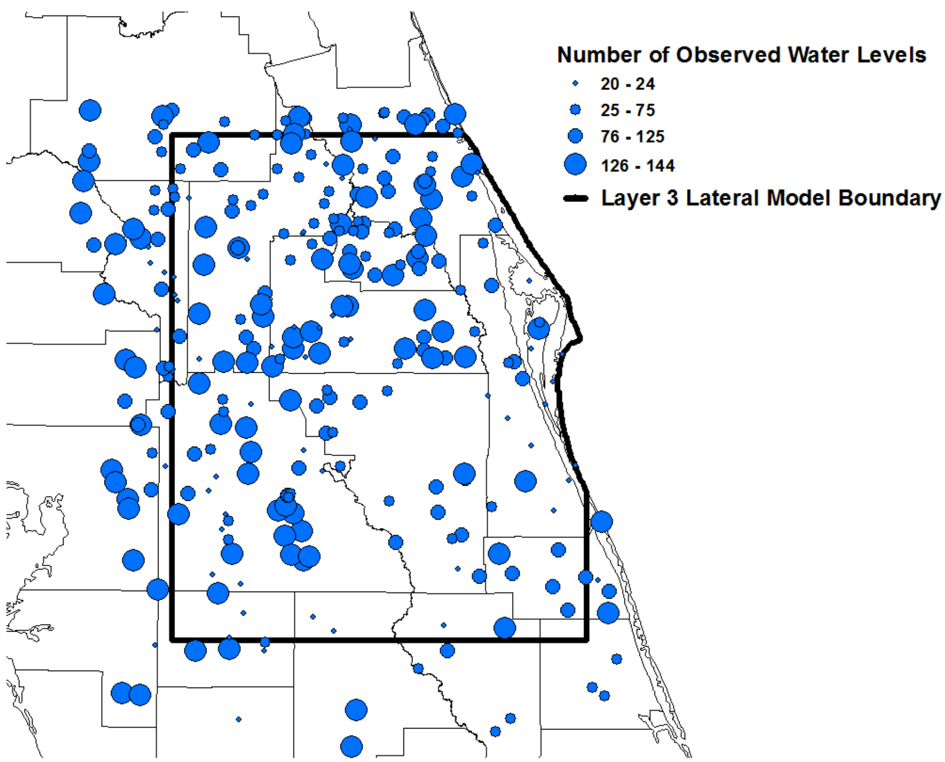

Figure 24. Layer 3 wells used to estimate the potentiometric surface.

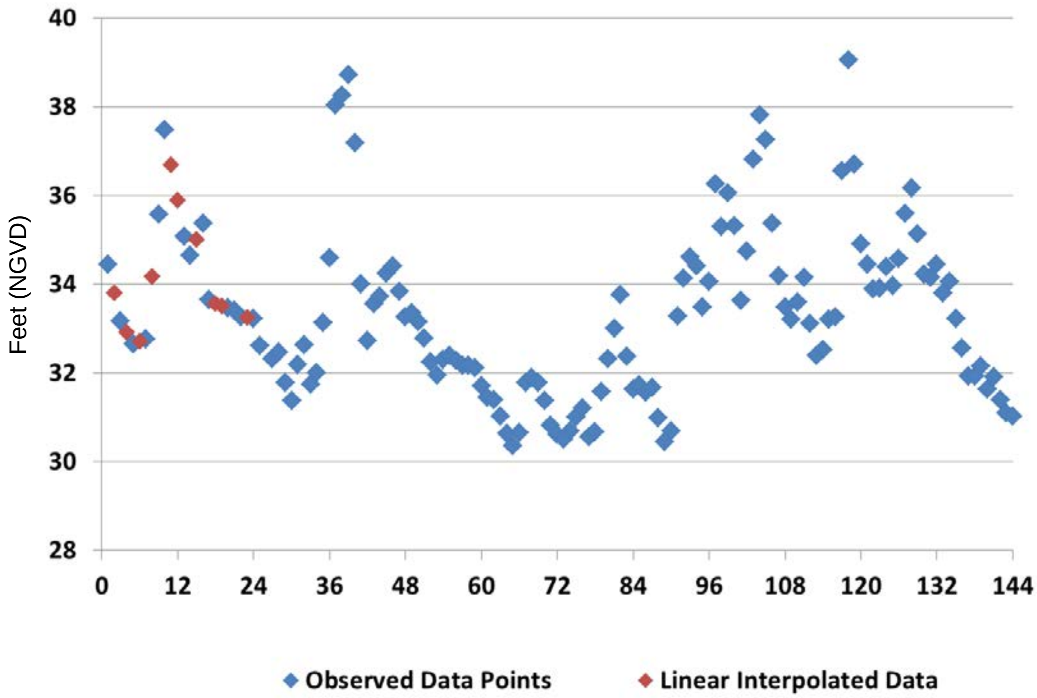

Figure 25. Linear interpolation technique (CE Dunnellon FLDN Well).

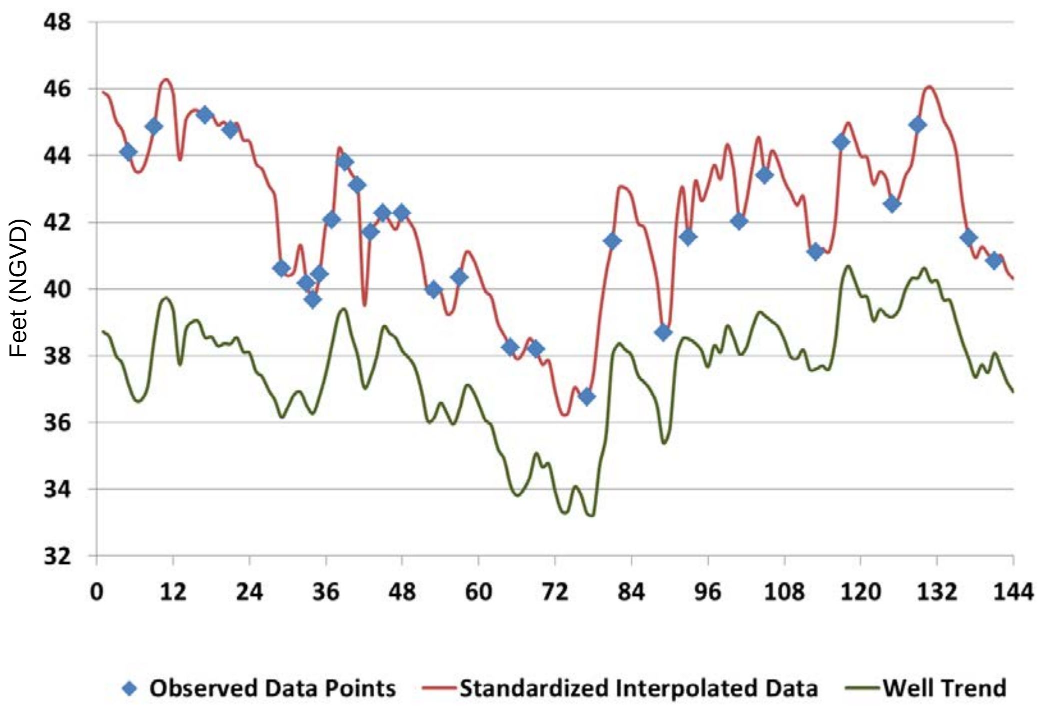

Figure 26. Standardized interpolation technique (Paul Shokley at Paisley Well).

Potentiometric Surface

Monthly potentiometric surfaces were created using a Python script developed in the Spatial Analyst Tools extension in ArcGIS using the splining interpolation method. The interpolation extended beyond the active model boundary to capture trends beyond the active model domain. The monthly value used for the lateral model boundary was selected as the value of the potentiometric surface located 1,250 feet from the center of the boundary cell in the direction outside the model grid perpendicular to the boundary (or 625 feet outside the model boundary) (**Figure 27**). For quality assurance, the generated May and September potentiometric surfaces were compared to the May and September potentiometric surfaces created by the USGS (**Figure 28**).

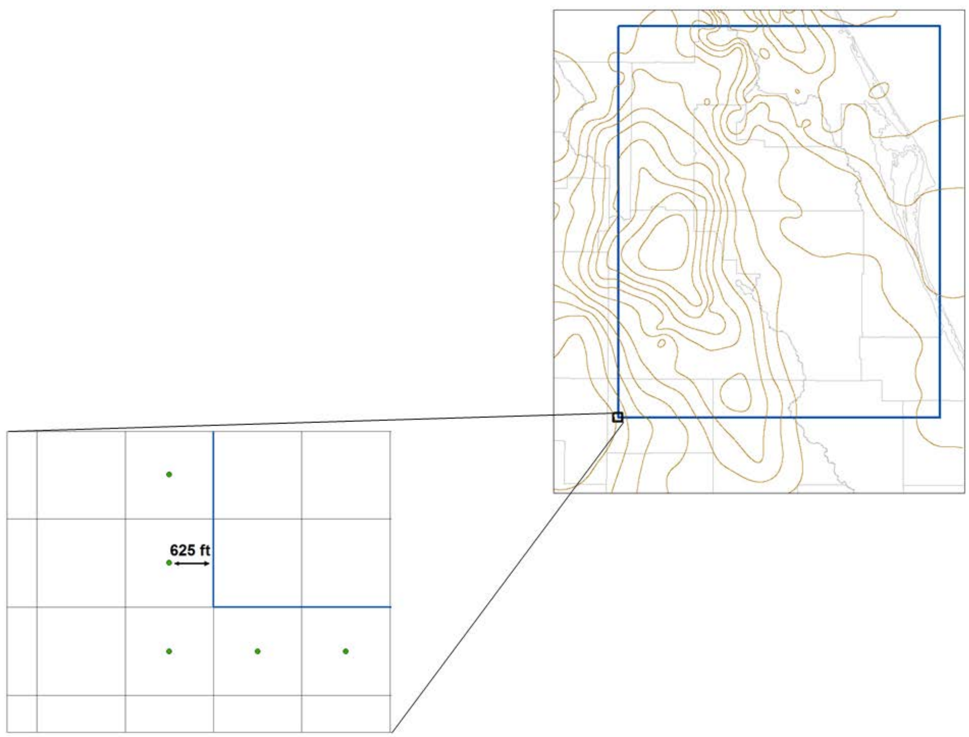

Figure 27. Distance of centroids from lateral model boundary used to create the Layer 3 monthly potentiometric surfaces

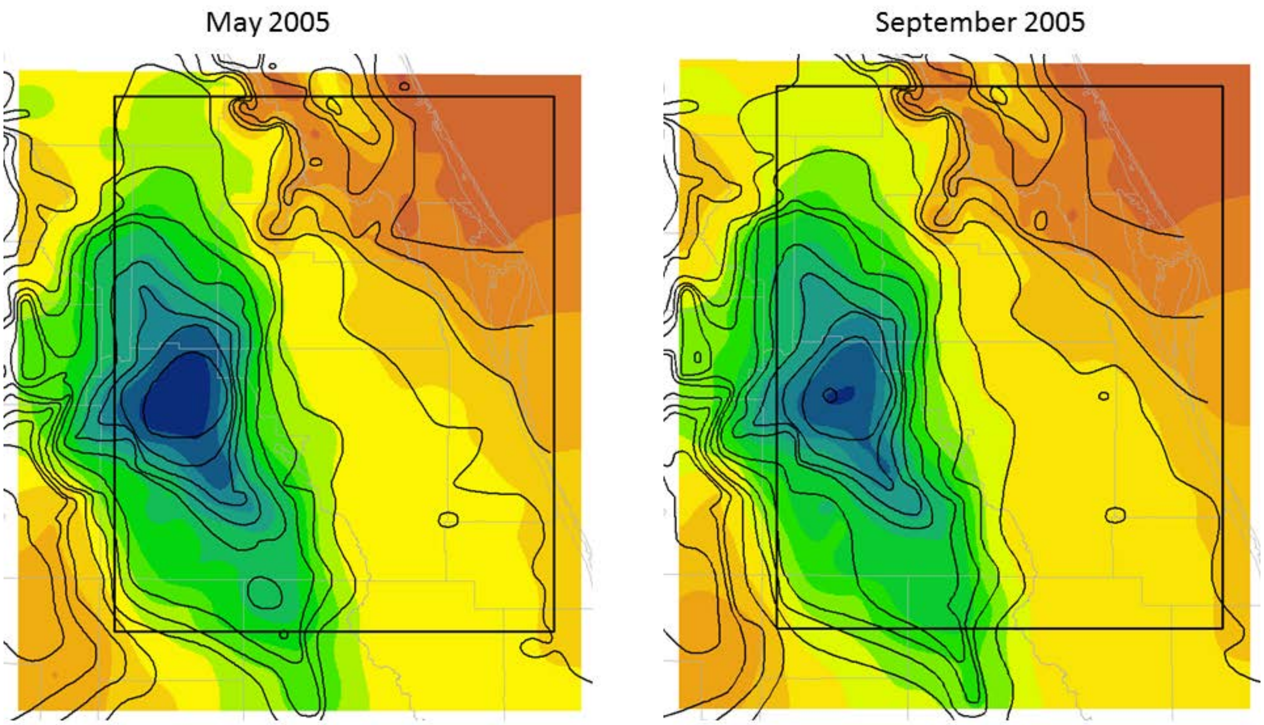

Figure 28. 2005 May/September comparison of HAT-generated potentiometric surfaces (color ramp) to USGS potentiometric surfaces (contour lines).

Estimation of Boundary Heads for Layer 5

Thirty-two wells (16 pairs) in Layers 3 and 5 were used to estimate the head differences between the two model layers. Only wells monitoring water levels in the Ocala permeable zone (Layer 3) and Avon Park permeable zone (Layer 5) were considered. Another consideration was the proximity of the Layer 5 well to the Layer 3 well. In order to compare head differences between layers, only Layer 5 wells in close proximity to a Layer 3 well were used as a paired well. Fourteen of the sixteen Layer 5 wells used were within a mile of a Layer 3 well. Paired wells outside the model domain were also identified and used to ensure trends beyond the active model area were captured and adequately characterized. The minimum data availability for inclusion was at least one observed value for every month during any given year for the paired wells. It was not necessary to infill missing data for the Layer 3 and 5 differences.

The Layer 3/Layer 5 differences were obtained by subtracting the observed water levels in Layer 5 from the observed water levels in Layer 3 for the same month and year. The average difference for each well pair for the 144 months of simulation was then calculated and contoured using the splining technique in ArcGIS to estimate the variability over the area. Though the differences varied along the model boundary, because these differences did not significantly change over time, the differences were held constant throughout the simulation period (**Figure 29**).

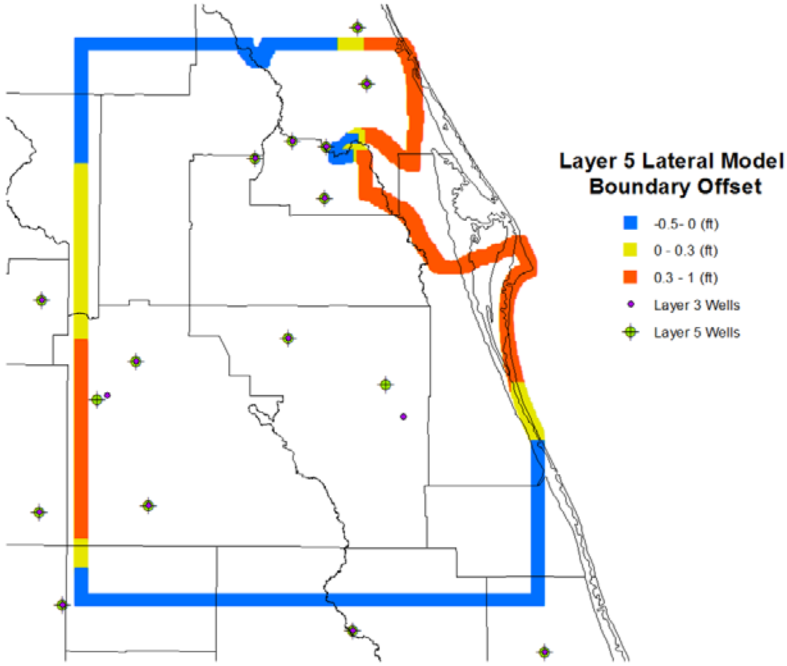

Figure 29. Lateral model boundary offset between Layers 3 and 5 and wells used to estimate the offset

Estimation of Boundary Heads for Layer 7

The process for selecting wells and obtaining differences between Layers 3 and 7 was the same as for determining differences between Layers 3 and 5. Forty wells were used to estimate the difference between the two layers. Only wells monitoring water levels in the Upper Floridan aquifer -- Ocala permeable zone (Layer 3) and the Lower Floridan aquifer (Layer 7) were considered. In order to compare head differences between layers, only Layer 7 wells in close proximity to a Layer 3 well were considered as a paired well. Fourteen of the twenty wells open to Layer 7 were within a mile of a Layer 3 well. Paired wells outside the model domain were also identified and used to ensure trends beyond the active model area were captured and adequately characterized. The minimum data availability for inclusion was at least one observed value for every month during any given year for the paired wells. It was not necessary to infill missing data for the Layer 3 and 7 wells.

The Layer 3/Layer 7 differences were created by subtracting the observed water levels in Layer 7 from the observed water levels in Layer 3. Though the differences varied along the model boundaries, the differences between Layers 3 and 7 did not significantly change over time and were held constant throughout the simulation period, with the exception of the southwest corner of the model. In this area, the fluctuation in Layer 3 was much greater than in Layer 7. As such, the average monthly difference was estimated using monitoring wells at the SWFWMD's ROMP 45.5 monitoring well site. An average value was obtained for each calendar month and applied throughout the simulation period. Differences between layers for the remaining well pairs were averaged over the 144-month simulation period. The averaged differences were then contoured to estimate the variability over the region (**Figure 30**).

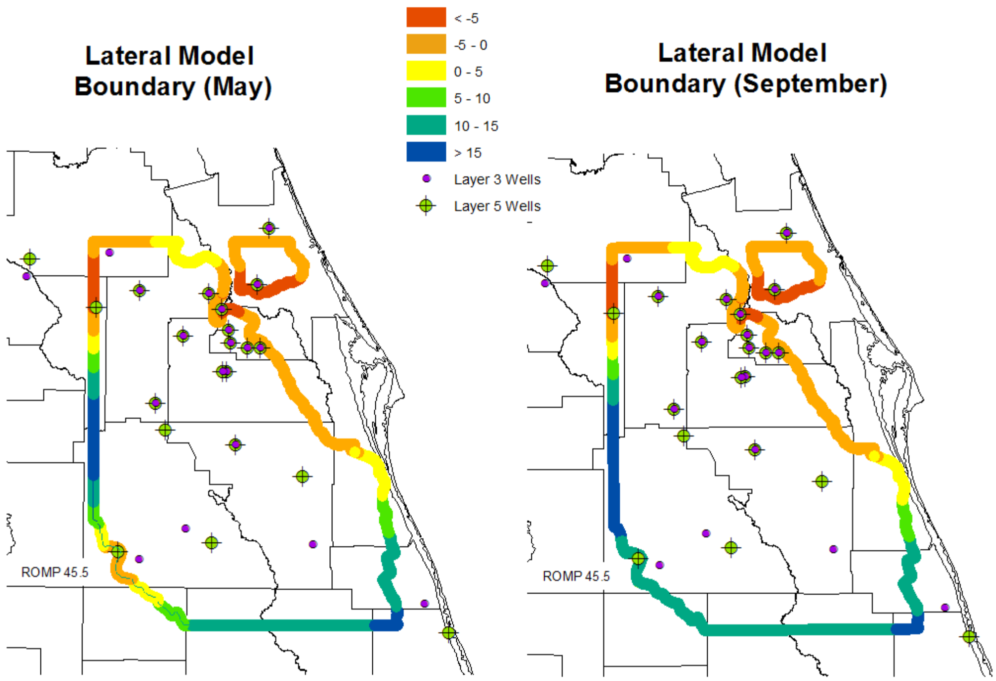

Figure 30. Lateral model boundary offset between Layers 3 and 7 and wells used to estimate the offset in feet.

Estimation of Boundary Heads for Layers 1, 2, 4 and 6

No changes were made to the GHB boundary heads in Layer 1. This was because the effects of annual changes in boundary conditions did not extend far into the model area largely due to the low permeabilities and high storativity of the aquifer. For the three confining layers in the model (Layers 2, 4, and 6) the boundary heads were linearly interpolated between the estimated heads for the two high producing layers vertically adjacent to the confining layer. Therefore, boundary heads for Layer 2 were linearly interpolated between heads in Layers 1 and 3; boundary heads for Layer 4 were linearly interpolated between heads in Layers 3, and 5; and for Layer 6, the boundary heads were linearly interpolated between Layers 5 and 7.

5

Model Data Set Construction, Time Variant Input Data Sets

IMPLEMENTATION OF PUBLIC WATER SUPPLY USES

Need for Normalized Public Water Supply Withdrawals

The interpretation of cause-and-effect relationships in groundwater modeling is easiest and clearest if the model can be used to test the effects of individual changes. When multiple causative factors are changed simultaneously, the influence of each factor on the results is often uncertain. For the withdrawal scenarios being considered in the CFWI process, it was possible to define a series of future long-term average withdrawal rates, each of which corresponded to a particular stage of projected population and urban development. For each such average condition, we were able to develop a series of monthly estimated PWS withdrawals to be represented in the model so that the month-to-month variations in withdrawals represent the response of PWS withdrawals to monthly weather patterns. These patterns of monthly variation in PWS withdrawals about a long-term average value were derived from the PWS calibration data, as described below. Once the method was developed, the consistency of variations in PWS pumpage was verified to confirm that there were consistent patterns of variations in PWS withdrawals across the region, and that these correlated with expected responses to weather (i.e., expected seasonal variations with higher withdrawal rates during dry years and lower withdrawal rates during wet years).

Calculating Public Water Supply Monthly Peaking Factors

To assess the effects of the future changes in groundwater withdrawals, we needed to compare the future modeled groundwater levels to a stable reference condition of withdrawals under the same weather conditions. Ideally, the reference condition should be similar to an observed historical condition to provide confidence that the reference condition potentiometric heads in the model are realistic. By using the same historical weather patterns to simulate a past historical condition and each future projected condition (represented by monthly rainfall and ET inputs to the model), we were able to capture the variable effects of weather on demands and groundwater responses, but avoided having weather as an inconsistent difference between the past and future simulations. For this purpose, the weather observations for the model calibration period of 1995 through 2006 were used as the standard weather variability to be applied. However, while the simulations of future conditions were each based on a single long-term average withdrawal estimate, the calibration period had a strong growth component in Public Water Supply instead of a stable constant long-term average. In order to compare the past condition and the future withdrawal scenarios directly, we needed to represent a past reference condition in the same way as the future conditions: a stable long-term average withdrawal that represented a stable level of population and development, with variation being driven only by weather effects. To create this Reference Condition, the year 2005 was used as the reference basis for population distribution and urban development. For this reference development condition, a corresponding long-term average groundwater withdrawal rate was calculated with monthly variations in withdrawals driven by weather conditions and groundwater withdrawal responses that were observed for 1995 through 2006. The steps to develop the long-term average reference condition groundwater withdrawal rate and the appropriate pattern of monthly variations are summarized below.

The steps to develop the Reference Condition pumpage were as follows:

(1) Linear regression was performed on the monthly pumpage for the 1995–2006 period to determine the trend in pumpage. For each PWS pumpage record, the following linear model was fitted:

$$Q = a + b\,T \qquad \text{(Eqn. 3)}$$

Where:

$a =$ A constant (the regression line intercept at a value of T = 0)

$b =$ The regression line gradient

$Q =$ The average daily PWS pumpage for each month (MGD)

$T =$ A time value representing the mid-point of each month (days from January 1, 1995)

(2) The monthly pumpage for the 1995–2006 period was detrended by normalizing with the trend line developed in Step 1. Each observed monthly pumpage was divided by the expected pumpage value for that month from the fitted trend line. The result was a monthly peaking factor series for the withdrawals during the 1995–2006 period:

$$\hat{Q}_i = a + b\,T_i \qquad \text{(Eqn. 4)}$$

Where:

$\hat{Q}_i =$ The expected value of the average daily PWS pumpage for month i (MGD)

$T_i =$ A time value representing the mid-point of month i (days from January 1, 1995)

$$PF_i = \frac{Q_i}{\hat{Q}_i} \qquad \text{(Eqn. 5)}$$

Where:

$PF_i =$ The observed monthly peaking factor for month i

$Q_i =$ The observed monthly pumpage for month i (MGD)

(3) The trend in average pumpage for the year 2005 was estimated for the midpoint of the year (July 2, 2005), using the monthly pumpage for the 1995–2006 as follows:

$$\hat{\hat{Q}}_{2005} = a + b\, T_{MP2005} \qquad \text{(Eqn. 6)}$$

Where:

$\hat{\hat{Q}}_{2005}$= The trend average pumpage for the year 2005

$T_{MP2005} =$ A time value representing the midpoint of the year 2005 (July 2, 2005) in days from January 1, 1995

(4) The monthly peaking factors developed in step 2 were multiplied by the 2005 average pumpage from step 3 to calculate the monthly reference condition pumpage for the whole 1995–2006 period as follows:

$$QRC_i = \bar{Q}_{2005} \times PF_i \qquad \text{(Eqn. 7)}$$

Where:

$QRC_i =$ The reference condition monthly pumpage for month i (MGD

Similarly, the monthly PWS pumpages for any other long-term average pumpage condition can be calculated by applying the monthly peaking factors to the long-term average pumpage rate as follows:

$$Q_{X,i} = \bar{Q}_X \times PF_i \qquad \text{(Eqn. 8)}$$

Where:

$Q_{X,i} =$ The monthly pumpage for some simulation condition "X" for month i (MGD)

$\bar{Q}_X =$ The long-term average pumpage for some simulation condition "X" (MGD)

The method described above was implemented on a wellfield level for larger utilities (total withdrawals greater than 1 MGD) and on a permit level for smaller utilities (total withdrawals less than 1 MGD).

Records Where the Fitted Trend Line Crosses the X-axis on a Date after January 1, 1995

There were some cases where a trend line fitted to the historical 1995–2006 data crossed the x-axis after 1995. This caused an abrupt, high-magnitude swing in the monthly peaking factors for the months on each side of the point where the trend line crossed the x-axis. The months where the value of the trend line value was close to zero would produce very high magnitude peaking factors because the observed flow was being divided by a trend line value close to zero. In addition, the peaking factor values prior to the point where the trend line crossed the x-axis would be negative (because the positive observed flow value was divided by a negative trend line flow value), while the peaking factor values after the point where the trend line crossed the x-axis would be positive (because the positive observed flow value was divided by a positive trend line flow value). These records were treated by breaking the record line into two segments and fitting a separate trend line to each segment of the record. This process is described further in the next section.

Records Containing Multiple, Distinct Trends

In some instances, a clear break in trend (a clear change of trend line gradient or a step change in the fitted trend line) caused large swings in the monthly peaking factor if a simple liner trend was fitted for the entire simulation period. Clear breaks in trend were identified using visual inspection and the trend lines in all these cases were modified to fit two or more separate trend lines on a piecewise basis (as shown in **Figure 31**). The trend average for the reference year (Step 3) was calculated using the equation of the trend line during the reference year (2005). For the example shown in **Figure 31**, the trend line was broken into two separate trend segments, the first from January 1995 through January 2004 and the second from February 2004 through December 2006, and the trend average 2005 pumpage was calculated for July 2, 2005 (Step 3 above) using the second trend line (February 2004–December 2006). The 2005 Reference Condition flows derived from this analysis of two trend line segments are shown in **Figure 32**.

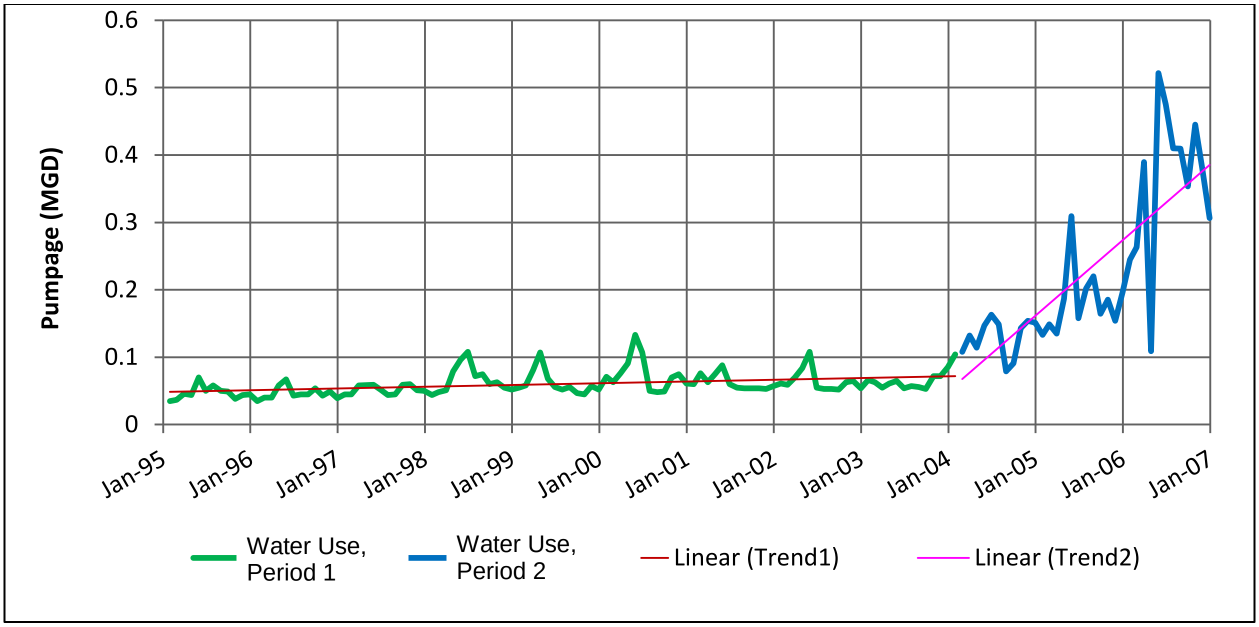

Figure 31. Example of trend line segments fitted to water use trends.

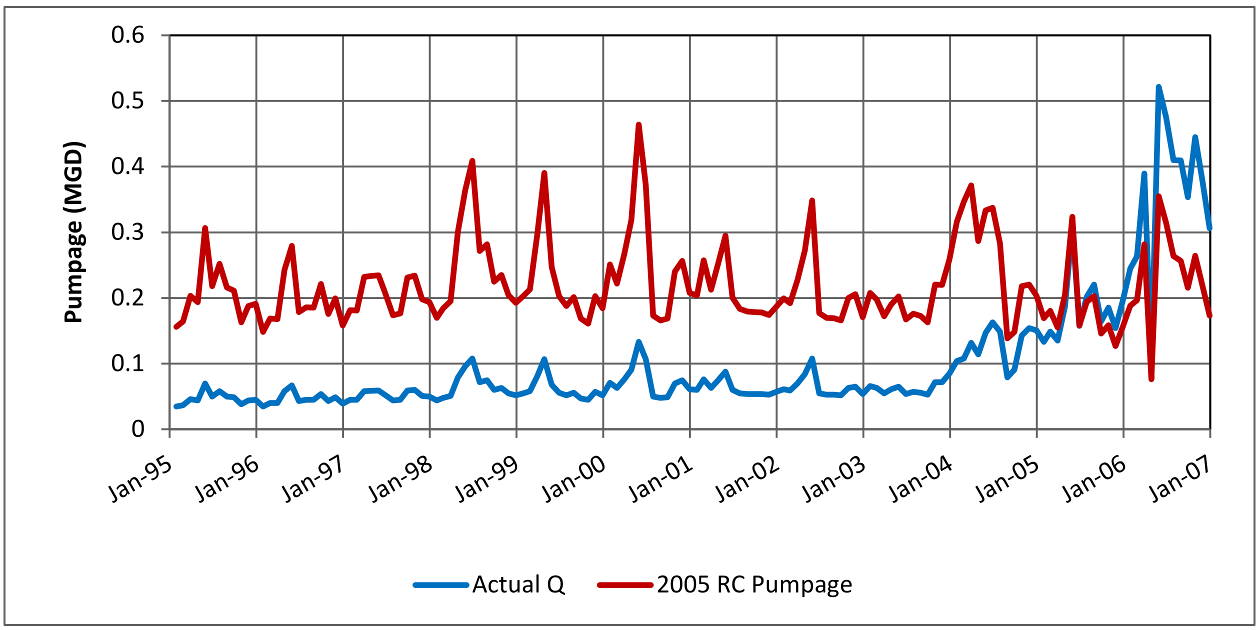

Figure 32. Reference condition flows for permitted pumpage shown in **Figure 31**.

Simulation of Wellfields Without Historical Data

There were cases when a permit had no recorded pumpage for some years, either due to missing data or because the wellfield was activated sometime during the calibration period. Due to a lack of data, a monthly peaking factor could not be developed for those months with no data, as shown in **Figure 33** for January 1995 to November 1999. All the cases that had missing pumpage or no pumpage during the calibration period were for utilities with less than 1.0 MGD of average pumpage, so their contribution to the total PWS impacts were small. However, even when the wellfield did not exist for a portion of the calibration period, monthly peaking factors were necessary to develop withdrawal series for the Reference Condition and the future simulations.

To develop monthly peaking factors for the missing months, average peaking factors were developed for the 144 stress periods for all utilities that had average pumpage of less than 1.0 MGD. These average peaking factors were developed by calculating the average combined peaking factor for each month of the simulation period. The monthly peaking factors for the individual permits with missing data were calculated using the available data. For the months where data was missing or where there was no historical pumpage, the average peaking factor for utilities less than 1.0 MGD was multiplied by the average monthly peaking factor for that utility to estimate the missing monthly peaking factors. This seemed to be the best approach to avoid a step change in the peaking factors for small utilities. An example of this approach is shown in **Figure 33**.

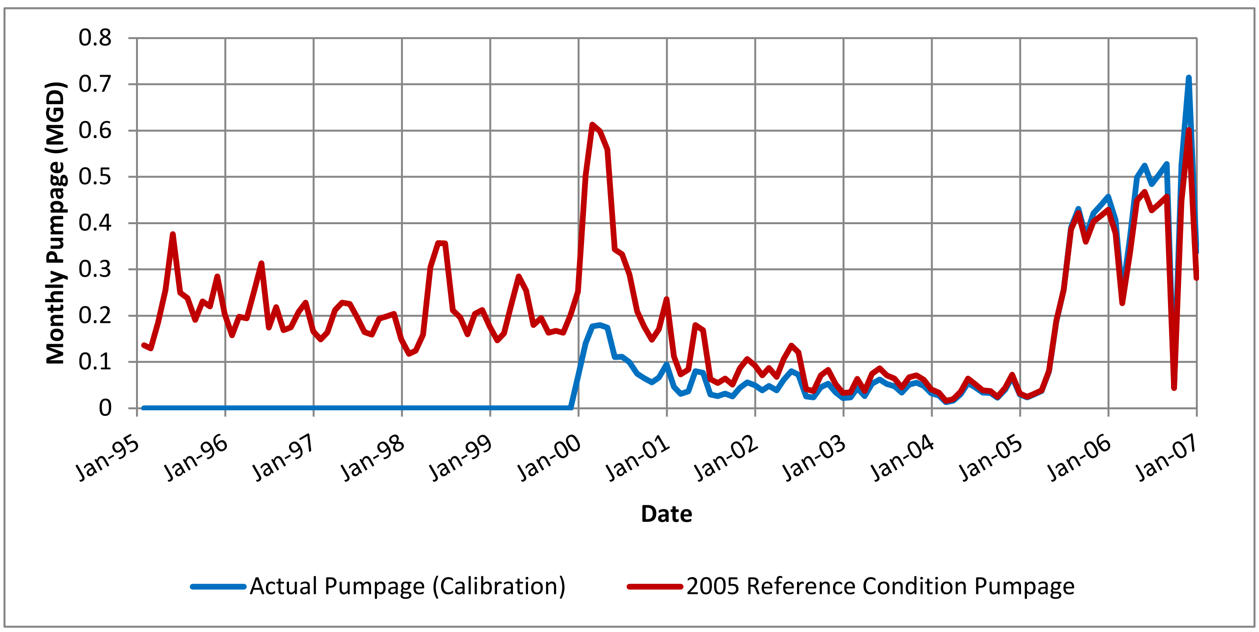

Figure 33. Example showing permitted pumpage with no data for a portion of the simulation period and the results of estimating pumpage for the Reference Condition based on other permits/withdrawals.

Simulation of Wellfields without Flows in 2005

For smaller utilities, there were some cases with no pumpage in 2005, but there may have been pumpage prior to or after 2005. To accurately represent the actual 2005 conditions, the Reference Condition pumpage for these cases was set to zero for the entire period of record (1995–2006), as shown in **Figure 34**.

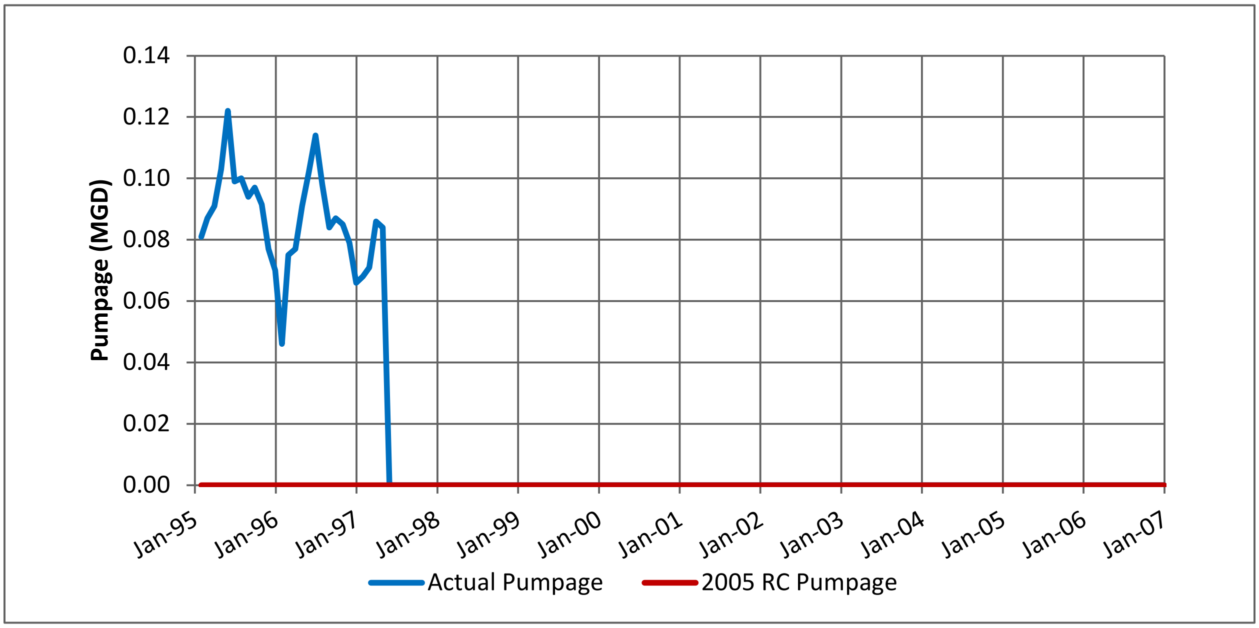

Figure 34. Example of permitted pumpage with no withdrawals during the reference year (2005) and adjustment to no pumpage for the Reference Condition.

Individual Utility Well/Wellfield Withdrawal Distribution

For the larger utilities, where information was available on individual wellfields, the actual pumpages for a WUP/CUP were further parsed out to develop individual pumpage time series for each wellfield. The monthly pumpages for the individual wellfields were used to determine the monthly peaking factor series for the individual wellfield for the period 1995-2006. Where data were sufficient to support it, the trend average pumpage for year 2005 was calculated for each individual well of the wellfield. The 2005 Reference Condition pumpage for each well was then estimated as a product of the monthly peaking factor for the wellfield and the 2005 trend average of a particular well.

Smaller utilities may not have multiple wellfields, or in some cases information was not readily available to assign their pumpages to individual wells or wellfields. For such utilities, the methods presented above were applied at the highest level of detail that could be supported by the available data. In some cases, this resulted in a monthly withdrawal pumpage for the utility being distributed evenly across all wells owned by the utility

Confirmation of Consistent Weather-Driven Variations in PWS Withdrawals

If our hypothesis about weather-driven PWS withdrawal variations is correct, we would expect the peaking factor series for all PWS withdrawals to look broadly similar because the region shows broadly consistent monthly variations in rainfall and ET. There is some significant local variation in monthly rainfall and ET estimates across the model grid (especially for rainfall), but this local variability can be viewed as local noise superimposed on top of a consistent regional signal of wetter and drier years. The effect of the local noise in weather patterns would be expressed in relatively small differences in the shape of the peaking factor series from one utility to another.

There is another difference between peaking factor series for different utilities that is driven by the percentage of Public Water Supply used for irrigation. Indoor uses of Public Water Supply are relatively consistent; they may show some seasonal variation but are not very sensitive to weather variations. As a result, we would expect that different Public Water Supply utilities would show similar shapes in their weather-driven pumpage peaking factors, but that the amplitudes of the peaking factor series would vary with the percentage of each utility's water that is used for indoor uses. The lower the percentage of indoor use, the higher the percentage of use that is subject to weather-driven variations outdoors, and therefore the higher the amplitude of the peaking factor series. We would anticipate that this effect could be largely filtered out by performing another normalization: by definition, the peaking factor series represents a series of variations about a mean value of 1 for all utilities. We can develop a standardized peaking factor shape series if we subtract the mean and divide by the standard deviation of the peaking factors:

$$SPF_i = \frac{PF_i - 1}{\sigma_{PF}} \qquad \text{(Eqn. 9)}$$

Where:

SPF_i = Standardized peaking factor for month i

σ_{PF} = Standard deviation of observed peaking factors

The resulting series of standardized peaking factors is shown in **Figure 35**. The variation of standardized peaking factors is very consistent for the larger utilities, but noisier for the small utilities. This probably reflects the fact that by serving a smaller population, the pumpages for smaller utilities are more vulnerable to very localized variations in rainfall patterns than those of larger, more geographically dispersed utilities. Smaller utilities are also more affected by the demand patterns of individual "extreme" users and more vulnerable to measurement errors at individual meters. **Figure 35** confirms that the PWS withdrawals show very consistent behavior for most of the larger PWS utilities, and as expected, withdrawals are higher in dry years and lower in wet years. This confirms that it is generally reasonable to use the peaking factor series for each utility as a template to calculate a representative series of monthly withdrawals for different total withdrawal quantities (i.e., for different model scenarios). This also confirms that it is generally reasonable to use an average value of the peaking factor series for each month from comparable PWS utilities to fill in months with missing data (e.g., for cases where a utility started operations part way through the calibration period – see the **Simulation of Wellfields Without Historical Data** section).

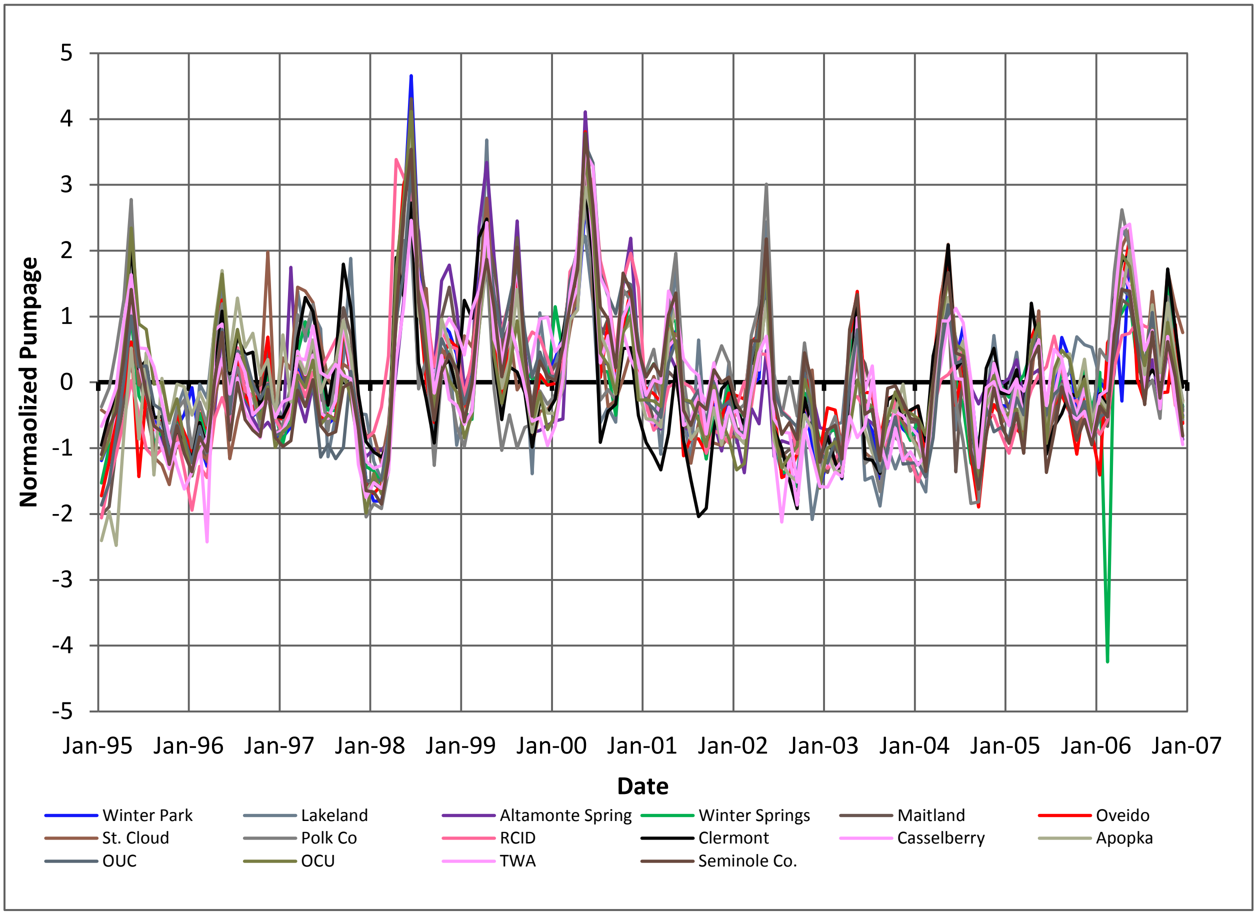

Figure 35. Normalized pumpage for large utilities (excluding outliers).

2005 Reference Condition PWS Withdrawals

The monthly withdrawal values for the 2005 Reference Condition were calculated by applying the monthly peaking factor series for each wellfield/utility to the trend average pumpage for the year 2005 ($\hat{\hat{Q}}_{2005}$), as shown in Equation 7 above.

Restrictions Imposed on Wellfields that Exceed Existing Permitted Demands

For the 2015, 2025, and 2035 scenarios, no constraints were imposed on the monthly PWS groundwater withdrawals. It was assumed for these simulations that they were to represent a "worst case" condition: what would happen if PWS groundwater withdrawals were driven solely by the PWS utilities' operational requirements for water.

For the End-of-Permit (EOP) scenario, PWS groundwater withdrawals were assumed to be maximized subject to the constraints of the PWS permits. The monthly groundwater demands were developed by using the long-term average permitted groundwater allocation as long-term average pumpage ($\overline{Q}_X$) in Equation 8. In months where this yielded groundwater withdrawals that would have exceeded permitted monthly maximum flow limits, or permitted annual and/or moving average flow limits, the groundwater withdrawals were reduced to comply with the permit requirements. This simulation assumed that where the available groundwater withdrawals were insufficient for normal utility operating requirements, the utility would adjust its operations to constrain demand so that they did not exceed the permitted supply or would satisfy the excess demand from alternative water sources.

Utilities with Surface Water and Groundwater Withdrawal Facilities

Some utilities have both surface water and groundwater withdrawal facilities currently permitted. The total water projections in the RWSP represent the sum of these water allocations. However, the ECFT model is not an integrated surface water/groundwater model and is not suitable for simulating the details of surface water flow systems. Because the surface water withdrawals have no material impact on groundwater levels and cannot be adequately represented in the ECFT model, only groundwater withdrawals were included as inputs to the ECFT model. This resulted in a difference between the sum of Public Water Supply withdrawals represented in the ECFT model and Public Water Supply withdrawals tabulated in the RWSP.

Distribution of Demands for Wells that Penetrate Multiple Model Layers

Production wells with open-hole sections that penetrate multiple model layers were examined. The affected wells were divided into two categories:

1. Wells where the straddling of layers was thought to be real

2. Wells where the straddling of layers was thought to be an artifact of the layer definition interpolation methods that were used to convert layer definitions at points with lithologic logs into cell-by-cell definitions across the model domain

For wells in the first category, the withdrawal at the affected well location was split between the contributing layers in proportion to the transmissivities of the contributing layers.

For wells in the second category, the apparent straddling of layers was overridden and the wells' withdrawals were assigned completely to the model layer within which the open-hole section of the well was thought to be contained.

IMPLEMENTATION OF AGRICULTURAL WATER USE

Agricultural demands for future scenarios were prepared using the EOP model run as the basis for adjusting quantities for the future withdrawal conditions. Using the EOP Condition as a basis ensured the most updated list of permitted wells was used and that the spatial distribution of withdrawals was consistent among the different future scenarios.

The permitting approach for the agricultural use class used by each WMD differs, and therefore the associated data in their respective databases upon which the most appropriate means of simulating these demands differs as well. Parts of this section describe agricultural use estimates for each WMD as applied in the HAT-ECFT simulations.

AFSIRS Model

General Description

The Agricultural Field-Scale Irrigation Requirements Simulation (AFSIRS) model was developed for Florida's water management districts by the University of Florida Institute of Food and Agricultural Sciences (IFAS) to provide a method to determine agricultural water use allocations for consumptive use permitting programs. The model estimates irrigation requirements for Florida crops, soils, irrigation systems, and climate conditions. The irrigation requirement for crop production is the amount of water, exclusive of precipitation, that should be applied to meet a crop's supplemental demand requirements without a significant reduction in yield.

The AFSIRS model is based on a water budget of the crop root zone and the concept that crop ET can be estimated from potential ET and crop water use coefficients. The water budget includes inputs to the crop root zone from rain and irrigation, and losses from the root zone by drainage and ET. The water storage capacity in the crop root zone is defined as the product of the water-holding capacity of the soil and the depth of the effective root zone for the crop being grown. Daily ET for each crop is calculated as the product of potential ET and the crop water use coefficient for that day. Irrigation is scheduled based on an allowable level of soil water depletion from the crop root zone. This level of simulation model development produces a functional model that could address the wide variety of crops, soils, and irrigation systems typical of Florida and include variations in daily rainfall and ET rates needed for a transient model simulation.

The model was last revised in 1990 and the user's guide (SJ2008-SP16; Smajstrla [1990]) and technical manual (SJ2008-SP17; Smajstrla [1990]) were created at that time.

The SJRWMD developed a modified version of the AFSIRS code to estimate the irrigation demand for crops grown in the region of the ECFT groundwater model during the model's calibration period (1995–2006). The estimates of irrigation were then incorporated in the groundwater model as land applied irrigation and withdrawals from the aquifer system. AFSIRS is a FORTRAN based computer program that runs with basic text file input for all required inputs. Input tables were developed by using GIS and overlaying the data layers to identify the necessary input components for each irrigated polygon. For this application of AFSIRS, the climate data were changed to better represent the information used in the groundwater model. The climate was changed by replacing the 30-year record with a single year in the calibration and then repeated for each subsequent year until all years in the calibration were run. This forced AFSIRS to return the best estimate of actual irrigation for each month in the specified year run through the model.

Reference Crop and Crop Coefficients

Reference crops were used to develop the water demands for various crops grown in Florida. Daily ET for each crop was calculated as the multiple of reference ET and the crop water use coefficient (Kc) for that day. These Kc values varied with the growth stage of the crop. Crop water use coefficients were obtained from the literature and revised by IFAS for bahiagrass, citrus, and sod. Three separate sets of Kc values were examined in this study and included in the AFSIRS updates used for this project.

SFWMD

The SFWMD generally uses a version of the SCS Blaney-Criddle method (SFWMD, 2013) to determine permitted irrigation demands within its boundaries. However, historical irrigation pumpage records are rare in the SFWMD because most irrigation users were not required to submit actual withdrawal data during the model simulation period of 1995 through 2006. Therefore, AFSIRS was needed as a secondary method to estimate the transient irrigation demands for a specific user. The SFWMD-modeled irrigated acreages were based upon individual permitted acreages with the demands placed at the permitted withdrawal facilities and not generated from a GIS-based approach. These demands were then increased or decreased on a crop type and county-by-county basis depending upon the scenario (e.g., 2015, 2025, 2035, EOP) within the CFWI area of the model and the demand estimates provided by the RWSP Team.

All individual and general irrigation permits issued within the SFWMD portion of the model domain (**Figure 36**) were reviewed. Information obtained from the permits included crop type or types, irrigation method and irrigated acreage for each crop, date when the crop was first planted, irrigation source, and irrigation withdrawal facilities. The permitted average annual allocations were also collected and divided accordingly by source if the user had multiple sources to meet the irrigation demands. The date the withdrawal facilities became, or were estimated to become, operational was also included. For those users that changed sources to reuse during the simulation period, the estimated date and the percentage of the overall demand the reuse would provide for meeting the crop demands were also obtained.

Individual demands were calculated on a crop-by-crop basis and aggregated up to a monthly irrigation demand for each permit. The amount of rainfall and ET at a permit location was also determined at a sub-county basis. The one exception to this method was pasture irrigation, which was not included for most of the area except those permits specifically identified as improved pasture. The amount of pasture simulated in the SFWMD area of the model is extremely small compared to the overall demands within the SFWMD portion of the CFWI Planning Area.

Aquaculture and livestock demands were also included but handled differently. Together, these users account for a minor fraction of the overall demand and were assigned their permitted allocation applied equally throughout the simulation period. Unimproved pasture areas can cover large percentages of some counties in the SFWMD portion of the study area. Unimproved pasture areas are associated with the livestock watering demands and the demand was calculated by multiplying the estimated number of livestock on the property by a gallon per day per livestock value with the assumption that the unimproved pasture is not irrigated unless specifically identified.

The well casing and total depth were also obtained for each groundwater withdrawal facility. The demand was placed into the model in the aquifer with the thickest penetration. For instance, a well that had 100 feet of the screened interval in the UFA (Layer 3) and 20 feet in the APPZ (Layer 5) was assigned to the UFA. Users that fulfill their irrigation needs from on-site lakes and do not have an open connection to the SFWMD regional canal system were assigned to the SAS (Layer 1) unless the lake was lined. Surface water users with surface water facilities on or that indirectly use the SFWMD canal systems or the Upper Kissimmee Chain of Lakes were not included in the data set. Withdrawals were distributed equally between individual facilities to meet the total demand of a permit unless additional information was available to allow for a more specific distribution.

As stated previously, calculations of crop demands were determined from AFSIRS. Specifically, demands were calculated at several sites within each county using a dominant soil type consistent with that location. Calculations were then done for a single acre for all crops projected for that county using a 100 percent efficient irrigation system. Irrigation demands were then generated on a daily basis for the 12-year simulation period using the historical daily ET and rainfall rates. Demands per permit were then calculated daily by multiplying the AFSIRS-generated irrigation requirement for each crop by the number of acres and the irrigation efficiency identified in each individual permit. The resulting demands were then rolled up into monthly values and adjusted by a fraction to approximate the RWSP Team's crop, county, and District breakout projections for any simulation.

Special attention was paid to those users that had complex irrigation practices. For instance, Adams Ranch in southern Osceola County uses surface water from Lake Marian and groundwater from the UFA. Most of the property is irrigated from the lake but a small section is irrigated strictly from wells. For that smaller area, monthly irrigation demands were calculated for each month of the simulation. However, for the larger area that uses the lake, irrigation demands were not included in the model except when the stage of Lake Marian fell below the level that requires termination of lake withdrawals. For those periods, the UFA wells were used to irrigate the entire property. Several other users had similar issues that were addressed on an individual basis.

The final demands developed for the SFWMD by irrigation use type and county are provided in **Table 8.** The table allows for a comparison of the simulated irrigation demands and the amount identified by the RWSP for the future simulations.

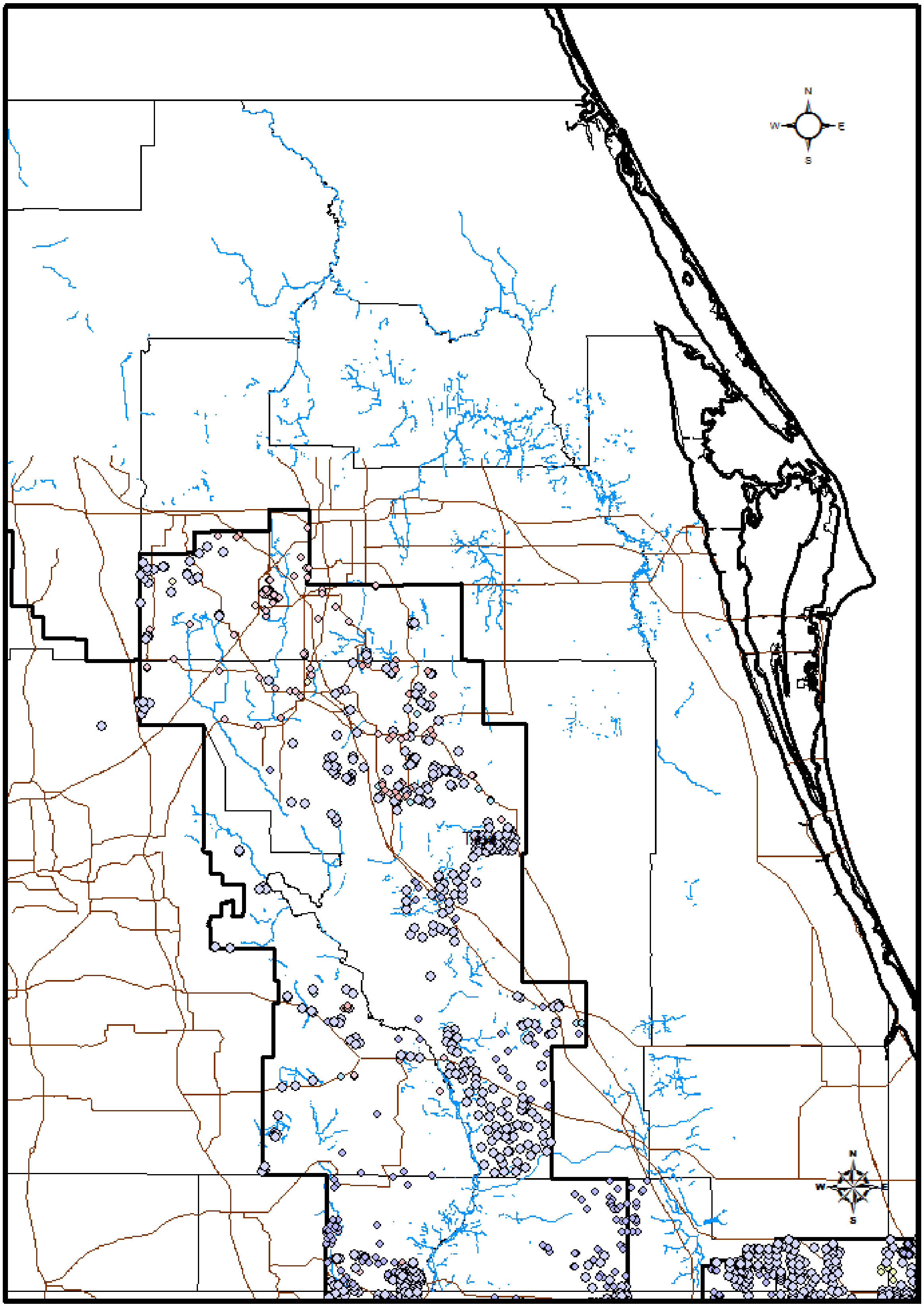

Figure 36. Agricultural well withdrawal locations within the SFWMD.

Table 8. Simulated Irrigation withdrawals (in MGD) by county and type within the SFWMD.

County	Type	2005 Model	2015 Plan	2015 Model	2025 Plan	2025 Model	2035 Plan	2035 Model	EOP Model
Orange	Landscape	8.03	6.99	6.99	9.71	9.71	14.61	14.61	13.50
Orange	Agriculture	1.49	4.51	4.51	3.17	3.17	1.84	1.84	1.97
Osceola	Landscape	5.18	3.04	3.04	4.94	4.94	6.02	6.02	6.07
Osceola	Agriculture	33.62	46.14	46.14	44.30	44.33	42.46	42.50	80.79
Polk	Landscape	1.95	0.58	0.58	0.89	0.89	1.30	1.30	0.98
Polk	Agriculture	2.38	8.11	8.11	7.61	7.61	7.10	7.10	4.57
Highlands	Irrigation	12.66	NA	12.92	NA	13.19	NA	13.46	13.46
Okeechobee	Irrigation	25.43	NA	25.59	NA	25.75	NA	25.90	25.90
St. Lucie	Irrigation	17.96	NA	17.96	NA	17.96	NA	17.96	17.96

Notes:
1) The modeled demands are the average annual withdrawal for the 12-year simulation period in million gallons per day (MGD).
2) Landscaping includes both landscaping and golf course uses that do not utilize reuse.
3) Livestock, aquaculture, and improved pasture demands are not included in the table for Orange, Osceola, and Polk Counties.
4) Highlands, Okeechobee, and St. Lucie Counties are the sum of all irrigation type uses.
5) Demands are for groundwater withdrawals and surface water withdrawals that only use on-site isolated lakes.

SJRWMD

Land Use-based Crop Demand Calculations

The SJRWMD developed a GIS database of locations of agricultural projects within its borders that use irrigation from land use and permit information for 1995, 2000, and 2005. The data were used to define the irrigated portion of agricultural lands. Soil data from the Natural Resources Conservation Services' Soil Survey Geographic (SSURGO) database available for the region. SJRWMD incorporated radar-detected rainfall and satellite (GOES ET) climate data into the calibration of the groundwater model.

Benchmark Farms Adjustments

After initial tests of the groundwater model, it was determined that the AFSIRS model was delivering more water than could be substantiated by the observation data. Additional checks showed that the water developed was more than was indicated by the limited metering data available for the area. Therefore, the model was further altered to return results more consistent with the available agricultural metering data from the SJRMWD's Benchmark Farms (BMF) program. This adjustment was accomplished by creating a ratio of average BMF application rates to the AFSIRS calculated rates for each month in the simulation for every available crop in the BMF database. The resulting revised rates were then incorporated into the groundwater on a monthly basis for the 144 months in the model calibration as land-applied irrigation and groundwater withdrawals.

Withdrawal Facilities (Centroid Based)

When the water use data set for the calibration of the groundwater model was developed, permitted wells were not associated with the areas where they provided irrigation water. To meet the schedule for the model development, the SJRWMD used the irrigated parcels as a surrogate for location of actual locations. In every grid cell that intersected an irrigated parcel, a well was placed at the cell's centroid and the estimated quantity was applied for the portion of the area associated with the particular cell. This created an easy way to estimate the water use and determine a withdrawal location.

SWFWMD

Since the early 1990s, the SWFWMD has compiled estimates of monthly water use on a permit and well basis. The basis for these estimates is metered withdrawal data that is reported to the SWFWMD. For permits and withdrawals without metered data, estimates are made based on reported pumping amounts for similar uses and quantities withdrawn. Currently, points for withdrawals permitted for 100,000 gallons per day (gpd) or more are required to be metered if they are in an area that has been designated as a Water Use Caution Area (WUCA). In 2011, metered withdrawals in the SWFWMD portion of Polk County accounted for about 72 percent of total withdrawals and 52 percent of total agricultural withdrawals. Locations for all withdrawal points are as reported by permittees and in some cases separately verified by SWFWMD staff. Model layer assignments for individual wells were made by correlating model layers with permitted casing and total well depths and assigning the well to the deepest model layer penetrated. Monthly quantities for individual withdrawal points within the SWFMWD are currently available for 1992 to 2011.

Reference Condition

More than 90 percent of agricultural withdrawals in the SWFWMD portion of the model are for citrus irrigation, so this was the focus for developing withdrawals for the Reference Condition. The process to estimate withdrawal quantities for citrus was developed at a countywide level and then applied to individual permits. The process was as follows:

1. Countywide citrus acreage totals (**Table 9**) were obtained for each year of the 12-year simulation from the Florida Agricultural Statistics Service (FASS).
2. Monthly irrigation application rates (**Table 10**) were calculated by dividing the estimated countywide citrus acreage by the monthly citrus withdrawal quantity
3. Countywide monthly multipliers (**Table 11**) were calculated by dividing the monthly irrigation application rate for a particular month/year of the simulation by the monthly application rate for the corresponding month of the reference year
4. Monthly withdrawal amounts for individual water use permits (WUPs)/wells were calculated as the product of the countywide monthly multiplier and the well withdrawal amount for the corresponding month of the reference year

Remaining agricultural withdrawals were included in the Reference Condition simulation at the same rates as used for the calibration period.

Table 9. Citrus acres obtained from FASS for the SWFWMD portion of Polk County (estimated as 91 percent of total acres reported for the county; acreage data in bold were interpolated from preceding and subsequent years).

Year	Acres
1994	100,827
1995	**100,767**
1996	100,708
1997	**99,543**
1998	98,379
1999	**98,380**
2000	98,381
2001	**97,760**
2002	97,138
2003	**94,641**
2004	92,144
2005	**87,950**
2006	83,756

Table 10. Monthly application rates for citrus irrigation for the 2005 reference year (inches per year per acre) in the SWFWMD portion of Polk County.

Month	Application Rate (in/yr/acre)
Jan	1.0
Feb	1.1
Mar	0.5
Apr	1.0
May	1.1
Jun	0.4
Jul	0.1
Aug	0.2
Sep	0.6
Oct	0.4
Nov	0.5
Dec	0.4
Total	7.3

Table 11. Monthly factor used to obtain monthly withdrawals for citrus in the SWFWMD portion of Polk County used in the Reference Condition (factor was multiplied by monthly pumping for 2005 to get pumping for the corresponding month of the specified year)

	1995	1996	1997	1998	1999	2000	2001	2002	2003	2004	2005	2006
Jan	0.3	0.9	1.5	0.1	1.0	1.3	2.7	2.0	1.5	0.8	1.0	0.9
Feb	0.9	1.6	1.2	0.1	1.3	1.2	1.6	1.3	0.7	0.5	1.0	0.9
Mar	1.6	1.7	3.0	0.6	4.1	3.7	3.0	3.3	1.1	2.2	1.0	3.4
Apr	1.4	1.3	1.5	2.1	3.0	2.3	1.9	2.3	1.3	1.9	1.0	2.2
May	2.2	1.4	1.2	2.3	1.6	2.7	2.1	2.4	1.3	1.9	1.0	1.9
Jun	1.9	1.8	2.5	8.3	1.9	5.8	3.2	2.9	1.6	4.0	1.0	3.5
Jul	5.5	8.4	4.4	10.0	6.3	4.2	3.0	4.1	3.7	6.1	1.0	4.3
Aug	1.3	4.0	3.6	4.2	2.2	2.0	2.3	1.8	0.9	0.9	1.0	2.7
Sep	0.6	1.4	2.7	0.7	1.2	0.7	0.5	0.7	0.9	0.1	1.0	0.7
Oct	0.7	2.1	3.8	3.7	0.7	3.5	1.5	2.3	2.3	0.9	1.0	3.0
Nov	1.6	3.4	0.7	2.9	2.4	3.7	2.6	2.0	1.9	2.3	1.0	3.0
Dec	4.1	2.8	0.4	3.1	2.8	4.4	3.3	1.1	2.9	1.7	1.0	2.3

End-of-Permit Scenario

In preparing agricultural water use in the SWFWMD for the EOP scenario, it was necessary to identify all currently active water use permits and withdrawal points. This was accomplished by comparing WUPs included in the Reference Condition (2005) scenario to a list of active WUPs as of December 31, 2012. Permits no longer active were deleted from the data set and permits issued since 2005 were added. The resulting list of permits and withdrawal points provided the basis for the EOP scenario, which in turn provided the basis for the future scenarios. The temporal variation in pumping for permits not included in the 2005 scenario was based on the average countywide temporal variation observed for the Reference Condition.

Though each of the districts have a different basis for permitting irrigation uses (i.e., quantities associated with a 1-in-10, 2-in-10, or 5-in-10 rainfall event), it was decided that for the EOP scenario, average agricultural demands over the 12-year simulation period would be prepared to reflect average conditions or demands based on a 5-in-10 rainfall. Annual average demands would then be compared to individual permitting criteria for the individual districts and reduced when the permitting criteria were exceeded. For example, in the SWFWMD, monthly estimates were compared to permitted peak month quantities and reduced when those values were exceeded. Additionally, the 12-month average withdrawal amounts were reduced when these quantities exceeded the 1-in-10 use in the SFWMD, and the 2 in 10 use in the SJRWMD and SWFWMD.

2015, 2025, and 2035 Withdrawal Conditions

Agricultural quantities associated with future withdrawal condition scenarios were calculated using countywide multipliers. The multipliers were calculated on a countywide basis as the ratio of average annual withdrawals over the 12-year simulation period for the specified withdrawal condition (e.g., 2015, 2025, or 2035) to the EOP values. Each withdrawal in the EOP simulation was multiplied by this ratio to yield the agricultural withdrawals for the specified withdrawal condition scenario. Withdrawal amounts for counties within the CFWI were obtained from the CFWI RWSP and for counties outside the CFWI, withdrawal quantities were obtained from the SWFMWD's RWSP documents.

IMPLEMENTATION OF LANDSCAPE / RECREATION / AESTHETIC (GOLF COURSE) WATER USE

The permitting approach for the Landscape/Recreation/Aesthetic (LRA) use class used by each WMD differs, and therefore the associated data in their respective databases upon which the most appropriate means of simulating these demands differs as well. The following sections describe LRA use estimates for each WMD as applied in the HAT-ECFT simulations.

SFWMD

For golf courses, an effort was undertaken to identify a timeframe of if and when a specific golf course began irrigating with reuse water. For the golf courses that employed reuse during the simulation period, groundwater irrigation withdrawals were reduced or stopped once reuse application began. Therefore, if a golf course began using reuse in the year 2001, in the model groundwater irrigation would occur for the entire 1995 scenario but not occur at all during the Reference Condition or any of the future simulations for that individual user. Golf course permits identified as having a groundwater source as back-up only were not simulated in the model. A list of the golf courses that have partial or total reuse simulated in the SFWMD portion of the model is provided in **Table 12. Figure 37** shows where groundwater was withdrawn to meet golf course and landscaping demands.

Table 12. Golf courses with water permits within the SFWMD portion of the CFWI Planning Area.

County	Name	Permit	Simulated as Reuse*
Orange	ISLEWORTH GOLF AND CC	48-00040-W	No
Orange	GRAND CYPRESS RESORT	48-00121-W	Partial
Orange	ORANGE LAKE RESORT AND CC	48-00135-W	Partial
Orange	ORANGE TREE GOLF CLUB	48-00179-W	Yes/Backup
Orange	LAKE NONA GOLF COURSE	48-00192-W	No
Orange	HUNTERS CREEK GOLF COURSE	48-00252-W	Yes/Backup
Orange	METROWEST GOLF CLUB	48-00264-W	Yes/Backup
Orange	WINDERMERE COUNTRY CLUB	48-00288-W	No
Orange	MARRIOTT GRANDE PINES	48-00300-W	No
Orange	BAY HILL GOLF COURSE	48-00760-W	Yes/Backup
Orange	MARRIOTT FALDO GOLF INSTITUTE	48-00891-W	No
Orange	WINDERMERE GOLF ACADEMY	48-00899-W	No
Orange	THE GOLDEN BEAR CLUB	48-00983-W	No
Orange	LAKE NONA SOUTH -TPCI	48-01053-W	No
Orange	GRANDE LAKES RESORT	48-01097-W	Yes/Backup
Orange	NORTH SHORE GOLF CLUB	48-01156-W	No
Orange	BONNET CREEK RESORT	48-01315-W	Yes/Backup
Orange	SHINGLE CREEK GOLF CLUB	48-01321-W	Yes/Backup
Orange	AUDUBON SILVER AWARD GOLF	48-01633-W	Yes/Backup
Orange	LAKE NONA CENTRAL	48-02021-W	No
Osceola	SERALAGO GOLF COURSE (TWA)	49-00118-W	Yes/Backup
Osceola	KISSIMMEE OAKS GOLF CLUB	49-00279-W	No
Osceola	KISSIMMEE BAY COUNTRY CLUB	49-00453-W	Partial
Osceola	REMINGTON GOLF COURSE	49-00780-W	Yes/Backup
Osceola	MYSTIC DUNES	49-00931-W	Partial
Osceola	CHAMPIONSGATE	49-00998-W	Yes/Backup
Osceola	HARMONY GOLF PRESERVE	49-01064-W	No
Osceola	KISSIMMEE GOLF CLUB	49-01225-W	No
Polk	RIVER RANCH RESORT	53-00017-W	No
Polk	SOLIVITA	53-00020-W	Yes/Backup
Polk	INDIAN LAKE GOLF COURSE	53-00151-W	No
Polk	PROVIDENCE GOLF COURSE	53-00165-W	No

* Permits identified as "partial" were generally multi-use developments where the golf course was irrigated with reuse water and the common grounds were irrigated from a groundwater or surface water source.

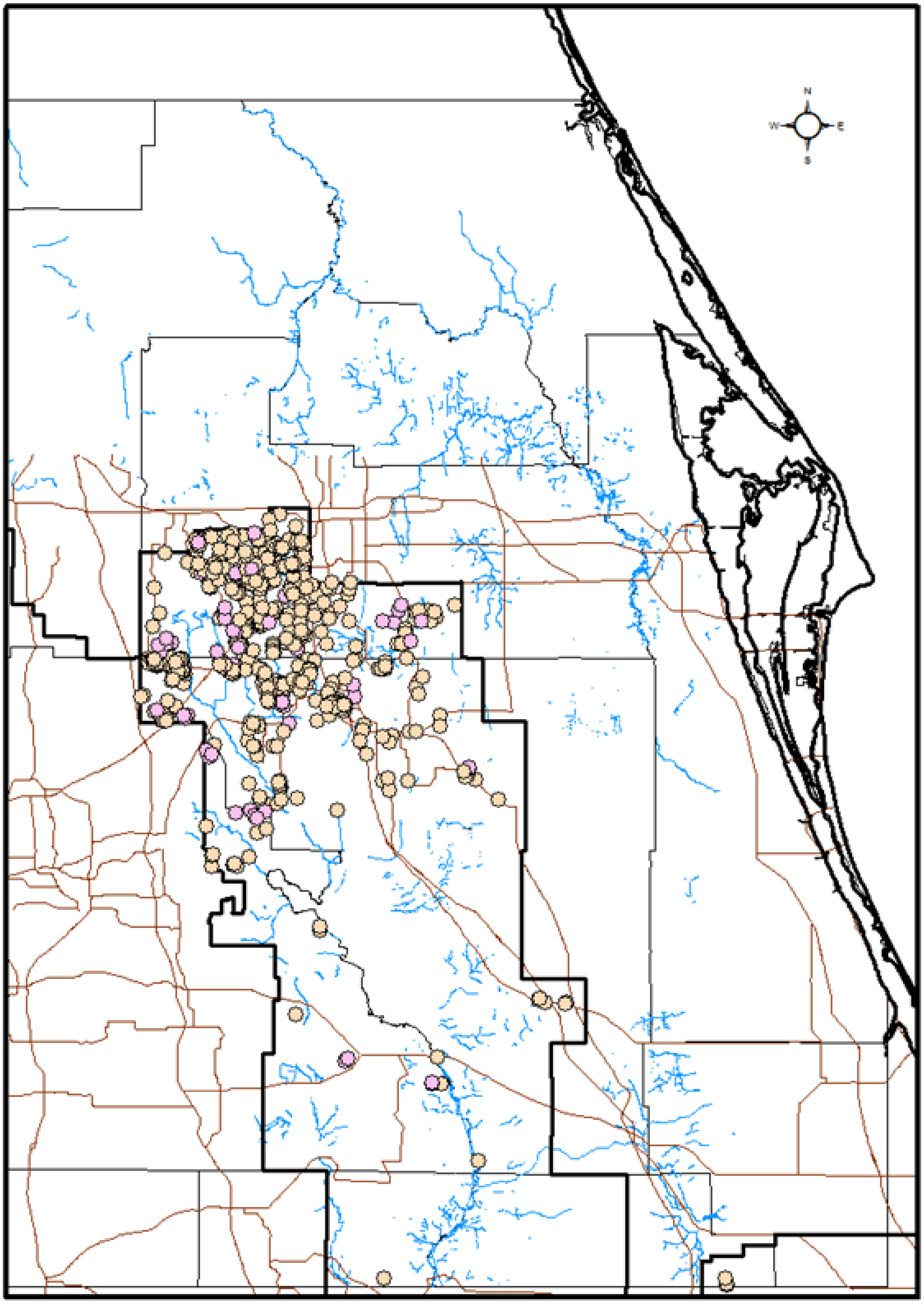

Figure 37. Golf course and landscape groundwater withdrawal locations in the SFWMD.

SWFWMD

Similar to agricultural withdrawals in the SWFWMD, withdrawals for Landscape/ Recreation/Aesthetic (LRA) use for the EOP model run served as the basis for the remaining future scenarios.

Reference Condition

LRA withdrawals used in the Reference Condition were prepared similar to how public supply withdrawals were prepared. That is, the volume of withdrawals for each year of the simulation was maintained at the levels observed for 2005. Monthly volumes, however, were adjusted from year to year to account for the intra-year monthly variations that occur due to differences in rainfall. Monthly pumping for each permit/withdrawal was calculated as follows:

$$QRC_{M,Y} = Q_{2005} * \left(\frac{Q_{M,Y}}{Q_{TY}}\right) \qquad \text{(Eqn. 10)}$$

Where:

$QRC_{M,Y}$	=	average pumping (mgd) for the Reference Condition for the specified month (M) and year (Y) of the simulation
Q_{2005}	=	average pumping (mgd) for the year 2005 as observed for the calibration period
$Q_{M,Y}$	=	average pumping (mgd) for the specified month (M) and year (Y) as observed for the calibration period
Q_{TY}	=	average pumping (mgd) for the specified year as observed for the calibration period

End-of-Permit Condition

LRA withdrawals for the EOP Condition were prepared using the same general approach as for agriculture. The first step was to identify currently active water use permits and withdrawal points by comparing WUPs in the Reference Condition (2005) to current WUPs as of December 31, 2012. Permits no longer active were deleted from the data set and permits issued since 2005 were added. The resulting list of permits and withdrawal points provided the basis for the EOP scenario, which in turn provided the basis for the future scenarios. Pumping for permits/wells included in the Reference Condition were calculated by multiplying monthly withdrawals by the ratio of EOP pumping to the annual average pumping for the Reference Condition simulation. The temporal variation in pumping for permits not included in the 2005 scenario was based on the countywide temporal variation observed for the Reference Condition.

2015, 2025, and 2035 Withdrawal Scenarios

LRA quantities associated with future withdrawal condition scenarios were calculated using countywide multipliers. The multipliers were calculated on a countywide basis as the ratio of average annual withdrawals over the 12-year simulation period for the specified withdrawal condition (e.g., 2015, 2025, or 2035) to the EOP values. Each withdrawal in the EOP simulation was multiplied by this ratio to yield the LRA withdrawals for the specified withdrawal condition scenario. For self-supplied golf courses, it was assumed the courses were built-out and that withdrawals for future scenarios would occur at the rates used in the EOP model run. Withdrawal amounts for counties within the CFWI were obtained from the CFWI RWSP and for counties outside the CFWI, withdrawal quantities were obtained from the SWFMWD's RWSP documents.

SJRWMD

Withdrawals for Landscape/Recreation/Aesthetic uses within SJRWMD are not included in the scenario runs because the SJRWMD demands are estimated from changes in land use and no updated land use maps for the future conditions were generated.

IMPLEMENTATION OF COMMERCIAL / INDUSTRIAL WATER USE

Similar to the SWFWMD agriculture calculations, Commercial/Industrial (C/I) withdrawals for the EOP model run served as the basis for the remaining future scenarios for the entire CFWI area.

Reference Condition

Commercial/Industrial withdrawals used in the Reference Condition were prepared similar to how public supply withdrawals were prepared. That is, the volume of withdrawals for each year of the simulation was maintained at the levels observed for 2005. Monthly volumes, however, were adjusted from year to year to account for the intra-year variation that occurs due to differences in rainfall throughout the year. Monthly pumping for each permit/withdrawal was calculated as follows:

$$QRC_{M,Y} = Q_{2005} * \left(\frac{Q_{M,Y}}{Q_{TY}}\right) \quad \text{(Eqn. 11)}$$

Where:

$QRC_{M,Y}$	=	average pumping (mgd) for the Reference Condition as observed for the specified month (M) and year (Y) of the simulation
Q_{2005}	=	average pumping (mgd) for the year 2005 as observed for the calibration period

$Q_{M,Y}$	=	average pumping (mgd) for the specified month (M) and year (Y) as observed for the calibration period
Q_{TY}	=	average pumping (mgd) for the specified year as observed for the calibration period

End-of-Permit Condition

C/I withdrawals for the EOP Condition were prepared using the same approach as used for SWFWMD Agricultural withdrawals. The first step was to identify all currently active water use permits and withdrawal points by comparing WUPs included in the Reference Condition (2005) scenario to current WUPs as of December 31, 2012. Permits no longer active were deleted from the data set and permits issued since 2005 were added. The resulting list of permits and withdrawal points provided the basis for the EOP scenario, which in turn provided the basis for the future scenarios. Of particular note was the consolidation of several permits and wells associated with the Mosaic mining company into one permit in the SWFWMD. That is, for the EOP and future scenarios, SWFWMD permit numbers 000029,001539, 002224, 002297, 003195, 003740, and 11400 were combined into permit number 11400. The temporal variation in pumping for permits not included in the 2005 scenario was based on the countywide temporal variation observed for the Reference Condition.

2015, 2025, and 2035 Future Withdrawal Condition Scenarios

C/I quantities associated with future withdrawal condition scenarios were calculated using countywide multipliers. The multipliers were calculated on a countywide basis as the ratio of average annual withdrawals over the 12-year simulation period for the specified withdrawal condition (e.g., 2015, 2025, or 2035) to the EOP values. Each withdrawal in the EOP simulation was multiplied by this ratio to yield the C/I withdrawals for the specified withdrawal condition scenario. Withdrawal amounts for counties within the CFWI were obtained from the CFWI RWSP. For counties outside the CFWI, withdrawal quantities were obtained from the SWFWMD's RWSP documents, remained at 2005 reference condition demand in the SFWMD, and to the projected future quantities from non-CFWI documents in the SJRWMD.

IMPLEMENTATION OF AQUIFER RECHARGE FACILITIES

Development of Monthly Flow Series

The development of monthly flow series for aquifer recharge facilities was based on metered flow data collected by public utilities and is directly analogous to the process for developing groundwater withdrawal flow series, as described in the **Implementation of Public Water Supply Uses** section of this chapter. As with groundwater withdrawals, the measured reclaimed water flow data generally includes an underlying trend driven by population growth and increased wastewater generation, and this is reflected in many utilities' records of aquifer recharge flows. While the measured flows were used for model calibration purposes, it is necessary to develop a de-trended flow series for use in the assessment of future conditions. As with the groundwater withdrawals, Equations 3 through 8 were used to develop de-trended flow series that could be scaled to represent other future flow conditions, if desired.

Aquifer Recharge Flow Series Used for Model Calibration

The measured flow data were used to represent aquifer recharge facilities in the model calibration run. Complete data records were used where they were available, but for some smaller facilities there were very few data available. Because of time limitations and the very small regional influence of recharge facilities that have capacities far less than 1 mgd, data infilling methods were not used for the small facilities with missing data.

The aquifer recharge facilities were mostly rapid infiltration basin facilities, except for those at Orange County's Northwest Water Reclamation Facility, which includes a substantial wetland treatment system that discharges several million gallons per day of treated reclaimed water to Lake Marden. Because Lake Marden is an isolated depressional lake, water discharged into it infiltrates from there to the underlying Upper Floridan aquifer. All these facilities were represented by "injection" of appropriate quantities of water into Layer 1 of the model (the surficial aquifer system). Treatment wetlands that discharge to free-flowing streams and rivers were not represented in the model because the discharge of reclaimed water at these locations has negligible effects on recharge to the groundwater system.

Aquifer Recharge Flow Series Used for 2005 Reference Condition

As for the groundwater withdrawal data, the 2005 Reference Condition was developed through use of Equation 7 to create a de-trended flow series scaled to the average fitted trendline flow for 2005. An example is shown in **Figure 38** for the rapid infiltration basin (RIB) systems operated by the Toho Water Authority.

Aquifer Recharge Flow Series Used for Future Simulation Conditions

The future development of aquifer recharge facilities systems will largely depend on the operational choices made by the public utilities that operate these systems. To ensure that the RWSP did not rely on increased aquifer recharge that might not happen if public utilities make other use of reclaimed water, the utilities requested that the future simulations not show increased flow to the aquifer recharge facilities. Accordingly, all the future simulations were run using the same aquifer recharge flows that were used in the Reference Condition.

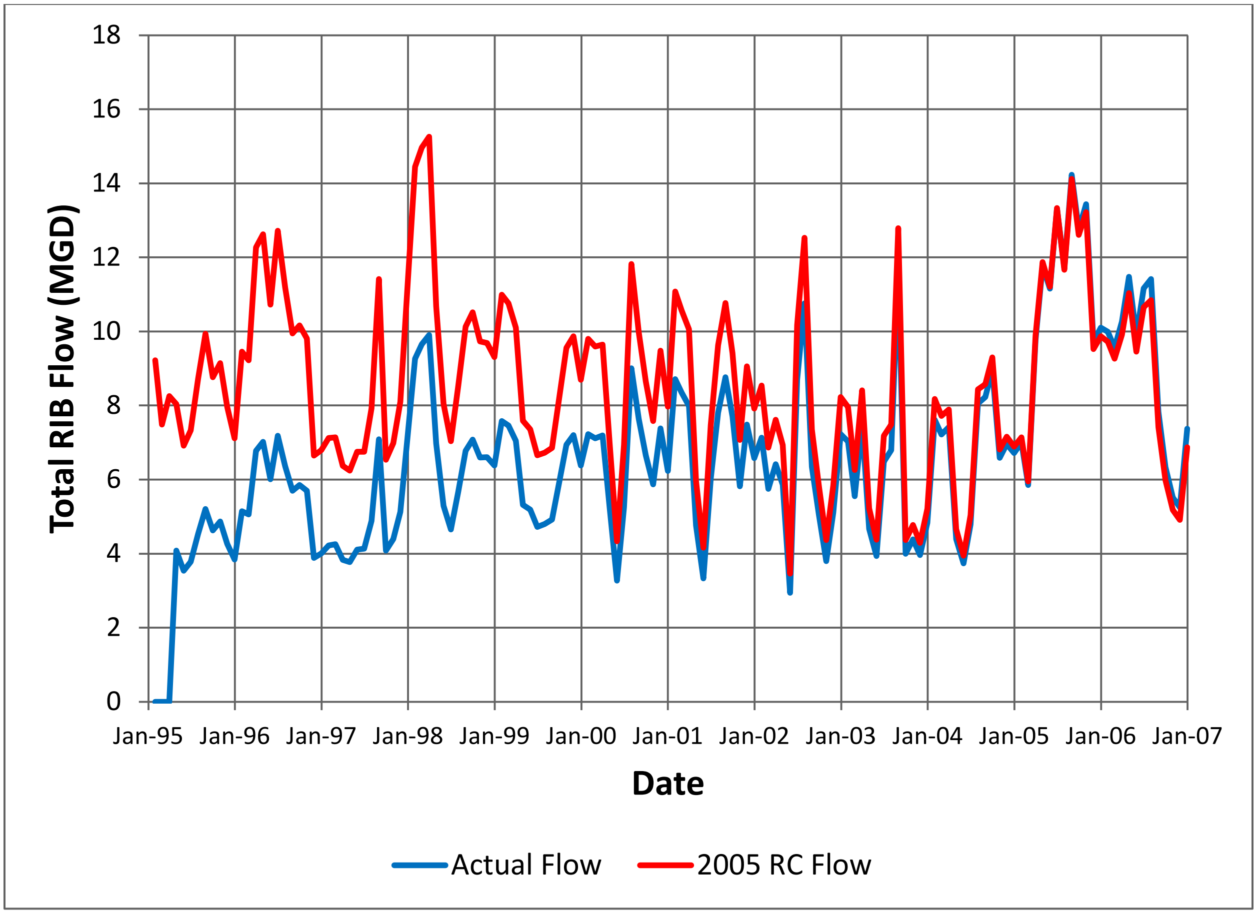

Figure 38. Recorded flow data and Reference Condition (RC) flows for Toho Water Authority RIB systems.

6

Comparison of Future Condition Simulation Results

INTRODUCTION

This chapter describes the results of the difference between simulated groundwater levels for the Reference Condition and future simulations, focusing on the simulated surficial aquifer system (i.e., Layer 1 of the model) and simulated Upper Floridan aquifer (i.e., Layer 3 of the model). This section will also describe the results of the difference between simulated spring flows for the Reference Condition and future simulations, which are simulated as flows from Layer 1 to Layer 3 in the model. The future simulations include the withdrawal conditions for the projected water demands associated with the years 2015, 2025, 2035 and end of permit. The Reference Condition (i.e., 2005 water demands) provides a common reference to allow comparison of relative changes associated with the future simulations.

2015 WITHDRAWAL SCENARIO

Figure 39 shows the difference in median simulated SAS groundwater levels between the Reference Condition and the 2015 Withdrawal Scenario. SAS groundwater levels are predicted to decrease 1 to 3 feet in some areas along the border of western Orange and Osceola counties, as well as some isolated parts of Polk County. Some slightly higher declines in SAS groundwater levels (i.e., 5 to 10 feet) occur in isolated areas in east-central Polk County.

Figure 40 shows the difference in median simulated UFA potentiometric surface levels between the Reference Condition and 2015 Withdrawal Scenario. Predicted decreases in UFA potentiometric surface levels of 1 to 3 feet occur in almost all of Osceola County, western Orange County, western Seminole County, central and south Lake County, and Polk County west of U.S. Route 27.

2025 WITHDRAWAL SCENARIO

Figure 41 shows the difference in median simulated SAS groundwater levels between the Reference Condition and the 2025 Withdrawal Scenario. Predicted decreases in SAS groundwater levels of 1 to 3 feet occur in some areas of western Orange, southwestern Lake, and Polk counties, with decreases of 3 to 5 feet in isolated areas of western Orange, Osceola, and Polk counties.

Figure 42 shows the difference in simulated UFA median water levels between the Reference Condition and the 2025 Withdrawal Scenario. The UFA potentiometric surface levels are expected to be 1 to 3 feet lower in most of the CFWI Planning Area and 3 to 5 feet lower in portions of south-central Orange and north-central Osceola counties, and isolated parts of the remainder of the area.

2035 WITHDRAWAL SCENARIO

Figure 43 shows the difference in median simulated SAS groundwater levels between the Reference Condition and the 2035 Withdrawal Scenario. The greatest decreases in SAS groundwater levels (> 5 feet) are predicted for the border between southwest Orange and northwest Osceola counties. Smaller areas with similar magnitude of drawdown are predicted for north-central Polk and eastern Lake counties.

Figure 44 shows the difference in median simulated UFA potentiometric surface levels between the Reference Condition and the 2035 Withdrawal Scenario. UFA potentiometric surface levels are predicted to be 5 to 10 feet lower in an area centered in southwest Orange and northwest Osceola counties, along with areas in north-central Polk County.

END-OF-PERMIT CONDITION

Figure 45 shows the difference in median simulated SAS groundwater levels between the Reference Condition and the EOP Condition. Decreases in SAS groundwater levels of 1 to 3 feet were predicted for isolated areas of western Seminole, Orange, and Osceola counties, as well as areas of southern Lake County and central Polk County. Some slightly higher drawdowns (i.e., 3 to 5 feet) occur along the border between southwest Orange and northwest Osceola counties.

Figure 46 shows the difference in median simulated UFA potentiometric surface levels between the Reference Condition and the EOP Condition. Potentiometric surface levels were predicted to decrease 1 to 3 feet occur across much of the CFWI Planning Area and 3 to 5 feet in most of Osceola and Orange counties. Potentiometric surface level declines of 5 to 10 feet were predicted in more isolated areas of north-central Osceola, south-central Orange, and Polk counties.

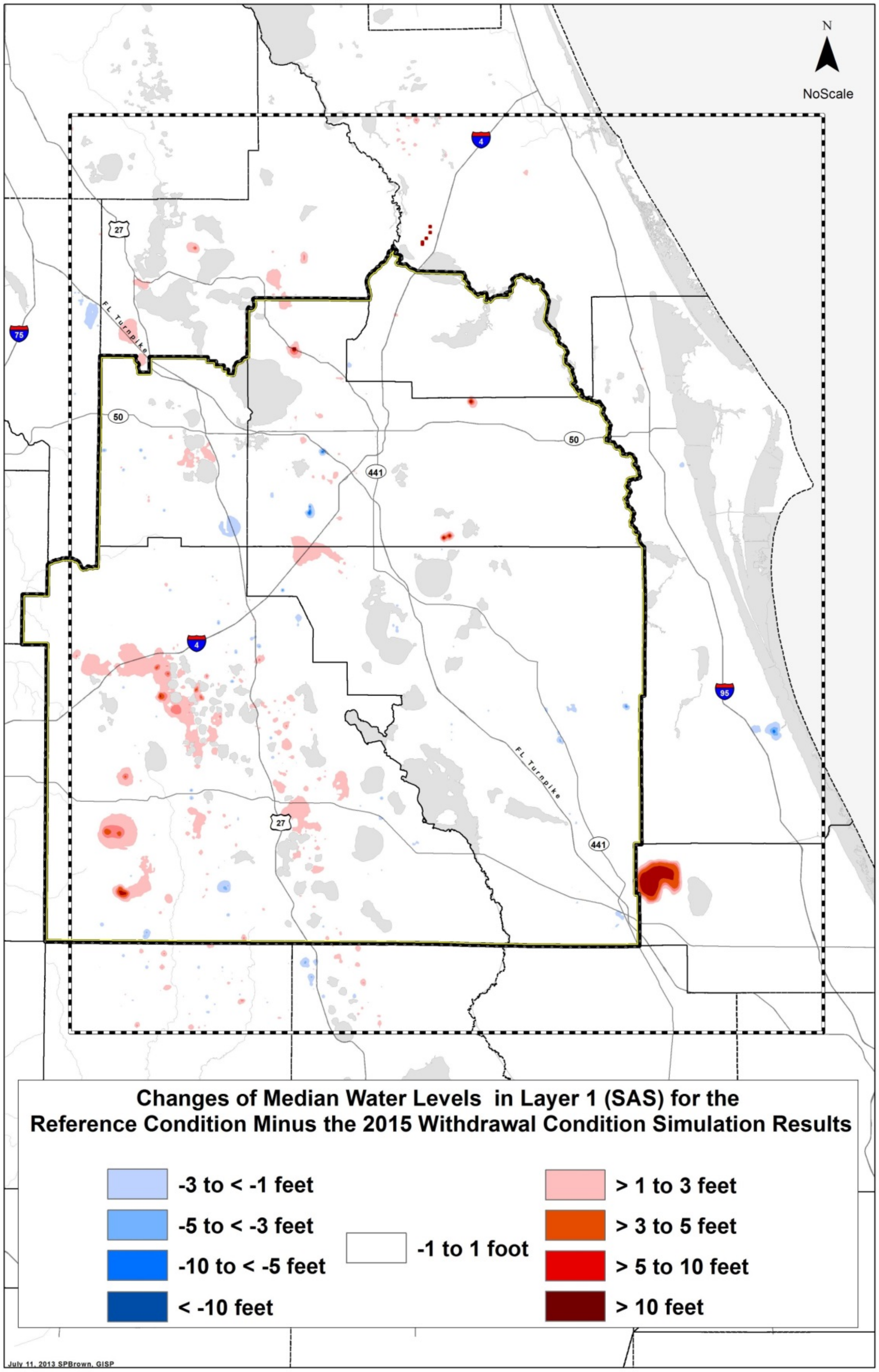

Figure 39. Changes in median water levels in Layer 1 (SAS) between the Reference Condition and the 2015 Withdrawal Scenario.

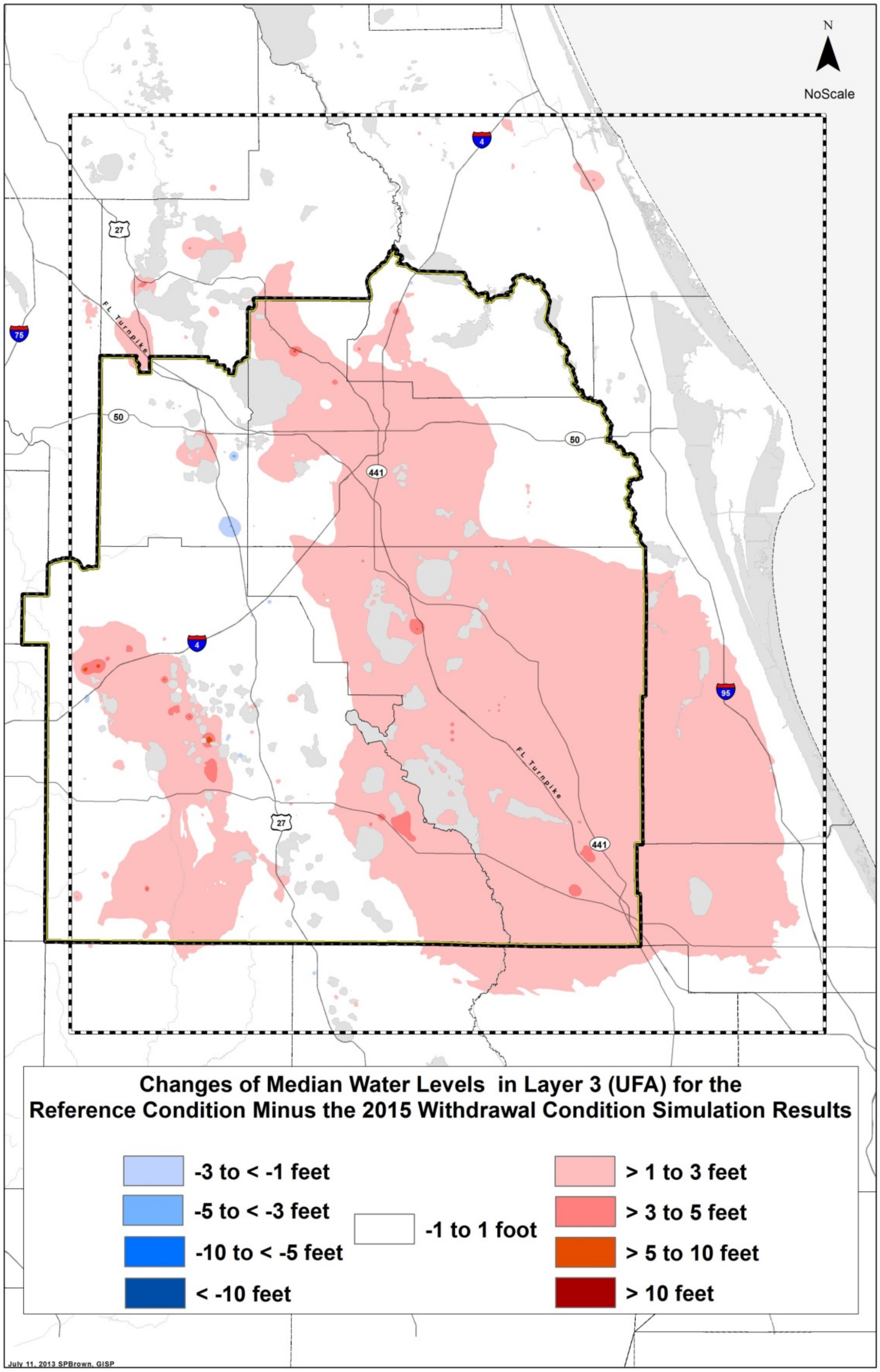

Figure 40. Changes in median water levels in Layer 3 (UFA) between the Reference Condition and the 2015 Withdrawal Scenario.

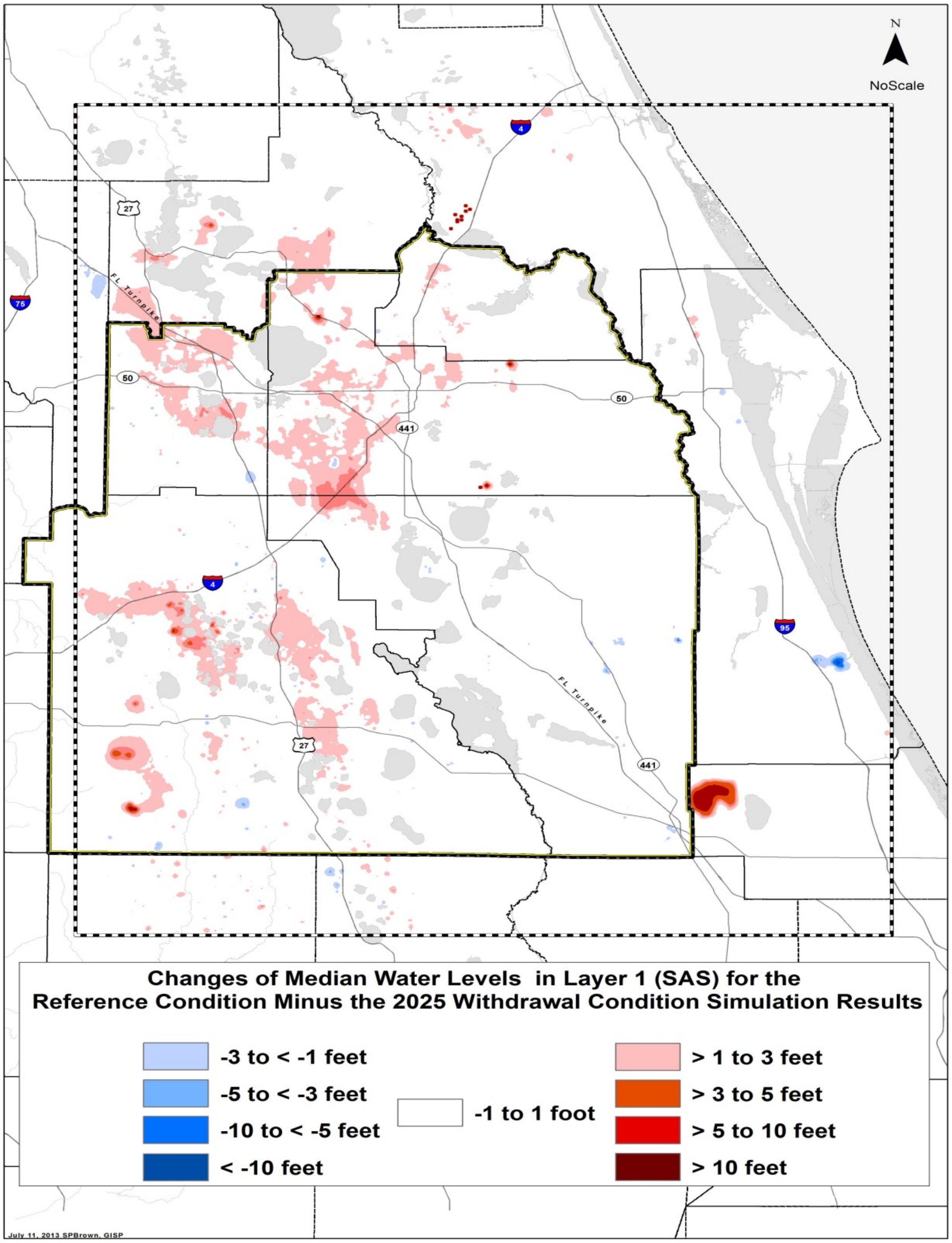

Figure 41. Changes in median water levels in Layer 1 (SAS) between the Reference Condition and the 2025 Withdrawal Scenario.

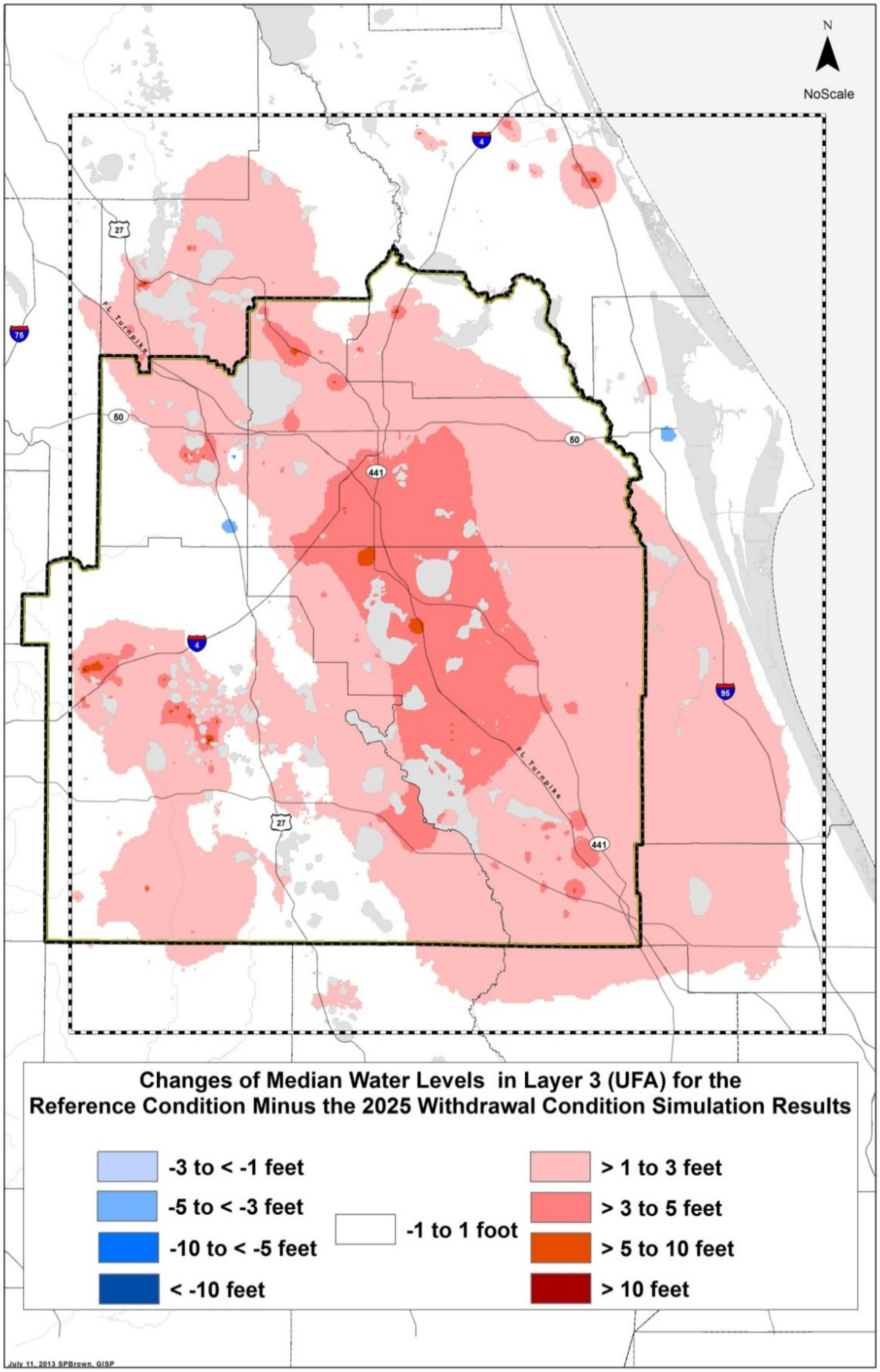

Figure 42. Changes in median water levels in Layer 3 (UFA) between the Reference Condition and the 2025 Withdrawal Scenario.

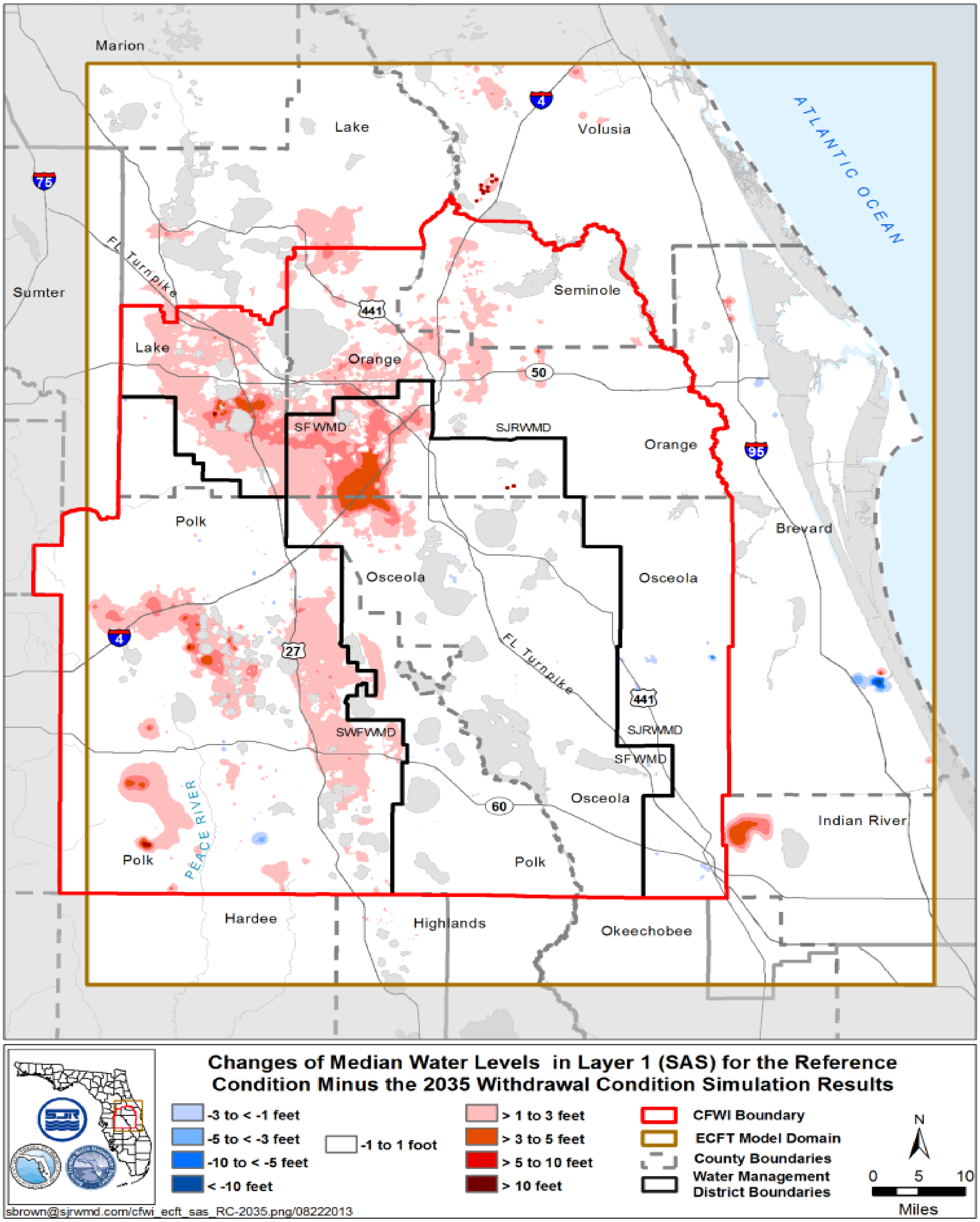

Figure 43. Changes in median water levels in Layer 1 (SAS) between the Reference Condition and the 2035 Withdrawal Scenario.

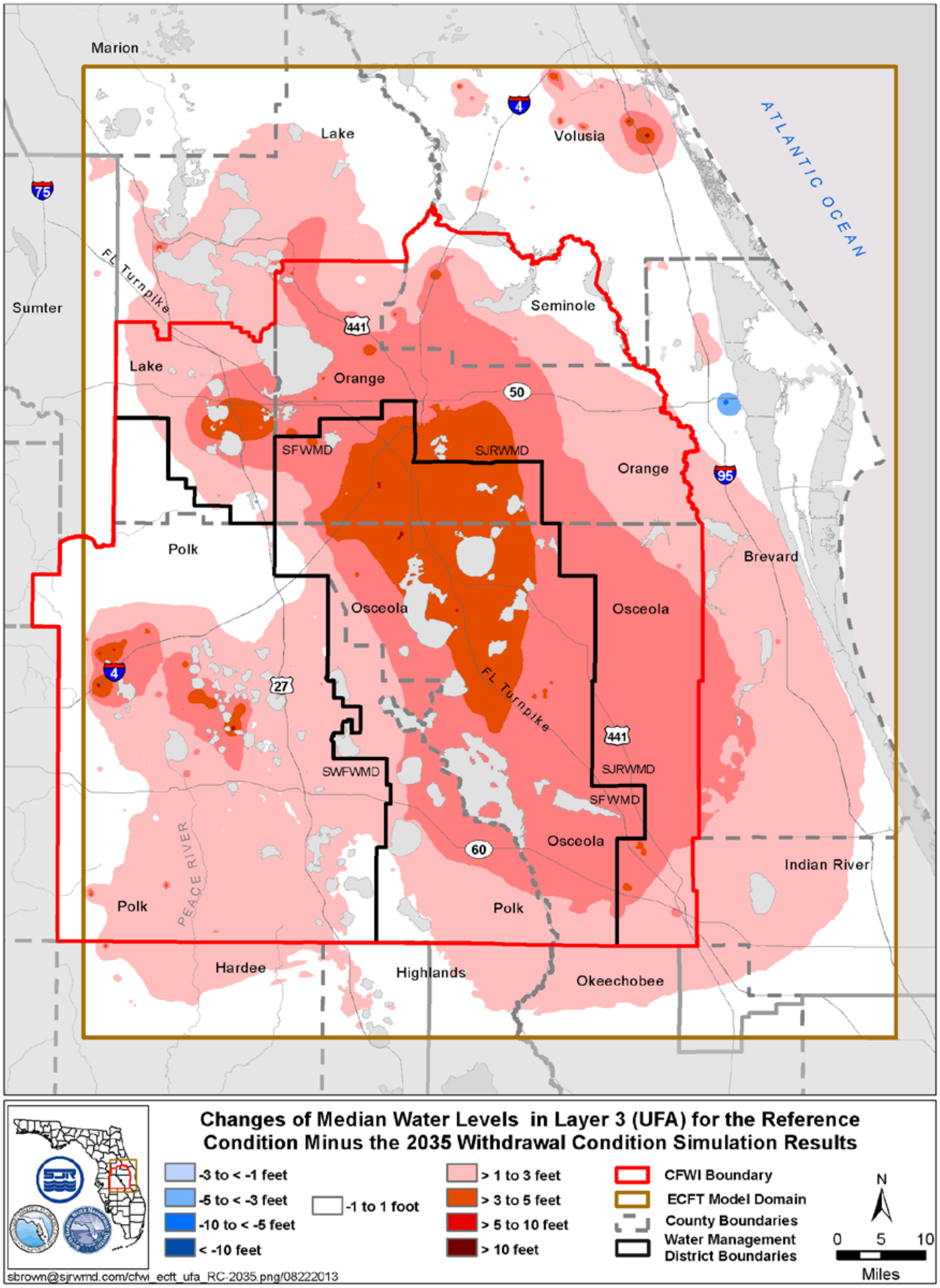

Figure 44. Changes in median water levels in Layer 3 (UFA) between the Reference Condition and the 2035 Withdrawal Scenario.

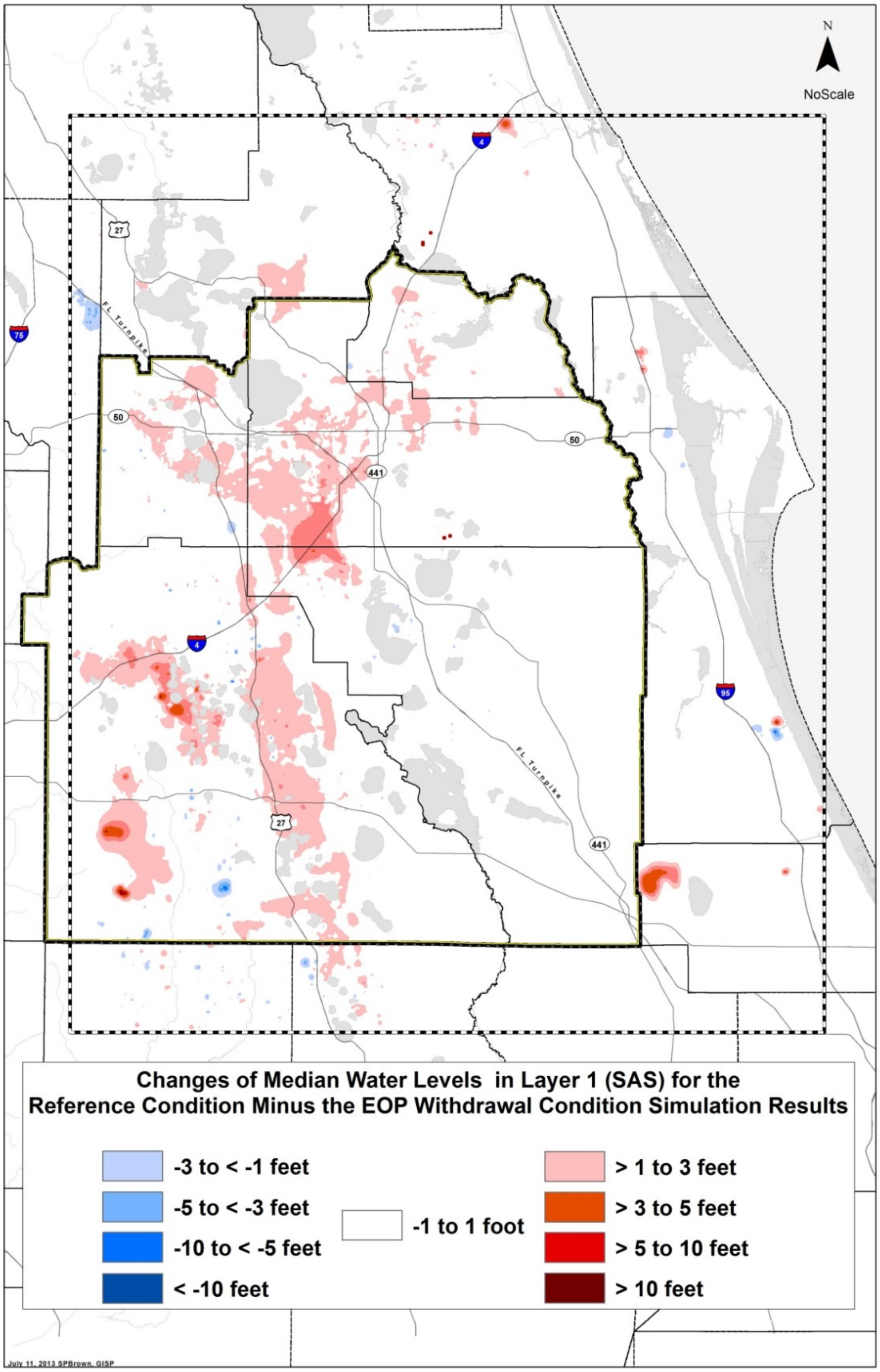

Figure 45. Changes in median water levels in Layer 1 (SAS) between the Reference Condition and the EOP Condition.

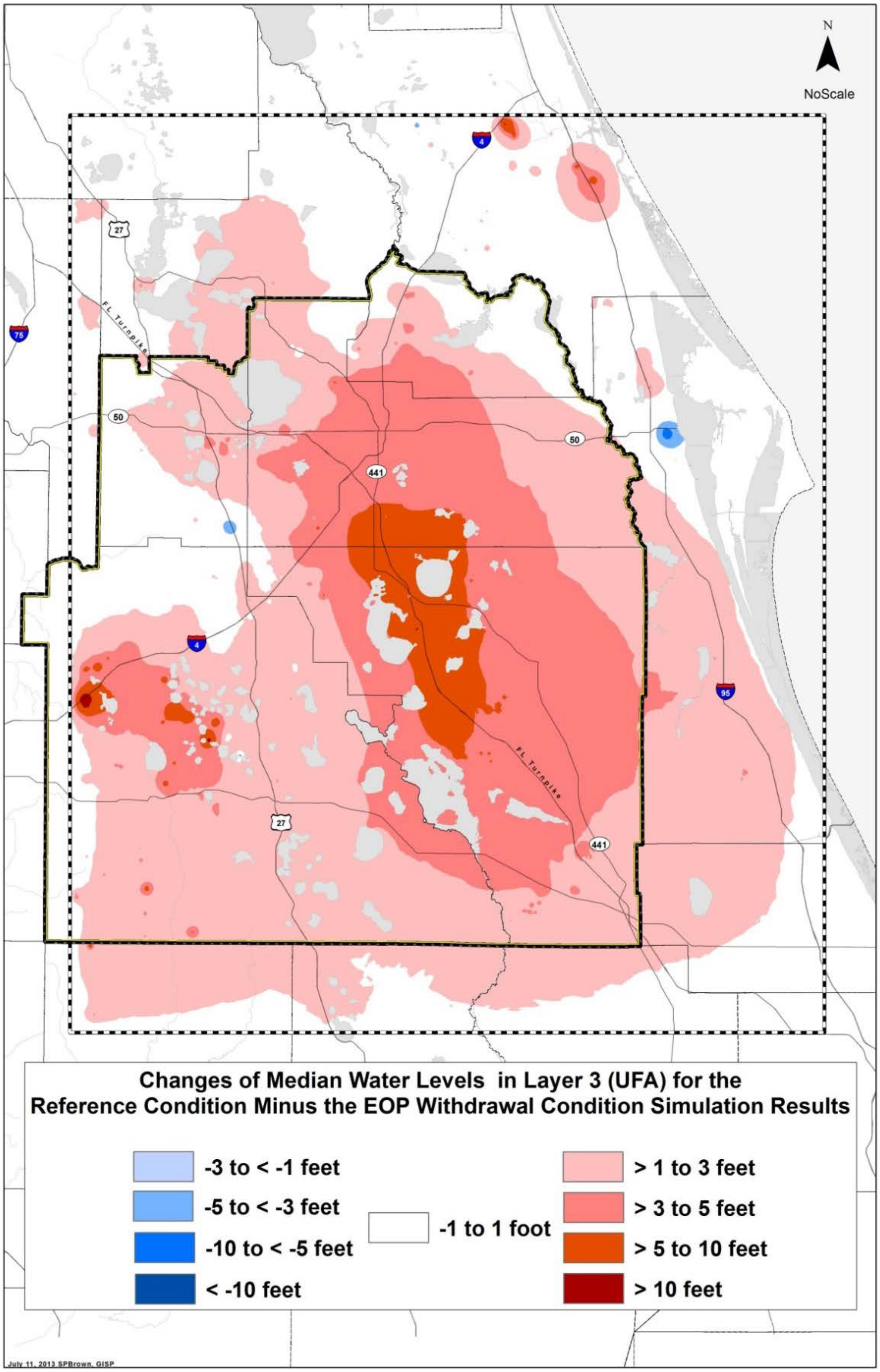

Figure 46. Changes in median water level in Layer 3 (UFA) between the Reference Condition and the EOP Condition.

SPRING DISCHARGES

Spring discharges are represented in the HAT-ECFT model as boundary conditions that simulate flow from the UFA to the SAS. A summary of spring flows for the Reference Condition and the predictive scenarios is provided in **Table 13**.

In general, spring flows incrementally decline with the increase in groundwater withdrawal from the Reference Condition to the 2035 Withdrawal Scenario. **Table 13** indicates that Blue Spring near Orange City (Volusia County), Palm Springs near Longwood, Rock Springs near Apopka, Sanlando Springs near Longwood, Seminole Spring near Sorrento, Starbuck Spring near Longwood, and Wekiva Springs near Apopka are all projected to experience a reduction in spring flows as a result of an increase in groundwater withdrawals that may result in an MFL exceedance.

The apparent MFL exceedances in **Table 13** may not truly be MFL exceedances or violations because timing and duration of the exceedance is not considered in the table. Rather, apparent MFL exceedances are intended to highlight springs whose flows are already low and are therefore susceptible to additional groundwater withdrawals that may cause an MFL exceedance or violation. More detailed analysis of MFLs is available in Appendix B of the CFWI RWSP.

Table 13. Comparison of spring flows (cfs) for Reference Condition and future withdrawal scenarios.

Spring	MFL	Reference Condition	2015	2025	2035	EOP
Alexander Spring near Astor		102.65	102.51	102.25	102.24	102.36
Apopka (Gourdneck) Spring near Montverde		24.85	24.37	22.27	17.54	21.05
Blue Spring near Orange City (Volusia Co)	142-157	152.53	150.55	**147.01**	**144.53**	**150.84**
Blue Springs near Yalaha (Lake Co)		2.45	2.19	1.88	1.85	2.09
Bugg Spring at Okahumpka		10.30	8.23	6.78	8.55	9.24
Camp La-No-Che Springs near Paisley		0.81	0.78	0.74	0.72	0.75
Clifton Springs near Oviedo		1.44	1.26	0.93	0.61	0.74
Droty Springs near Sorrento		0.67	0.55	0.38	0.26	0.41
Gemini Springs near Debary		10.14	10.02	9.76	9.58	9.92
Green Spring near Osteen		1.91	1.85	1.74	1.66	1.79
Holiday Springs near Yalaha		3.19	2.70	2.10	2.04	2.47
Island Spring in Wekiva River near Sanford		7.84	7.69	7.38	7.16	7.38
Messant Spring near Sorrento	12.00	15.45	14.95	14.25	13.74	14.41
Miami Springs near Longwood	4.00	5.80	5.40	5.18	4.94	5.28
Palm Springs near Longwood	7.00	**5.81**	**5.45**	**5.08**	**4.66**	**4.95**
Rock Springs near Apopka	53.00	53.65	**51.24**	**48.61**	**46.46**	**49.69**
Sanlando Springs near Longwood	15.00	20.14	18.50	16.84	**14.99**	16.32
Seminole Spring near Sorrento	34.00	**29.11**	**28.43**	**27.47**	**26.75**	**27.69**
Starbuck Spring near Longwood	13.00	13.56	**12.65**	**11.79**	**10.85**	**11.58**
Wekiva Falls Resort (flowing 14" borehole)		18.28	17.88	17.19	16.65	17.28
Wekiva Springs near Apopka	62.00	63.64	**61.02**	**59.24**	**57.37**	**59.99**
Witherington Springs near Apopka		1.98	1.79	1.64	1.49	1.70

NOTE: Values in bold indicate predicted exceedances of the spring’s MFL.

7

Conclusions

MODEL PERFORMANCE

From a performance statistics perspective, the recalibrated HAT-ECFT model was similar to the USGS-ECFT calibration. Recalibration for the full model domain resulted in a slight improvement over the original calibration; however, depending on the model layer or the metric being evaluated, the recalibration results varied from a slight degradation to a slight improvement in the model calibration statistics.

The main benefit of the recalibration effort was improvement in the transient response of many of the water levels and flows simulated by the model. This was the result of identifying specific assumptions made in the original calibration effort that the HAT modified. These changes include:

- The general head boundary condition input parameter assignment for head was held constant for each individual year of the calibration. To fix this, they were modified to simulate monthly variability in groundwater levels based on available observed data.

- The spring pool elevations assigned to the drain node boundary conditions utilized for springs was used as a calibration parameter. For the recalibration, these elevations were modified based on available observation data.

- The storage coefficient/storativity parameters assigned to the model were held constant across each individual model layer. The HAT modified the parameters to represent the variable hydrogeologic conditions across the area.

- Historical well pumping data was found to have errors. An extensive review of historical pumping data was performed and the model well package was updated accordingly.

As seen in **Figure 4**, transient groundwater level response was improved through model recalibration at observation well ROMP 60 (located in west-central Polk County). **Figure 47** illustrates the improvement of the transient spring flow response achieved through model recalibration at Alexander Springs (located in north Lake County). Though the overall recalibration was similar, the modifications implemented resulted in a notable improvement in transient response of the HAT-ECFT model.

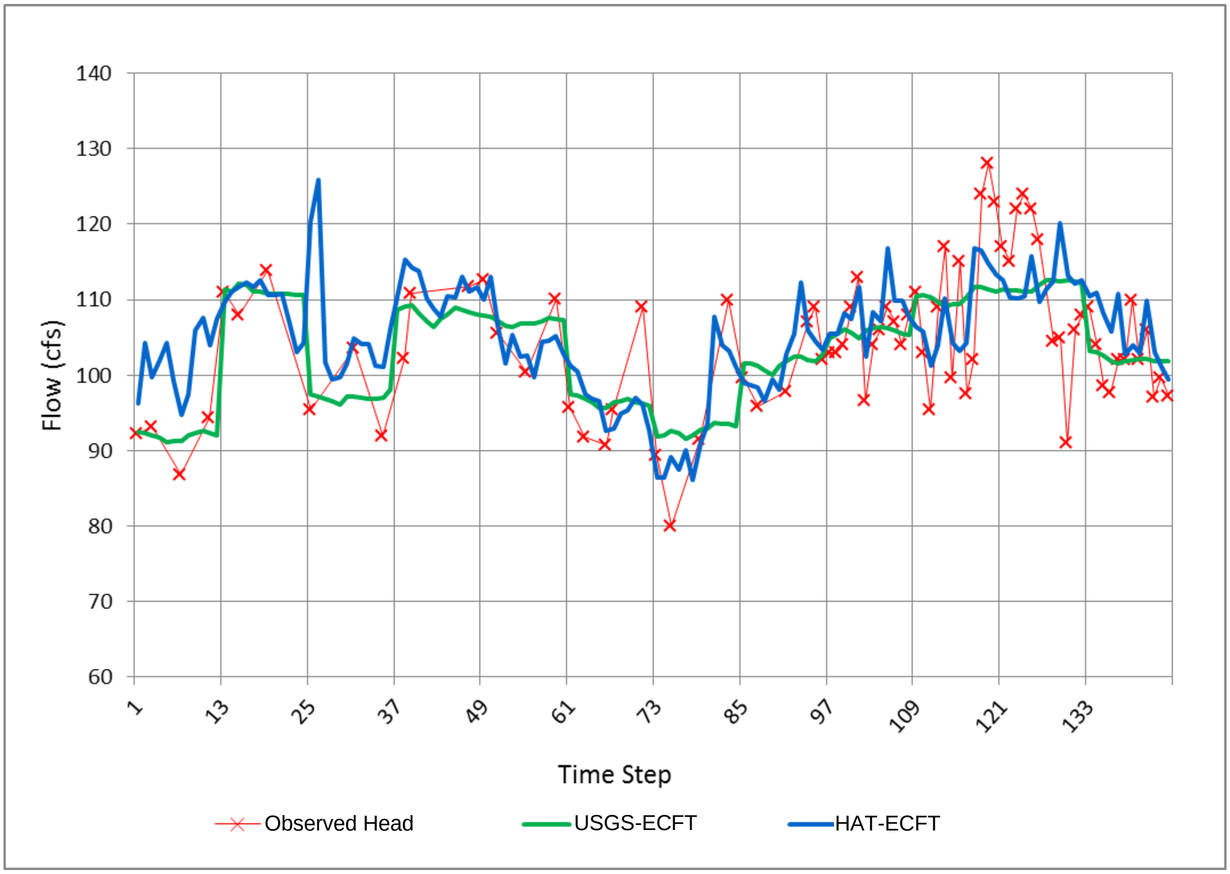

Figure 47. Hydrograph of observed and simulated spring flows at Alexander Springs in Lake County for the USGS-ECFT and HAT-ECFT models.

References

CFWI. 2014. *Central Florida Water Initiative Regional Water Supply Plan Planning Document*, Final Draft. Central Florida Water Initiative. http://www.cfwiwater.com.

Harbaugh, A.W., 2005, *MODFLOW-2005, The U.S. Geological Survey Modular Ground-Water Model—the Ground-Water Flow Process: U.S. Geological Survey Techniques and Methods*, Book 6, Chapter 16, Modeling Techniques, Section A, Ground Water, 196 p.

Hoblit, B.B., C. Castello, L. Liu, and D. Curtis, 2003, *Creating a seamless map of gage-adjusted radar rainfall estimates for the state of Florida:* Proceedings of the EWRI World Water and Environmental Congress, Philadelphia, PA.

Merritt, M.L., and L.F. Konikow, 2000, *Documentation of a computer program to simulate lake-aquifer interaction using the MODFLOW ground-water model and the MOC3D solute-transport model:* U.S. Geological Survey Water Resources-Investigations Report 00-4167, 146 p.

Niswonger, R.G., and D.E. Prudic, 2006, *Documentation of the Streamflow-Routing (SFR2) Package to include unsaturated flow beneath streams—A modification to SFR1*: U.S. Geological Survey Techniques and Methods, Book 6, Chapter A13, 48.

Niswonger, R.G., D.E. Prudic, and S. Regan, 2006*, Documentation of the Unsaturated-Zone Flow (UZF1) Package for modeling unsaturated flow between the land surface and the water table with MODFLOW-2005*: U.S. Geological Survey Techniques and Methods, Book 6, Chapter A19, 62 p.

Prudic, D.E., L.F. Konikow, and E.R. Bant, 2004, *A new stream-flow routing (SFR1) package to simulate stream-aquifer interaction with MODFLOW-2000*: U.S. Geological Survey Open-File Report 2004-1042, 95 p.

Sepúlveda, N., C.R. Tiedeman, A.M. O'Reilly, J.B. Davis, and P. Burger, 2012, *Groundwater flow and water budget in the surficial and Floridan aquifer systems in east-central Florida*: U.S. Geological Survey Open-File Report 2012-1132, 195 p.

Shah, N., M. Nachabe, and M. Ross. 2007. *Extinction depth and evapotranspiration from ground water under land covers*: Ground Water 45(3):329-338.

SFWMD, 2013. *Volume III, Water Use Permitting Manual,* South Florida Water Management District, West Palm Beach, FL.

Smajstrla, A.G. 1990. *Technical Manual. Agricultural Field Scale Irrigation Requirements Simulation (AFSIRS) Model, Version 5.5.* Agricultural Engineering Department, University of Florida, Gainesville, FL.

Smajstrla, A.G. 1990. *User's Guide. Agricultural Field Scale Irrigation Requirements Simulation (AFSIRS) Model, Version 5.5.* Agricultural Engineering Department, University of Florida, Gainesville, FL.

Winsburg, M.D. 2003. *Florida Weather*. Second Edition. University Press of Florida, Gainsville, FL.

Zahina-Ramos, J., D. MacIntyre, J. Bays, S. Denton, A. Janicki, and C. Uranowski, 2013, *Development of Environmental Measures for Assessing Effects of Water Level Changes on Lakes and Wetlands in the Central Florida Water Initiative Area, Final Report*, (http://cfwiwater.com/pdfs/CFWI_Environmental_Measures_finalreport.pdf)

Appendix A. Summary Calibration Graphics per Layer, USGS-ECFT and HAT-ECFT Models

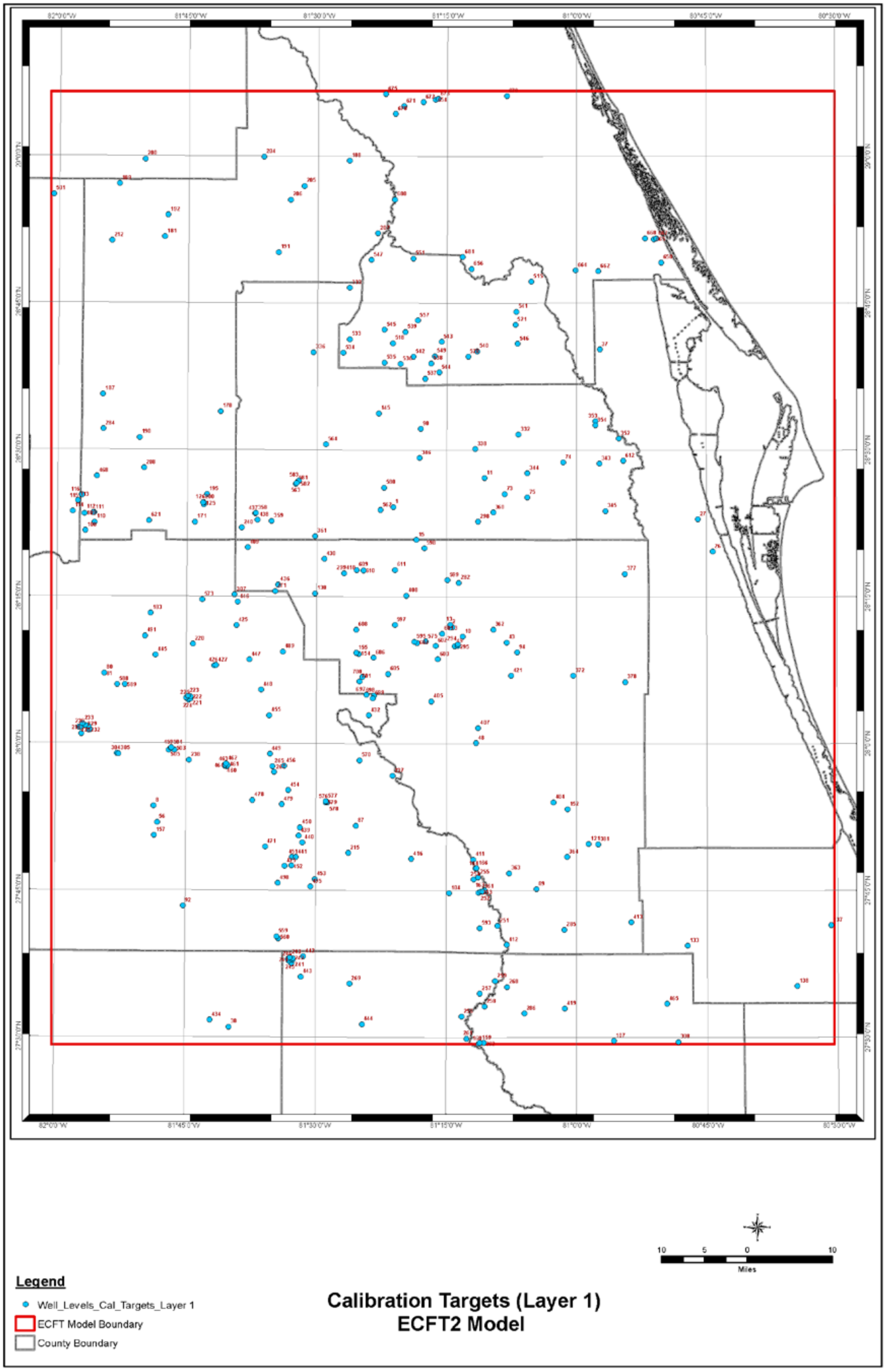

Calibration Targets (Layer 1)
ECFT2 Model

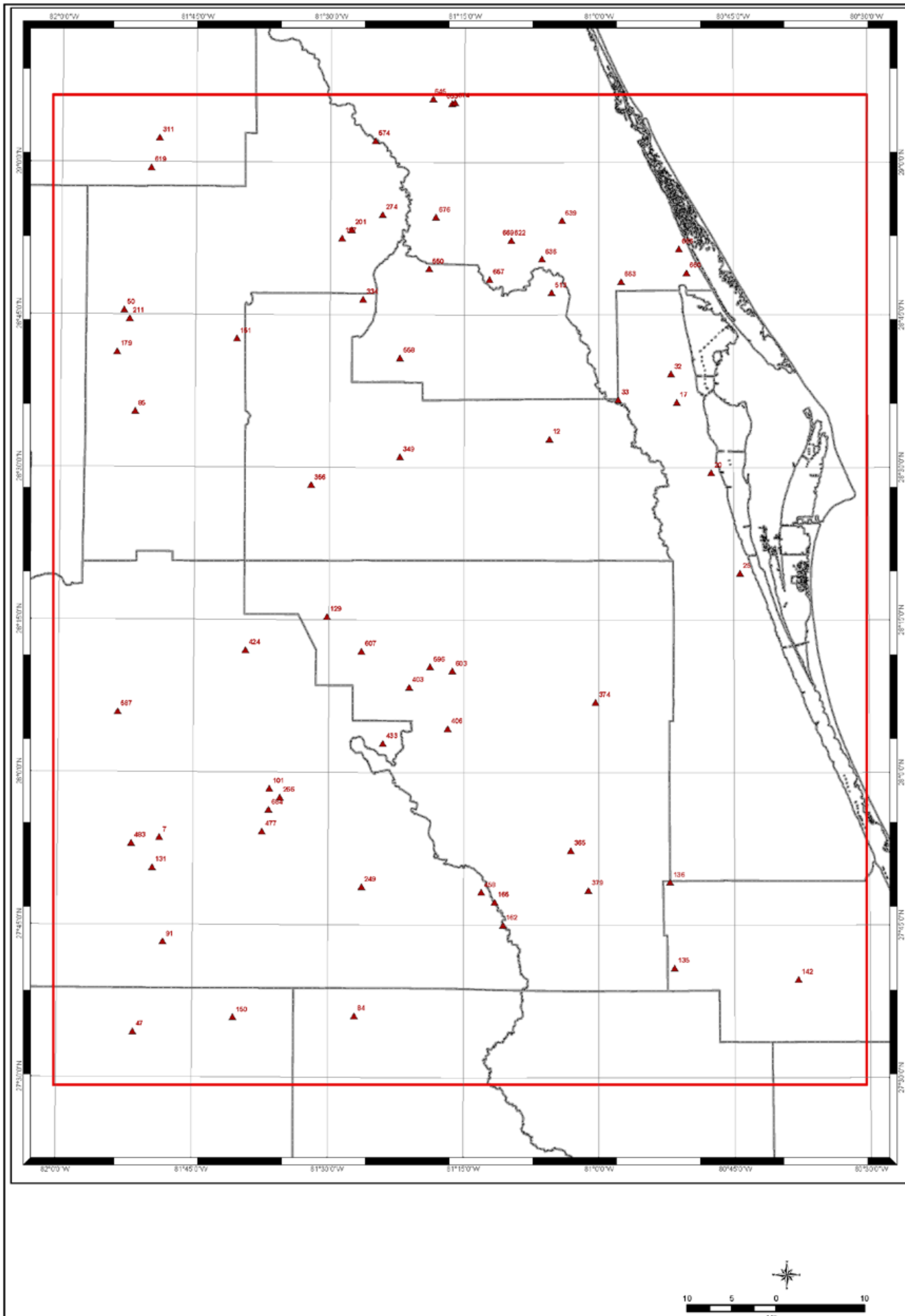

Legend

▲ Well_Levels_Cal_Targets_Layer 2

ECFT Model Boundary

County Boundary

Calibration Targets (Layer 2)
ECFT2 Model

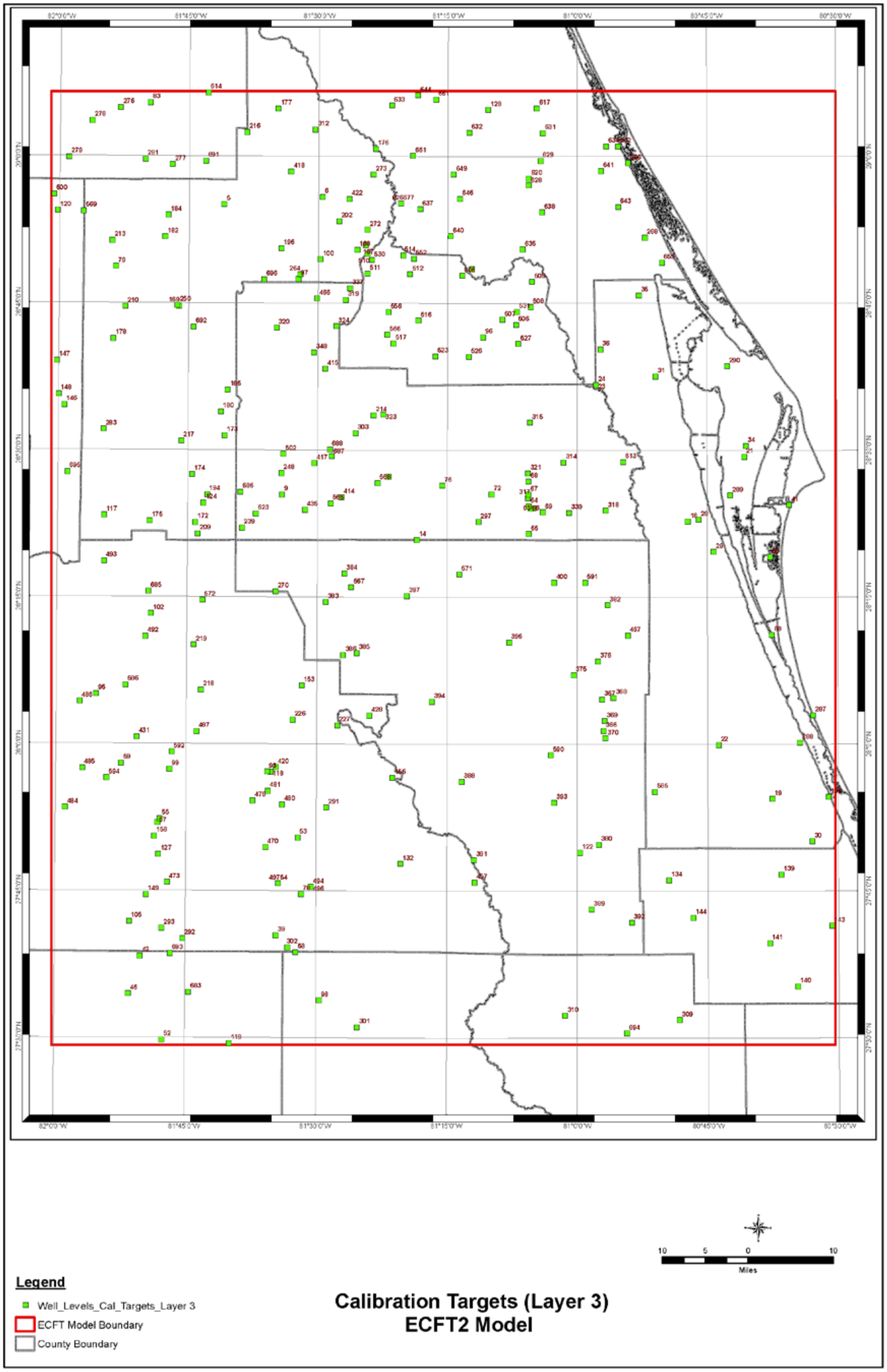

**Calibration Targets (Layer 3)
ECFT2 Model**

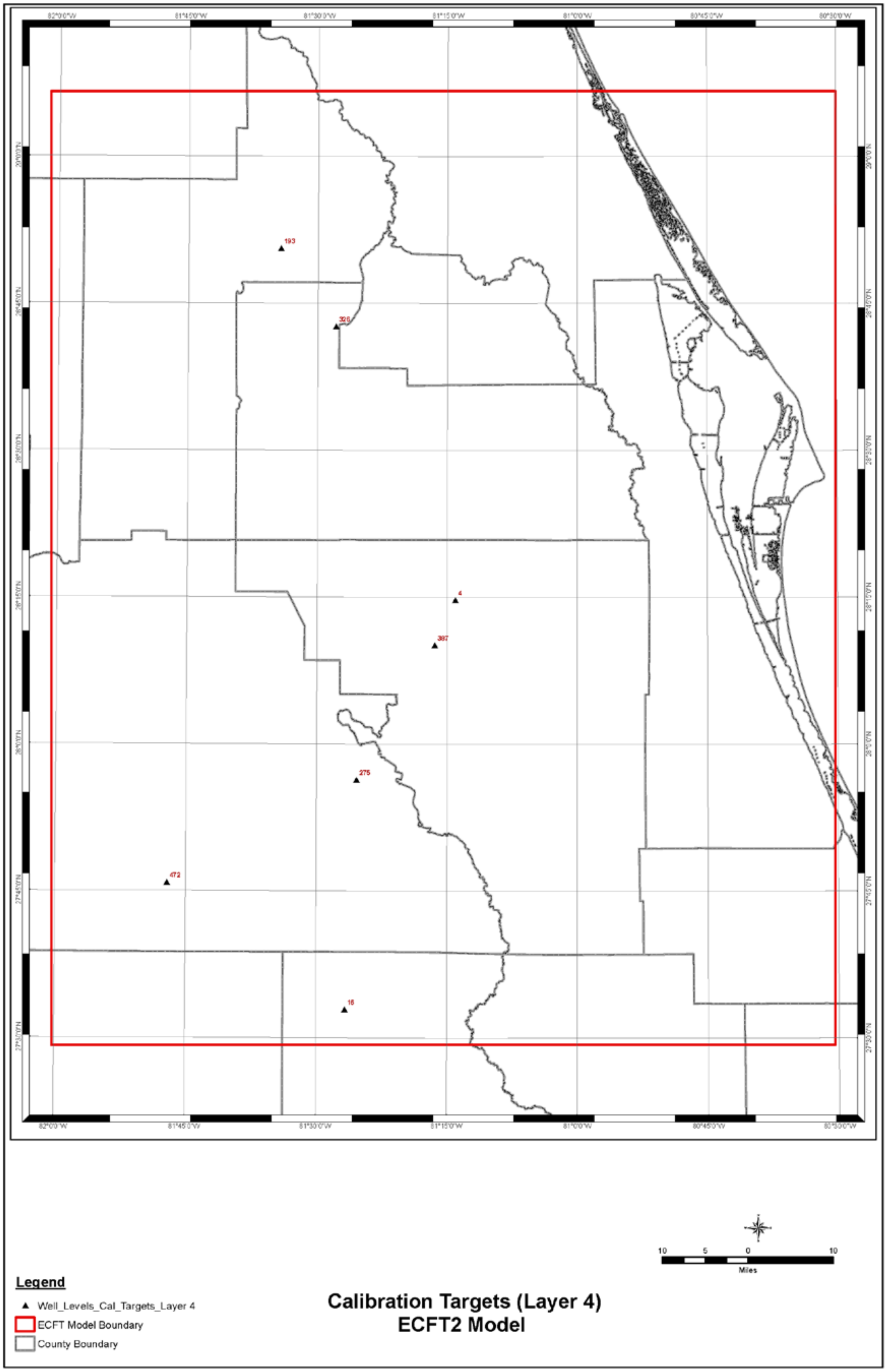

Calibration Targets (Layer 4)
ECFT2 Model

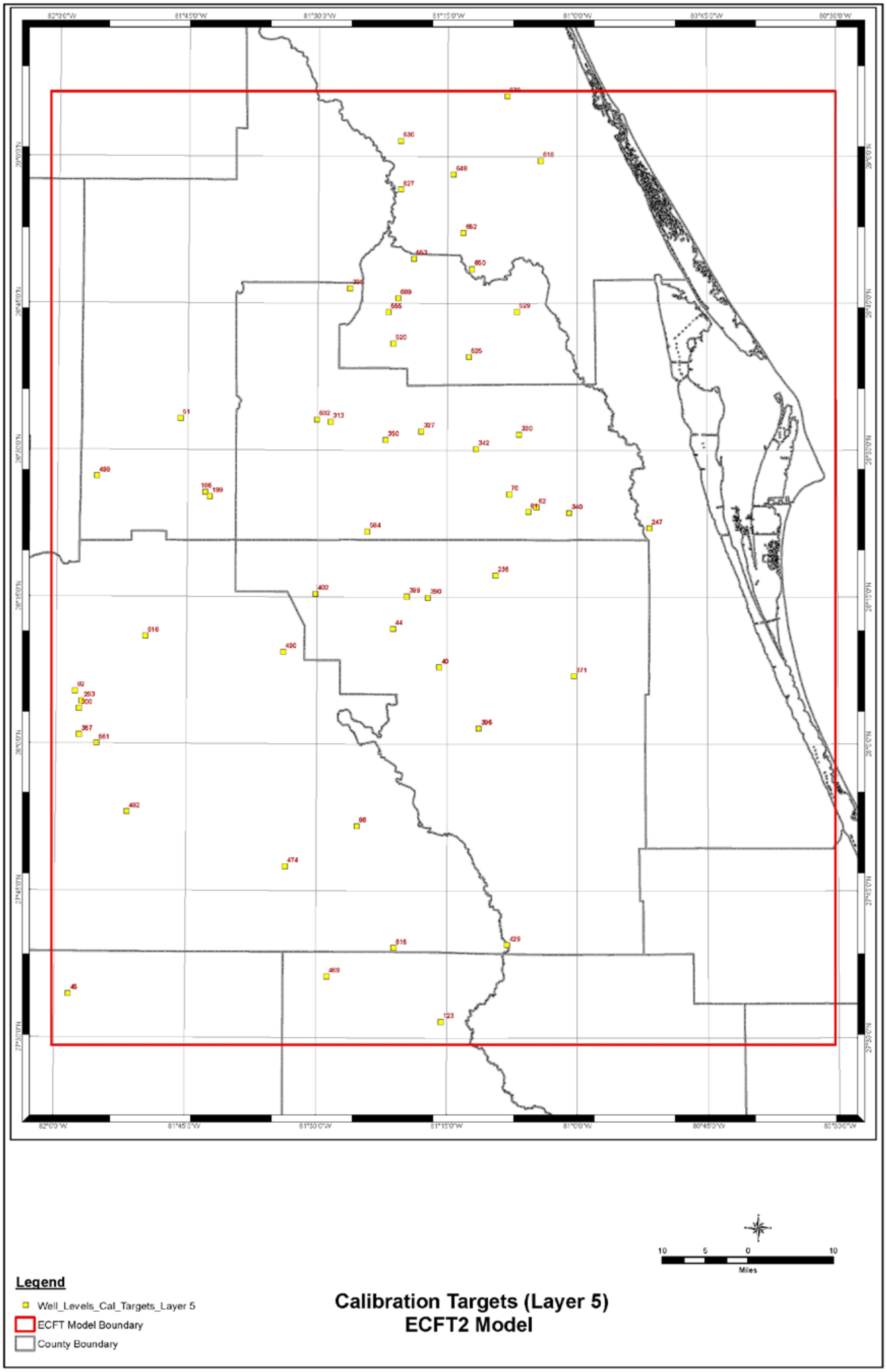

Calibration Targets (Layer 5)
ECFT2 Model

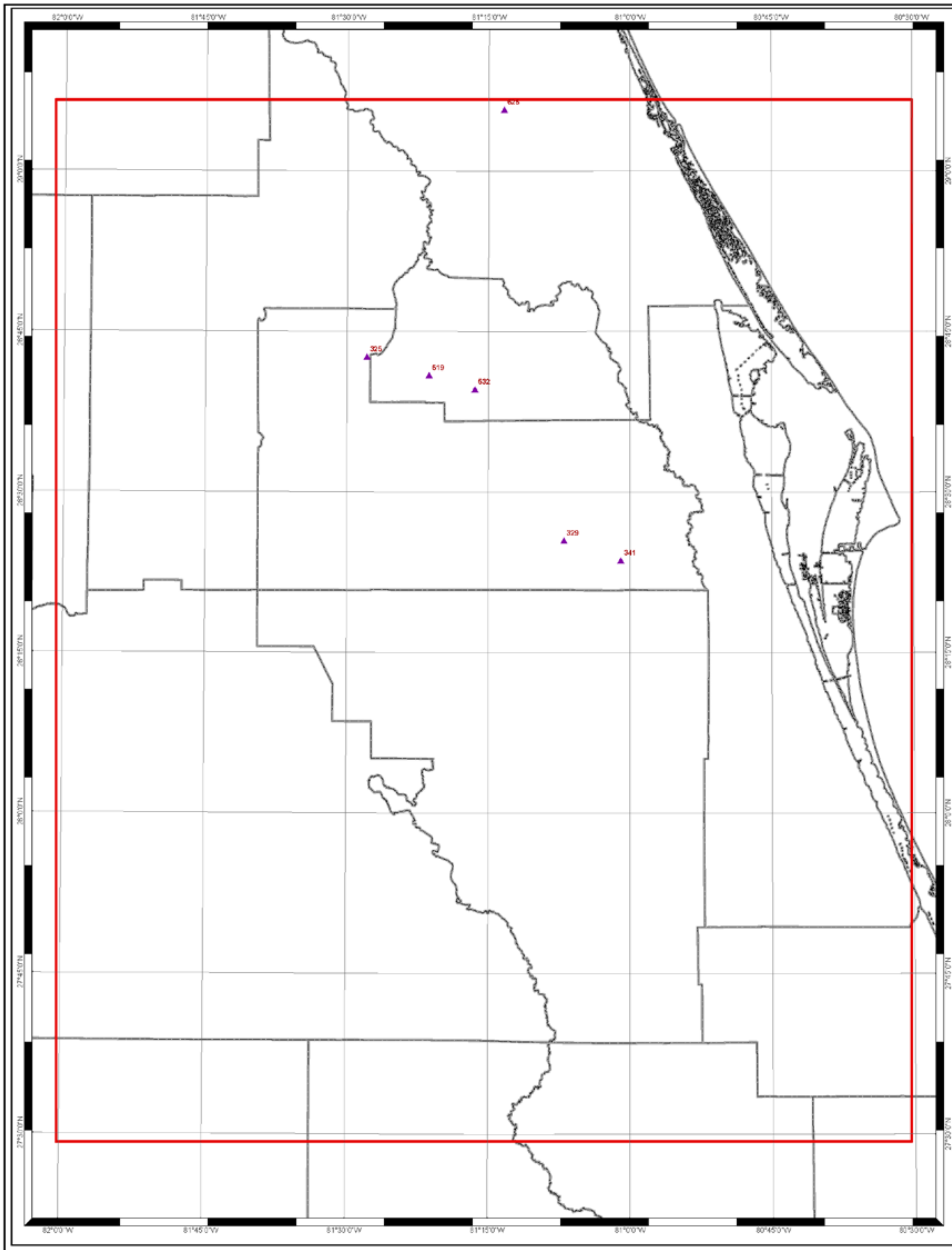

Calibration Targets (Layer 6)
ECFT2 Model

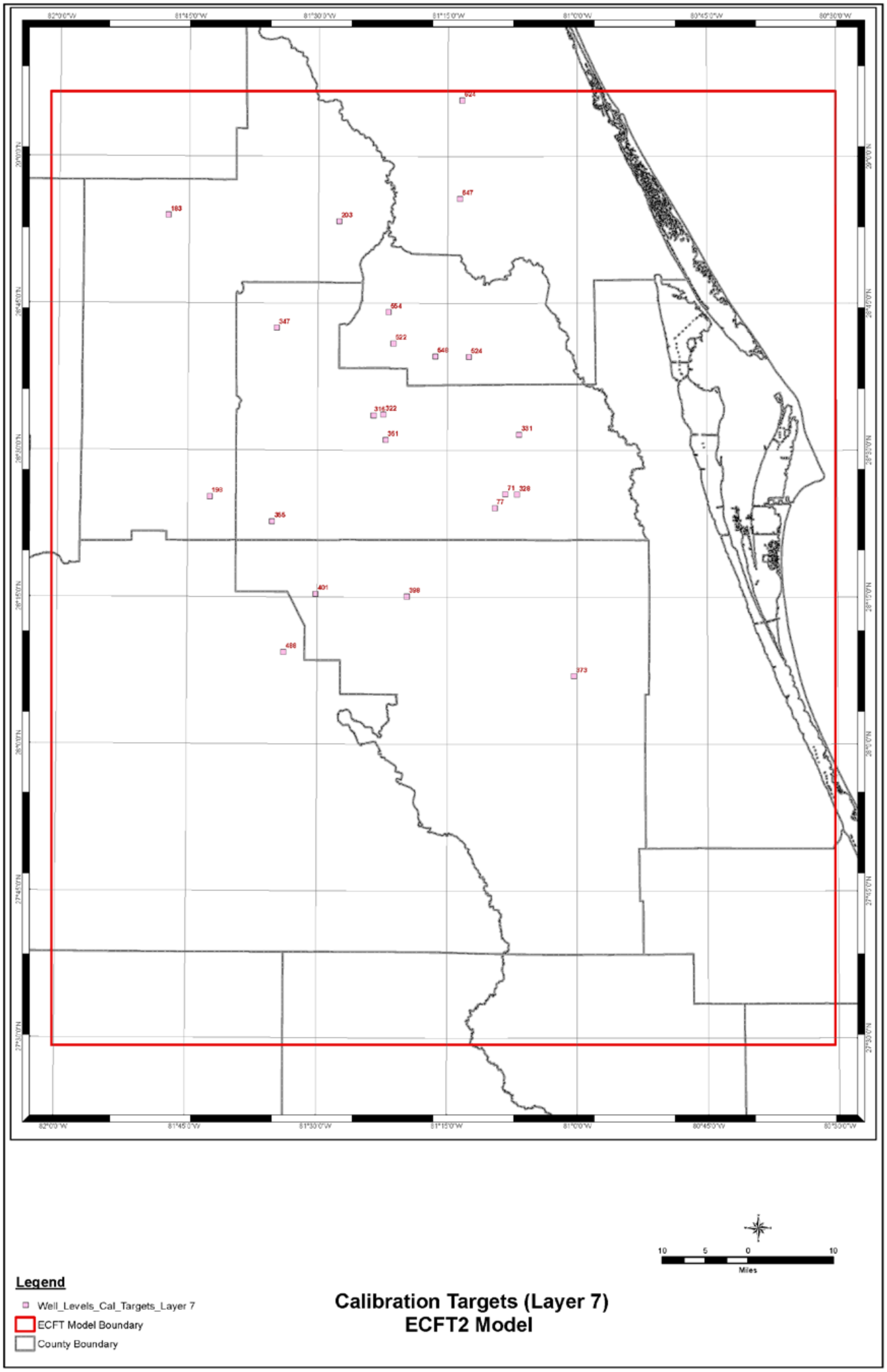

Calibration Targets (Layer 7)
ECFT2 Model

Table A-1. Coordinates and model layer of observation wells used in the USGS-ECFT and HAT-ECFT models.

WELL_ID	REFERENCE_ID	X_UTMW	Y_UTMW	LATITUDE	LONGITUDE	Layer
air19_g_s	1	465332.72	3141936.76	28° 24' 12.111"	-81° 21' 14.097"	1
all1w2	2	476096.51	3119233.18	28° 11' 55.192"	-81° 14' 36.829"	1
all2w2	3	476455.71	3119229.8	28° 11' 55.105"	-81° 14' 23.653"	1
bartow_sas	8	420074.58	3085651.16	27° 53' 36.009"	-81° 48' 43.487"	1
beekw2	10	478467.95	3117455.08	28° 10' 57.556"	-81° 13' 9.724"	1
beeline_g	11	482561.2	3147373.6	28° 27' 10.024"	-81° 10' 41.218"	1
blackw2	13	476074.08	3119692.51	28° 12' 10.117"	-81° 14' 37.686"	1
boggy_cres	15	469693.71	3135768.08	28° 20' 52.044"	-81° 18' 33.243"	1
br1548	26	525621.88	3133493.01	28° 19' 38.473"	-80° 44' 19.028"	1
br1549	27	522826.21	3139582.5	28° 22' 56.545"	-80° 46' 1.269"	1
br1661	32	513084.4	3169678.71	28° 39' 15.024"	-80° 51' 57.994"	1
br1940	37	504282.78	3171682.92	28° 40' 20.364"	-80° 57' 22.210"	1
buckhorn_c	38	434216.32	3043901.07	27° 31' 2.016"	-81° 39' 57.994"	1
castw2	43	486720.23	3116372.91	28° 10' 22.780"	-81° 8' 7.018"	1
chapman_g	48	480958.2	3097403.93	28° 0' 6.078"	-81° 11' 37.221"	1
chestw2	49	476897.66	3115645.68	28° 9' 58.659"	-81° 14' 7.187"	1
cl_sprsa	56	420710.59	3082591.21	27° 51' 56.711"	-81° 48' 19.489"	1
cocoa_g	73	486364.98	3144353.08	28° 25' 32.032"	-81° 8' 21.228"	1
cocoa_k	74	497384.15	3150376.62	28° 28' 48.020"	-81° 1' 36.217"	1
cocoa_m	75	490635.56	3143702.62	28° 25' 11.030"	-81° 5' 44.225"	1
combee_rdd	80	410806.55	3110707.22	28° 7' 8.072"	-81° 54' 29.277"	1
combee_rds	81	410779.01	3110676.63	28° 7' 7.072"	-81° 54' 30.278"	1
east_lksh	87	458261.63	3081799.47	27° 51' 37.101"	-81° 25' 26.256"	1
elmax_g	89	492384.52	3069822	27° 45' 10.110"	-81° 4' 38.213"	1
englewoods	90	470562.72	3156660.16	28° 32' 11.019"	-81° 18' 3.242"	1
ep_claymon	91	420666.9	3066725.37	27° 43' 21.125"	-81° 48' 17.287"	1
ep_moncw1	92	425596.48	3066786.53	27° 43' 24.127"	-81° 45' 17.283"	1
exotgw	94	488702.93	3114461.82	28° 9' 20.741"	-81° 6' 54.241"	1
fussell_sh	103	419532.5	3122031.38	28° 13' 18.056"	-81° 49' 12.272"	1
gac_g	104	475821.42	3069074.32	27° 44' 45.105"	-81° 14' 43.225"	1
griffith_g	107	506963.94	3041238.11	27° 29' 41.146"	-80° 55' 46.205"	1
gs_1_upl_s	108	407210.01	3137603.47	28° 21' 41.113"	-81° 56' 48.798"	1
gs_2_upl_s	109	407088.76	3140885.23	28° 23' 27.713"	-81° 56' 54.200"	1
gs_3_upl_s	110	408970.17	3139217.81	28° 22' 34.011"	-81° 55' 44.599"	1
gs_4_upl_s	111	408779.49	3140961.23	28° 23' 30.611"	-81° 55' 52.099"	1
gs_4_wtl_s	112	408842.4	3141000.74	28° 23' 31.911"	-81° 55' 49.799"	1
gs_5_upl_s	113	405826.27	3143317.39	28° 24' 46.413"	-81° 57' 41.300"	1
gs_6_upl_s	114	404835.87	3141306.38	28° 23' 40.814"	-81° 58' 17.101"	1
gs_b_upl_s	115	406528.13	3144330.48	28° 25' 19.512"	-81° 57' 15.802"	1

WELL_ID	REFERENCE_ID	X_UTMW	Y_UTMW	LATITUDE	LONGITUDE	Layer
gs_b_wtl_s	116	406595.96	3144299.25	28° 25' 18.515"	-81° 57' 13.300"	1
hayman_w1	121	502209.93	3078373.74	27° 49' 48.107"	-80° 58' 39.222"	1
hiloche_b	125	429610.8	3142462.01	28° 24' 24.011"	-81° 43' 6.995"	1
hiloche_m	126	429558.54	3142831.58	28° 24' 36.010"	-81° 43' 8.996"	1
ic_sas	130	450583.5	3125656.57	28° 15' 21.371"	-81° 30' 13.646"	1
ir0025	133	520899.22	3059191.91	27° 39' 24.130"	-80° 47' 17.207"	1
ir0900	137	547971.61	3063016.03	27° 41' 25.921"	-80° 30' 48.558"	1
ir0902	138	541589.49	3051579.64	27° 35' 15.012"	-80° 34' 42.990"	1
ivanhoe_s	145	462609.42	3159606.28	28° 33' 46.017"	-81° 22' 56.247"	1
kenans1_g	152	498217.49	3084896.62	27° 53' 20.095"	-81° 1' 5.209"	1
kirchoff	154	458838.43	3114167.99	28° 9' 9.057"	-81° 25' 9.231"	1
kircof	155	458338.63	3114439.03	28° 9' 17.808"	-81° 25' 27.591"	1
kissengen1	157	420136.02	3080062.38	27° 50' 34.412"	-81° 48' 39.887"	1
krcffm	159	481649.76	3040790.17	27° 29' 26.205"	-81° 11' 8.771"	1
krcnnd	160	481445.6	3040673.84	27° 29' 22.415"	-81° 11' 16.205"	1
kreffm	161	482177.87	3069401.49	27° 44' 56.096"	-81° 10' 51.050"	1
krennm1	163	482546.82	3069592.58	27° 45' 2.324"	-81° 10' 37.582"	1
krfffm	164	480868.19	3073676.18	27° 47' 14.955"	-81° 11' 39.139"	1
krfnnm	166	481012.75	3073768.89	27° 47' 17.975"	-81° 11' 33.862"	1
l_0044	170	432756.95	3160045.42	28° 33' 55.956"	-81° 41' 15.071"	1
l_0050	171	427927.66	3139198.62	28° 22' 37.641"	-81° 44' 8.118"	1
l_0289	181	422283.25	3193018.17	28° 51' 45.193"	-81° 47' 48.664"	1
l_0693	187	410598.56	3163342.47	28° 35' 38.270"	-81° 54' 51.522"	1
l_0695	188	457137.13	3207263.02	28° 59' 33.948"	-81° 26' 24.147"	1
l_0696	189	413739.78	3203077.53	28° 57' 10.056"	-81° 53' 6.761"	1
l_0697	190	417488.25	3155191.53	28° 31' 15.073"	-81° 50' 35.775"	1
l_0701	191	443722.69	3190048.88	28° 50' 12.745"	-81° 34' 36.806"	1
l_0703	192	422897.79	3197123.61	28° 53' 58.716"	-81° 47' 26.993"	1
l_0710	195	430152.54	3144436.74	28° 25' 28.282"	-81° 42' 47.516"	1
l_0714	196	444177.97	3190795.64	28° 50' 37.081"	-81° 34' 20.138"	1
l_0797	200	429395.35	3142832.56	28° 24' 36.010"	-81° 43' 14.994"	1
l_0829	204	440977.59	3208029.21	28° 59' 56.519"	-81° 36' 21.497"	1
l_0841	205	448578.02	3202539.4	28° 56' 59.328"	-81° 31' 39.688"	1
l_0851	206	446004.78	3199925.31	28° 55' 34.008"	-81° 33' 14.296"	1
l_0869	207	462494.07	3193563.65	28° 52' 9.420"	-81° 23' 4.524"	1
l_0872	208	418310.54	3149452.11	28° 28' 8.772"	-81° 50' 4.056"	1
l_0926	212	412303.94	3192373.7	28° 51' 21.937"	-81° 53' 56.802"	1
lakweo_g	215	456787.46	3076684.64	27° 48' 50.710"	-81° 26' 19.492"	1
lk_alfsha	220	427538.07	3116163.79	28° 10' 9.064"	-81° 44' 17.267"	1
lk_gelses	221	427037.87	3105734.84	28° 4' 30.076"	-81° 44' 33.272"	1
lk_geunes	222	427095.51	3106226.91	28° 4' 46.077"	-81° 44' 31.271"	1
lk_geunw	223	426523.04	3106353.5	28° 4' 50.077"	-81° 44' 52.273"	1

WELL_ID	REFERENCE_ID	X_UTMW	Y_UTMW	LATITUDE	LONGITUDE	Layer
lk_geuss	224	426682.3	3105613.94	28° 4' 26.077"	-81° 44' 46.272"	1
lk_geuws	225	426220.4	3105955.33	28° 4' 37.078"	-81° 45' 3.271"	1
lk_holes	228	407804.05	3099959.22	28° 1' 18.090"	-81° 56' 16.283"	1
lk_holns	229	407237.51	3100855.97	28° 1' 47.087"	-81° 56' 37.282"	1
lk_holws	230	406388.61	3100554.92	28° 1' 37.090"	-81° 57' 8.282"	1
lk_houes	231	408077.63	3100018.6	28° 1' 20.088"	-81° 56' 6.282"	1
lk_houne	232	407837.06	3100697.57	28° 1' 42.090"	-81° 56' 15.282"	1
lk_hounw	233	406666.74	3101198.96	28° 1' 58.088"	-81° 56' 58.281"	1
lk_houses	234	406460.65	3099292.62	28° 0' 56.092"	-81° 57' 5.283"	1
lk_houws	235	406033.14	3100496.11	28° 1' 35.089"	-81° 57' 21.282"	1
lk_kisssh	237	465180.53	3091193.13	27° 56' 43.090"	-81° 21' 14.250"	1
lk_mcleod	238	426749.16	3094227.74	27° 58' 16.091"	-81° 44' 41.275"	1
lk_oli_sh	240	436709.19	3138083.4	28° 22' 3.038"	-81° 38' 45.262"	1
lk_olle	241	446335.39	3056553.75	27° 37' 55.133"	-81° 32' 38.268"	1
lk_ollne	242	446309.42	3056861.48	27° 38' 5.130"	-81° 32' 39.265"	1
lk_olunw	243	445789.26	3056986.96	27° 38' 9.134"	-81° 32' 58.266"	1
lk_olus	244	446112.9	3055816.23	27° 37' 31.133"	-81° 32' 46.267"	1
lk_olusw	245	445539.59	3056311.05	27° 37' 47.131"	-81° 33' 7.266"	1
lk_oluw	246	445431.49	3056650.05	27° 37' 58.133"	-81° 33' 11.266"	1
lkba1a	251	485005.68	3062879.05	27° 41' 24.244"	-81° 9' 7.457"	1
lkba2a	252	481434.98	3069129.44	27° 44' 47.218"	-81° 11' 18.172"	1
lkba2b	253	481874.75	3069352.64	27° 44' 54.494"	-81° 11' 2.120"	1
lkba3a	254	480500.72	3071655.95	27° 46' 9.280"	-81° 11' 52.448"	1
lkba3b	255	481306	3072089.9	27° 46' 23.424"	-81° 11' 23.051"	1
lkbb1a	256	478206.89	3045763.43	27° 32' 7.655"	-81° 13' 14.565"	1
lkbb2a	257	481657.91	3050107.14	27° 34' 29.010"	-81° 11' 8.983"	1
lkbb2b	258	482531.06	3047683.47	27° 33' 10.282"	-81° 10' 37.011"	1
lkbb3a5	259	484546.3	3052483.74	27° 35' 46.380"	-81° 9' 23.747"	1
lkbb3b_gw2	260	486805.89	3051340.16	27° 35' 9.299"	-81° 8' 1.275"	1
lkbc3a	261	479137.17	3041613.13	27° 29' 52.821"	-81° 12' 40.391"	1
lkbc3b	262	482371.39	3040813.14	27° 29' 26.986"	-81° 10' 42.473"	1
lkst_stlne	265	442535.22	3093033.99	27° 57' 40.089"	-81° 35' 3.263"	1
lkst_wts9	267	442803.24	3091955.74	27° 57' 5.091"	-81° 34' 53.266"	1
lotela_g	269	457035.56	3052018.97	27° 35' 29.135"	-81° 26' 7.239"	1
loughmans	271	443052.94	3126082.25	28° 15' 34.108"	-81° 34' 50.090"	1
m_0481	280	418579.85	3207691.61	28° 59' 41.111"	-81° 50' 9.173"	1
mako	282	477648.92	3127632.04	28° 16' 28.226"	-81° 13' 40.465"	1
mascottes	284	410636.37	3156778.59	28° 32' 5.009"	-81° 54' 48.288"	1
maxcey_n_g	285	497666.29	3062158.51	27° 41' 1.120"	-81° 1' 25.210"	1
maxcey_s_g	286	490093.3	3046409.2	27° 32' 29.143"	-81° 6' 1.219"	1
moon1w2	294	477524.61	3116072.2	28° 10' 12.559"	-81° 13' 44.226"	1
moon2w2	295	477537.15	3115749.7	28° 10' 2.080"	-81° 13' 43.744"	1

WELL_ID	REFERENCE_ID	X_UTMW	Y_UTMW	LATITUDE	LONGITUDE	Layer
mosspk_s	298	481296.96	3139128.67	28° 22' 42.032"	-81° 11' 27.222"	1
mr_0162	299	456085.65	3129440.7	28° 17' 25.043"	-81° 26' 52.231"	1
oak_hill_p	304	413187.53	3095546.57	27° 58' 56.010"	-81° 52' 57.988"	1
oak_hill_s	305	413487.63	3095482.91	27° 58' 54.012"	-81° 52' 46.986"	1
obs_well27	307	435415.43	3125442.66	28° 15' 12.054"	-81° 39' 30.261"	1
ok_3_g	308	519174.6	3041005.1	27° 29' 33.150"	-80° 48' 21.195"	1
or0649	332	488993.37	3155598.02	28° 31' 37.536"	-81° 6' 44.997"	1
or0650	333	457180.95	3183289.84	28° 46' 34.990"	-81° 26' 19.251"	1
or0661	336	450315.12	3171180.83	28° 40' 0.637"	-81° 30' 30.562"	1
or0665	338	480822.15	3152843.36	28° 30' 7.680"	-81° 11' 45.489"	1
or0713	343	504263.4	3150100.11	28° 28' 39.019"	-80° 57' 23.213"	1
or0714	344	490639.22	3148287.6	28° 27' 40.024"	-81° 5' 44.224"	1
or0715	345	505382.29	3141176.87	28° 23' 49.033"	-80° 56' 42.213"	1
or0722	346	470304.18	3151152.55	28° 29' 12.026"	-81° 18' 12.243"	1
or0830	352	507876.02	3154803.4	28° 31' 11.796"	-80° 55' 10.233"	1
or0833	353	503460.21	3158111.49	28° 32' 59.364"	-80° 57' 52.665"	1
or0834	354	503460.43	3157349.29	28° 32' 34.596"	-80° 57' 52.666"	1
ors_0029	358	439391.21	3140807.94	28° 23' 32.027"	-81° 37' 7.246"	1
ors_4	359	442413.02	3139306.16	28° 22' 43.719"	-81° 35' 15.937"	1
ors_5	360	484182.65	3140936.4	28° 23' 40.914"	-81° 9' 41.281"	1
ors_6	361	450621.35	3136461.47	28° 21' 12.488"	-81° 30' 13.911"	1
os_181_g	362	484181.29	3118815.46	28° 11' 42.055"	-81° 9' 40.247"	1
os_182_g	363	487213.21	3072811.1	27° 46' 47.112"	-81° 7' 47.242"	1
os_183_g	364	498133.44	3075942.87	27° 48' 29.107"	-81° 1' 8.232"	1
os0024	372	499284.39	3110056.65	28° 6' 57.756"	-81° 0' 26.240"	1
os0171	377	509010.51	3129301.3	28° 17' 23.045"	-80° 54' 29.209"	1
os0179	378	509135.03	3108900.54	28° 6' 20.073"	-80° 54' 25.212"	1
os0232	381	504022.24	3078256.1	27° 49' 44.268"	-80° 57' 32.971"	1
osf62_gw2	404	495585.25	3086202.76	27° 54' 2.521"	-81° 2' 41.505"	1
osf64_gw1	405	472526.44	3105254.08	28° 4' 20.659"	-81° 16' 46.604"	1
osf66_gw1	407	481347.73	3100234.31	28° 1' 38.080"	-81° 11' 23.120"	1
osf70_gw1	408	467806.68	3125201.94	28° 15' 8.521"	-81° 19' 41.504"	1
oss_102	409	437886.12	3134371.21	28° 20' 2.615"	-81° 38' 1.309"	1
oss_71	410	456028.39	3129468.5	28° 17' 25.940"	-81° 26' 54.337"	1
oss_73	411	480469.82	3075401.65	27° 48' 11.010"	-81° 11' 53.798"	1
oss_74	412	486762.95	3059331.17	27° 39' 29.005"	-81° 8' 3.158"	1
oss_76	413	510236.92	3063612.68	27° 41' 48.247"	-80° 53' 46.235"	1
p_49	416	468746.99	3075490.72	27° 48' 13.106"	-81° 19' 2.247"	1
peavine_g	419	497690.78	3047297.56	27° 32' 58.138"	-81° 1' 24.213"	1
pine_isl_g	421	487580.88	3110072.6	28° 6' 58.066"	-81° 7' 35.215"	1
po0002	425	435772.59	3119673.63	28° 12' 4.652"	-81° 39' 16.010"	1
po0023	426	431554.83	3112077.28	28° 7' 57.044"	-81° 41' 49.117"	1

WELL_ID	REFERENCE_ID	X_UTMW	Y_UTMW	LATITUDE	LONGITUDE	Layer
po0024	427	431906.95	3112169.43	28° 8' 0.104"	-81° 41' 36.229"	1
poinci_g	430	452337.54	3132163.07	28° 18' 53.038"	-81° 29' 10.233"	1
pos_12	432	460737.33	3102622.36	28° 2' 54.067"	-81° 23' 58.218"	1
prescott_s	434	430621.9	3045217.39	27° 31' 44.149"	-81° 42' 9.284"	1
reedgw10_g	436	443599.88	3127339.27	28° 16' 15.040"	-81° 34' 30.236"	1
ribs_ii_15	437	439309	3140777.89	28° 23' 31.037"	-81° 37' 10.261"	1
ribs_ii_16	438	439710.86	3139544.92	28° 22' 51.039"	-81° 36' 55.263"	1
ridge_clp3	439	447466.49	3079931.06	27° 50' 35.012"	-81° 32' 0.692"	1
ridge_clp5	440	448202.32	3078663.15	27° 49' 53.911"	-81° 31' 33.591"	1
ridge_clp7	441	446937.48	3075930.01	27° 48' 24.912"	-81° 32' 19.390"	1
ridge_h_1	442	448351.65	3057190.67	27° 38' 16.116"	-81° 31' 24.794"	1
ridge_h_2	443	447825.48	3053331.14	27° 36' 10.613"	-81° 31' 43.392"	1
ridge_h_5	444	459367.84	3044349.48	27° 31' 20.140"	-81° 24' 41.236"	1
ridge_p_1	445	420479.59	3114120.55	28° 9' 1.207"	-81° 48' 35.589"	1
ridge_p_4	446	435974.07	3124081.04	28° 14' 27.906"	-81° 39' 9.490"	1
ridge_p_5	447	438201.48	3113218.54	28° 8' 35.308"	-81° 37' 45.689"	1
ridge_p_6	448	440393.3	3107502.06	28° 5' 29.909"	-81° 36' 24.290"	1
ridge_p_8	449	442015.93	3095422	27° 58' 57.610"	-81° 35' 22.690"	1
ridge_vc_1	450	447714.1	3081514.66	27° 51' 26.510"	-81° 31' 51.890"	1
ridge_vc_2	451	446128.71	3075936.35	27° 48' 25.002"	-81° 32' 48.950"	1
ridge_vc_4	452	446117.79	3074345.76	27° 47' 33.310"	-81° 32' 49.090"	1
ridge_vc_5	453	450524.18	3071757.62	27° 46' 9.811"	-81° 30' 7.681"	1
ridge_vc_7	454	445503.24	3088538.58	27° 55' 14.450"	-81° 33' 13.890"	1
ridge_vc_9	455	441923.83	3102678.83	28° 2' 53.417"	-81° 35' 27.349"	1
ridge_vc12	456	444720.92	3093107.8	27° 57' 42.820"	-81° 33' 43.280"	1
rlnw_nrsd	459	423294.35	3096588.03	27° 59' 32.089"	-81° 46' 48.277"	1
rnd_rolsw	460	433573.34	3093111.04	27° 57' 41.092"	-81° 40' 31.272"	1
rnd_roue	461	434066.17	3093292.99	27° 57' 47.092"	-81° 40' 13.272"	1
rnd_roun	462	433767.21	3093571.58	27° 57' 56.092"	-81° 40' 24.270"	1
rnd_rounw	463	433492.94	3093388.43	27° 57' 50.091"	-81° 40' 34.271"	1
rnd_rouse	464	433900.95	3093047.75	27° 57' 39.094"	-81° 40' 19.270"	1
rock_k_g	465	517042.74	3048240.53	27° 33' 28.406"	-80° 49' 38.522"	1
romp_101_s	468	409396.38	3147936.68	28° 27' 17.412"	-81° 55' 31.403"	1
romp_44_nr	471	441105.3	3077895.61	27° 49' 27.912"	-81° 35' 52.891"	1
romp_55_sa	475	444803.78	3074253.2	27° 47' 30.109"	-81° 33' 37.092"	1
romp_57_nr	478	438739.77	3086683.51	27° 54' 13.110"	-81° 37' 20.990"	1
romp_57a_n	479	444271.84	3085872.01	27° 53' 47.611"	-81° 33' 58.490"	1
romp_74x_s	489	444506.59	3114689.22	28° 9' 24.107"	-81° 33' 54.790"	1
romp_76_sa	491	418474.78	3117716.36	28° 10' 57.610"	-81° 49' 49.990"	1
romp_cl_2s	495	449666.75	3070336.46	27° 45' 23.512"	-81° 30' 38.792"	1
romp_cl_3s	498	443519.1	3071034.3	27° 45' 45.310"	-81° 34' 23.489"	1
romp_wr_3s	501	401327.62	3201152.51	28° 56' 4.281"	-82° 0' 44.646"	1

WELL_ID	REFERENCE_ID	X_UTMW	Y_UTMW	LATITUDE	LONGITUDE	Layer
rue_nrsd	503	424029.34	3096183.32	27° 59' 19.089"	-81° 46' 21.276"	1
run_nrsd	504	423431.34	3096648.75	27° 59' 34.090"	-81° 46' 43.276"	1
rusw_nrsd	505	422936.49	3096159.61	27° 59' 18.092"	-81° 47' 1.277"	1
s_0266	515	491426.32	3184442.41	28° 47' 14.904"	-81° 5' 16.258"	1
s_1015	518	465278.04	3172850.56	28° 40' 56.652"	-81° 21' 19.474"	1
s_1023	521	488392.64	3176286.65	28° 42' 49.800"	-81° 7' 7.857"	1
s_1211	528	479500.21	3170277.64	28° 39' 34.140"	-81° 12' 35.241"	1
s_1275	533	457111.26	3173610.07	28° 41' 20.449"	-81° 26' 20.506"	1
s_1276	534	455885.43	3171081.99	28° 39' 58.153"	-81° 27' 5.326"	1
s_1277	535	463637.01	3169180.72	28° 38' 57.240"	-81° 22' 19.521"	1
s_1278	536	466747.93	3168911.09	28° 38' 48.780"	-81° 20' 24.897"	1
s_1279	537	471354	3166128.1	28° 37' 18.744"	-81° 17' 34.977"	1
s_1280	538	472500.6	3169012.44	28° 38' 52.560"	-81° 16' 53.001"	1
s_1281	539	467616.97	3174973.17	28° 42' 5.844"	-81° 19' 53.505"	1
s_1286	540	481150.36	3171300.74	28° 40' 7.476"	-81° 11' 34.509"	1
s_1288	541	488585.53	3178779.17	28° 44' 10.800"	-81° 7' 0.837"	1
s_1291	542	469132.29	3170286.06	28° 39' 33.672"	-81° 18' 57.201"	1
s_1292	543	474439.7	3173098.29	28° 41' 5.472"	-81° 15' 41.901"	1
s_1293	544	473997.97	3167327.27	28° 37' 57.912"	-81° 15' 57.705"	1
s_1297	545	463666.02	3175358.19	28° 42' 17.976"	-81° 22' 19.162"	1
s_1301	546	488783.77	3172712.29	28° 40' 53.664"	-81° 6' 53.313"	1
s_1310	547	461238.79	3188561.12	28° 49' 26.736"	-81° 23' 50.243"	1
s_1337	549	473196.68	3170397.88	28° 39' 37.632"	-81° 16' 27.477"	1
s_1386	551	469126.69	3188794.45	28° 49' 35.088"	-81° 18' 59.218"	1
s_1477	557	469974.67	3177133.87	28° 43' 16.260"	-81° 18' 26.817"	1
saddle_sbn	559	443259.08	3060967.75	27° 40' 18.128"	-81° 34' 31.271"	1
saddle_sbs	560	443558.48	3060535.57	27° 40' 4.128"	-81° 34' 20.269"	1
sas_or_pk	562	462905.08	3141357.2	28° 23' 53.038"	-81° 22' 43.248"	1
sas_tibet	563	446899.41	3146311.21	28° 26' 32.030"	-81° 32' 32.258"	1
sas_trkyl	564	452641.47	3153733.92	28° 30' 34.026"	-81° 29' 2.257"	1
snively_g	570	458933.34	3094135.82	27° 58' 18.080"	-81° 25' 3.233"	1
spread_rsh	573	429251.4	3124523.69	28° 14' 41.051"	-81° 43' 16.265"	1
sungw	575	471470.38	3116567.59	28° 10' 28.237"	-81° 17' 26.288"	1
swim_swln	576	452700.47	3086343.19	27° 54' 4.094"	-81° 28' 50.257"	1
swim_swun	577	452618.75	3086435.89	27° 54' 7.097"	-81° 28' 53.260"	1
swim_swus	578	452863.71	3086158	27° 53' 58.097"	-81° 28' 44.259"	1
swim_swuw	579	452563.04	3086159.18	27° 53' 58.097"	-81° 28' 55.258"	1
taft_g	580	463625.98	3145570.53	28° 26' 10.026"	-81° 22' 17.233"	1
tb1_g	581	447088.13	3146438.16	28° 26' 36.183"	-81° 32' 25.341"	1
tb2_g	582	447418.72	3146747.44	28° 26' 46.281"	-81° 32' 13.238"	1
tb3_g	583	447558.12	3146981.13	28° 26' 53.895"	-81° 32' 8.151"	1
tenoroc_rp	588	413219.36	3108566.01	28° 5' 59.074"	-81° 53' 0.277"	1

WELL_ID	REFERENCE_ID	X_UTMW	Y_UTMW	LATITUDE	LONGITUDE	Layer
tenoroc_sa	589	414692.74	3108524.71	28° 5' 58.077"	-81° 52' 6.276"	1
tick_isl_g	593	481615.11	3062418.27	27° 41' 9.118"	-81° 11' 11.221"	1
toho1_gw	595	469342.19	3116500.97	28° 10' 25.900"	-81° 18' 44.328"	1
toho10_gw	597	465609.02	3119683.12	28° 12' 8.978"	-81° 21' 1.570"	1
toho12_gw	598	471207.42	3134101.59	28° 19' 58.012"	-81° 17' 37.492"	1
toho13_gw	599	475510.72	3128147.73	28° 16' 44.848"	-81° 14' 58.991"	1
toho14_gw	600	473699.76	3113214.61	28° 8' 39.441"	-81° 16' 4.258"	1
toho15_gw	601	474578.42	3118025.61	28° 11' 15.847"	-81° 15' 32.420"	1
toho16_w1	602	473355.04	3115736.82	28° 10' 1.381"	-81° 16' 17.103"	1
toho2_gw	604	469842.75	3116275.03	28° 10' 18.599"	-81° 18' 25.950"	1
toho3_gw	605	464374.91	3110417.13	28° 7' 7.745"	-81° 21' 45.825"	1
toho4_gw	606	461612.27	3113496.5	28° 8' 47.536"	-81° 23' 27.449"	1
toho6_gw	608	458340.64	3118803.79	28° 11' 39.648"	-81° 25' 28.077"	1
toho7_gw	609	458413.39	3130078.73	28° 17' 46.050"	-81° 25' 26.858"	1
toho8_gw	610	459716.69	3129980.51	28° 17' 43.004"	-81° 24' 38.996"	1
toho9_gw	611	465684.41	3130050.04	28° 17' 45.874"	-81° 20' 59.904"	1
tosohatchd	612	508695.2	3150656.42	28° 28' 57.018"	-80° 54' 40.207"	1
usgs_oweva	621	419277.36	3139481.4	28° 22' 45.011"	-81° 49' 25.996"	1
v_0813	654	473335.76	3218793.14	29° 5' 50.184"	-81° 16' 26.471"	1
v_0821	656	480161.67	3186843.69	28° 48' 32.484"	-81° 12' 11.913"	1
v_0836	658	515859.04	3188080.64	28° 49' 12.876"	-80° 50' 14.854"	1
v_1032	662	504036.31	3186435.25	28° 48' 19.740"	-80° 57' 31.102"	1
v_1034	664	499756.39	3186596.3	28° 48' 24.996"	-81° 0' 8.998"	1
v_1035	665	514505.23	3192402.97	28° 51' 33.384"	-80° 51' 4.606"	1
v_1037	667	514940.97	3192578.57	28° 51' 39.072"	-80° 50' 48.514"	1
v_1039	668	512805.97	3192631.41	28° 51' 40.872"	-80° 52' 7.318"	1
v_1040	669	484042.38	3193933.76	28° 52' 23.064"	-81° 9' 49.102"	1
v_1056	670	465808.56	3216108.61	29° 4' 22.308"	-81° 21' 4.645"	1
v_1059	671	467419.71	3217577.49	29° 5' 10.188"	-81° 20' 5.208"	1
v_1060	672	471070.12	3218308.92	29° 5' 34.272"	-81° 17' 50.244"	1
v_1062	673	473849.89	3218937.1	29° 5' 54.900"	-81° 16' 7.463"	1
v_1064	675	463971.87	3219829.19	29° 6' 23.016"	-81° 22' 13.009"	1
v_1096	678	486768.11	3219463.35	29° 6' 12.720"	-81° 8' 9.563"	1
v_4037	680	465687.39	3199930.91	28° 55' 36.636"	-81° 21' 7.344"	1
v_4042	681	478463.09	3189087.98	28° 49' 45.311"	-81° 13' 14.733"	1
wr11_gw1	697	460258.91	3106531.88	28° 5' 1.064"	-81° 24' 16.218"	1
wr15_gw1	698	461677.6	3106373.38	28° 4' 56.063"	-81° 23' 24.216"	1
wr16_gw1	699	461457.71	3105881.79	28° 4' 40.065"	-81° 23' 32.215"	1
wr6_gw1	700	459478.9	3109888.57	28° 6' 50.061"	-81° 24' 45.216"	1
wr8_gw1	701	459011.95	3108997.72	28° 6' 21.059"	-81° 25' 2.218"	1
bartow_ha	7	420071.83	3085651.17	27° 53' 36.009"	-81° 48' 43.587"	2
bithlo_2	12	491000.14	3157857.44	28° 32' 51.013"	-81° 5' 31.222"	2

WELL_ID	REFERENCE_ID	X_UTMW	Y_UTMW	LATITUDE	LONGITUDE	Layer
br0001	17	514116.7	3164530.59	28° 36' 27.696"	-80° 51' 20.194"	2
br0586	20	520385.15	3151766.36	28° 29' 32.616"	-80° 47' 30.189"	2
br1547	25	525621.88	3133493.01	28° 19' 38.473"	-80° 44' 19.028"	2
br1744	33	503488.48	3164986.78	28° 36' 42.780"	-80° 57' 51.550"	2
cfind_uf_6	47	415212.94	3050363.15	27° 34' 28.216"	-81° 51' 32.293"	2
church_god	50	413727.15	3181499.75	28° 45' 28.984"	-81° 53' 1.295"	2
dresslers	84	455476.29	3053101.46	27° 36' 4.134"	-81° 27' 4.260"	2
drphillips	85	415682.72	3163081.19	28° 35' 31.006"	-81° 51' 44.286"	2
freemanha	101	440128.97	3094464.92	27° 58' 26.207"	-81° 36' 31.590"	2
ic_hcu	129	450550.95	3125659.37	28° 15' 21.458"	-81° 30' 14.841"	2
ir0365	135	513800.02	3061766.28	27° 40' 48.126"	-80° 51' 36.214"	2
ir0366	136	512940.3	3077392.8	27° 49' 16.008"	-80° 52' 6.991"	2
ir0956	142	536246.42	3059747.51	27° 39' 41.016"	-80° 37' 56.994"	2
john_w_627	150	433415.05	3052921.27	27° 35' 55.014"	-81° 40' 28.992"	2
keen_ranch	151	434201.17	3176226.55	28° 42' 41.996"	-81° 40' 25.272"	2
krennd	162	482549.57	3069587.49	27° 45' 2.158"	-81° 10' 37.482"	2
krfnnd	165	481014.32	3073764.57	27° 47' 17.835"	-81° 11' 33.804"	2
l_0096	179	412477.07	3173905.17	28° 41' 21.926"	-81° 53' 45.282"	2
l_0715	197	453279.21	3194373.85	28° 52' 34.656"	-81° 28' 44.798"	2
l_0815	201	455069.63	3195870.22	28° 53' 23.508"	-81° 27' 38.918"	2
l_0904	211	414754.68	3179934.63	28° 44' 38.378"	-81° 52' 22.985"	2
lk_weohy	249	456793.5	3076573.77	27° 48' 47.107"	-81° 26' 19.257"	2
lkst_ufa	266	441987.68	3092821.27	27° 57' 33.090"	-81° 35' 23.265"	2
lower_weki	274	460704.04	3198664.5	28° 54' 54.970"	-81° 24' 11.241"	2
onf4_hcam	311	420235.09	3212722.67	29° 2' 24.947"	-81° 49' 9.293"	2
or0546	324	454520.28	3176076.11	28° 42' 40.261"	-81° 27' 56.339"	2
or0651	334	457180.95	3183289.84	28° 46' 34.990"	-81° 26' 19.251"	2
or0824	349	463797.29	3154619.5	28° 31' 4.092"	-81° 22' 11.960"	2
orh_1	356	447656.81	3149579.77	28° 28' 18.351"	-81° 32' 4.948"	2
os_243	365	494908.19	3083143.87	27° 52' 23.102"	-81° 3' 6.225"	2
os0030	374	499358.05	3110051.11	28° 6' 57.577"	-81° 0' 23.540"	2
os0229	379	498109.3	3075887.26	27° 48' 27.300"	-81° 1' 9.114"	2
osf53_gw2	403	465489.18	3112762.27	28° 8' 24.061"	-81° 21' 5.231"	2
osf64_gw2	406	472526.44	3105254.08	28° 4' 20.659"	-81° 16' 46.604"	2
po0001	424	435772.56	3119669.2	28° 12' 4.508"	-81° 39' 16.010"	2
pos_13	433	460737.33	3102622.36	28° 2' 54.067"	-81° 23' 58.218"	2
river_ranw	458	478597.43	3075561.66	27° 48' 16.108"	-81° 13' 2.240"	2
romp_57_ha	477	438739.77	3086683.51	27° 54' 13.110"	-81° 37' 20.990"	2
romp_59_ha	483	414943.63	3084646.13	27° 53' 2.210"	-81° 51' 50.888"	2
s_0202	513	491426.32	3184442.41	28° 47' 14.904"	-81° 5' 16.258"	2
s_1385	550	469126.69	3188794.45	28° 49' 35.088"	-81° 18' 59.218"	2
s_1511	558	463853.83	3172610.05	28° 40' 48.696"	-81° 22' 11.926"	2

WELL_ID	REFERENCE_ID	X_UTMW	Y_UTMW	LATITUDE	LONGITUDE	Layer
tenoroc_rd	587	412536.64	3108509.51	28° 5' 57.076"	-81° 53' 25.279"	2
toho1_gw2	596	469342.19	3116500.97	28° 10' 25.900"	-81° 18' 44.328"	2
toho16_w2	603	473355.04	3115736.82	28° 10' 1.381"	-81° 16' 17.103"	2
toho5_gw	607	456861.93	3119370.38	28° 11' 57.889"	-81° 26' 22.390"	2
usgs_ow48	619	418709.23	3207316.47	28° 59' 28.953"	-81° 50' 4.294"	2
usgs_owg2	622	484039.21	3193900.28	28° 52' 21.976"	-81° 9' 49.217"	2
v_0166	636	489654.48	3190537.23	28° 50' 32.904"	-81° 6' 21.814"	2
v_0199	639	493265.84	3197538.68	28° 54' 20.496"	-81° 4' 8.686"	2
v_0743	645	469933.94	3219594.84	29° 6' 15.960"	-81° 18' 32.400"	2
v_0812	653	473335.76	3218793.14	29° 5' 50.184"	-81° 16' 26.471"	2
v_0822	657	480161.67	3186843.69	28° 48' 32.484"	-81° 12' 11.913"	2
v_0841	660	515859.04	3188080.64	28° 49' 12.876"	-80° 50' 14.854"	2
v_1033	663	504036.31	3186435.25	28° 48' 19.740"	-80° 57' 31.102"	2
v_1036	666	514505.23	3192402.97	28° 51' 33.384"	-80° 51' 4.606"	2
v_1063	674	473849.89	3218937.1	29° 5' 54.900"	-81° 16' 7.463"	2
v_1077	676	470348.75	3198151.97	28° 54' 39.252"	-81° 18' 15.010"	2
w222_fl	684	439918.54	3090616.35	27° 56' 21.108"	-81° 36' 38.589"	2
w84513005	690	450908.8	3181283.61	28° 45' 28.995"	-81° 30' 10.259"	2
well_sr42	691	429966.51	3207304.19	28° 59' 30.957"	-81° 43' 8.282"	2
austin_gr	5	433437.04	3199097.14	28° 55' 4.968"	-81° 40' 58.278"	3
b_rogers_d	6	451937.73	3200451.79	28° 55' 51.967"	-81° 29' 35.253"	3
baylake_dp	9	444278.96	3144384.57	28° 25' 29.032"	-81° 34' 8.261"	3
boggy_crer	14	469693.71	3135768.08	28° 20' 52.044"	-81° 18' 33.243"	3
br0202	18	520792.91	3139224.24	28° 22' 45.025"	-80° 47' 16.005"	3
br0288	19	536706.47	3086921.71	27° 54' 24.095"	-80° 37' 37.192"	3
br0608	21	531376.19	3151441.59	28° 29' 21.276"	-80° 40' 45.945"	3
br0645	22	526612.72	3097104.31	27° 59' 55.873"	-80° 43' 45.619"	3
br0660	23	503488.48	3164986.78	28° 36' 42.780"	-80° 57' 51.550"	3
br1526	24	503488.48	3164986.78	28° 36' 42.780"	-80° 57' 51.550"	3
br1557	28	522826.21	3139582.5	28° 22' 56.545"	-80° 46' 1.269"	3
br1558	29	525621.88	3133493.01	28° 19' 38.473"	-80° 44' 19.028"	3
br1559	30	544280.53	3078946.98	27° 50' 4.106"	-80° 33' 1.190"	3
br1572	31	514671.42	3166558.65	28° 37' 33.576"	-80° 50' 59.674"	3
br1748	34	531695.52	3153527.42	28° 30' 29.028"	-80° 40' 33.993"	3
br1835	35	511551.71	3181886.91	28° 45' 51.780"	-80° 52' 54.010"	3
br1914	36	504282.78	3171682.92	28° 40' 20.364"	-80° 57' 22.210"	3
burnetts	39	443068.51	3061214.78	27° 40' 26.127"	-81° 34' 38.269"	3
cape_cantp	41	539856.2	3142319.76	28° 24' 24.025"	-80° 35' 35.178"	3
cargill_fa	42	417440.7	3057460.86	27° 38' 19.364"	-81° 50' 12.803"	3
cfind_lf_6	46	415212.81	3050344.65	27° 34' 27.615"	-81° 51' 32.293"	3
city_z_242	52	421499.25	3041606.56	27° 29' 45.015"	-81° 47' 40.995"	3
cl_1_fldn	53	447191.62	3079627.62	27° 50' 25.112"	-81° 32' 10.692"	3

WELL_ID	REFERENCE_ID	X_UTMW	Y_UTMW	LATITUDE	LONGITUDE	Layer
cl_3_hawth	54	443519.1	3071034.3	27° 45' 45.310"	-81° 34' 23.489"	3
cl_spris	55	421221.2	3083304.85	27° 52' 20.010"	-81° 48' 0.989"	3
cl_sprsu	57	420730.03	3082627.97	27° 51' 57.910"	-81° 48' 18.787"	3
clenny_dp	58	446815.35	3058055.77	27° 38' 44.015"	-81° 32' 20.994"	3
cntl_hawth	59	413945.64	3093820.8	27° 58' 0.109"	-81° 52' 29.785"	3
cocoa_04	60	536240.02	3132522.7	28° 19' 6.040"	-80° 37' 49.184"	3
cocoa_12b	63	491722.35	3141670.91	28° 24' 5.033"	-81° 5' 4.225"	3
cocoa_4	64	490743.06	3142040.87	28° 24' 17.032"	-81° 5' 40.225"	3
cocoa_44	65	490793.36	3136840.51	28° 21' 28.040"	-81° 5' 38.228"	3
cocoa_4a1	66	491042.06	3141702.21	28° 24' 6.034"	-81° 5' 29.227"	3
cocoa_7	67	490717.63	3144318.03	28° 25' 31.030"	-81° 5' 41.226"	3
cocoa_9	68	490719.58	3146779.74	28° 26' 51.026"	-81° 5' 41.226"	3
cocoa_a	69	493463.46	3140962.05	28° 23' 42.033"	-81° 4' 0.222"	3
cocoa_d	72	483780.54	3144356.37	28° 25' 32.032"	-81° 9' 56.231"	3
cocoa_p	76	474507.18	3145972.92	28° 26' 24.030"	-81° 15' 37.243"	3
coley_well	78	447818.77	3068999.58	27° 44' 39.812"	-81° 31' 46.090"	3
college_st	79	413012.44	3187475.81	28° 48' 42.977"	-81° 53' 29.298"	3
deep_onf	83	419544.03	3218329.1	29° 5' 26.943"	-81° 49' 36.296"	3
eau_gal_09	88	536639.22	3117876.63	28° 11' 10.055"	-80° 37' 36.184"	3
esteve_fas	93	441410.31	3092085.53	27° 57' 9.090"	-81° 35' 44.264"	3
fish_lkdp	95	409195.07	3106903.46	28° 5' 4.080"	-81° 55' 27.278"	3
florida_av	96	482193.46	3173961.74	28° 41' 33.998"	-81° 10' 56.227"	3
florida_ca	97	447372.96	3184991.95	28° 47' 28.988"	-81° 32' 21.259"	3
floyd_deva	98	451190.71	3048960.23	27° 33' 49.015"	-81° 29' 39.992"	3
foodtwndp	99	423050.59	3092650.77	27° 57' 24.095"	-81° 46' 56.277"	3
free_sr46a	100	451536.51	3188697.54	28° 49' 29.983"	-81° 29' 48.255"	3
fussell_dp	102	419532.5	3122031.38	28° 13' 18.056"	-81° 49' 12.272"	3
gardinier	105	415384.69	3064015.74	27° 41' 51.914"	-81° 51' 29.489"	3
grant_82	106	547311.52	3087327.88	27° 54' 36.093"	-80° 31' 9.184"	3
gs_lk751w	117	410758.5	3140589.67	28° 23' 19.030"	-81° 54' 39.281"	3
hart_fas	118	442120.6	3092051.29	27° 57' 8.089"	-81° 35' 18.264"	3
hass_bryan	119	434219.92	3040920.54	27° 29' 25.154"	-81° 39' 57.280"	3
hatcher	120	402014.13	3198027.98	28° 54' 22.959"	-82° 0' 18.313"	3
hayman_w2	122	500459.24	3076804.41	27° 48' 57.111"	-80° 59' 43.224"	3
hiloche_12	124	429476.95	3142832.07	28° 24' 36.010"	-81° 43' 11.995"	3
homeland9	127	420944.89	3076601.18	27° 48' 42.110"	-81° 48' 9.489"	3
i_4_dp	128	483178.94	3216859.27	29° 4' 47.953"	-81° 10' 22.213"	3
imc_hy98	131	418780.08	3080188.3	27° 50' 38.210"	-81° 49' 29.488"	3
indian_lk	132	466583.23	3074696.52	27° 47' 47.107"	-81° 20' 21.247"	3
ir0189	134	517264.94	3071616.66	27° 46' 8.113"	-80° 49' 29.209"	3
ir0921	139	538424.65	3072678.1	27° 46' 41.029"	-80° 36' 35.995"	3
ir0954	140	541589.49	3051579.64	27° 35' 15.012"	-80° 34' 42.990"	3

WELL_ID	REFERENCE_ID	X_UTMW	Y_UTMW	LATITUDE	LONGITUDE	Layer
ir0955	141	536246.42	3059747.51	27° 39' 41.016"	-80° 37' 56.994"	3
ir0963	143	547971.61	3063016.03	27° 41' 25.921"	-80° 30' 48.558"	3
ir0968	144	521854.74	3064512.86	27° 42' 17.004"	-80° 46' 41.982"	3
jc_51_hug	146	403199.81	3161392.59	28° 34' 33.005"	-81° 59' 23.297"	3
jc_65	147	401857.27	3169775.11	28° 39' 4.993"	-82° 0' 15.301"	3
jc_67	148	402157.49	3163463.3	28° 35' 40.002"	-82° 0' 2.298"	3
jc_barnet	149	418587.24	3069012.93	27° 44' 35.014"	-81° 49' 33.791"	3
kimbell	153	447957.25	3108364.12	28° 5' 59.071"	-81° 31' 47.258"	3
kiss_stpk	156	465097.87	3090947.23	27° 56' 35.091"	-81° 21' 17.249"	3
kissengen2	158	420152.28	3080049.97	27° 50' 34.012"	-81° 48' 39.290"	3
l_0032	167	460116.57	3191343.58	28° 50' 57.024"	-81° 24' 32.004"	3
l_0037	168	458481.22	3190486.27	28° 50' 28.981"	-81° 25' 32.246"	3
l_0043	169	424896.58	3179940.07	28° 44' 40.826"	-81° 46' 9.087"	3
l_0051	172	427927.66	3139198.62	28° 22' 37.641"	-81° 44' 8.118"	3
l_0052	173	433475.82	3155548.7	28° 31' 29.976"	-81° 40' 47.674"	3
l_0053	174	427298.46	3148245.3	28° 27' 31.475"	-81° 44' 33.285"	3
l_0057	175	419303.91	3139509.25	28° 22' 45.922"	-81° 49' 25.028"	3
l_0059	176	461978.03	3209507.32	29° 0' 47.423"	-81° 23' 25.514"	3
l_0066	177	443631.54	3217083.58	29° 4' 51.143"	-81° 34' 45.052"	3
l_0095	178	412477.07	3173905.17	28° 41' 21.926"	-81° 53' 45.282"	3
l_0199	180	432756.95	3160045.42	28° 33' 55.956"	-81° 41' 15.071"	3
l_0290	182	422283.25	3193018.17	28° 51' 45.193"	-81° 47' 48.664"	3
l_0620	184	422897.79	3197123.61	28° 53' 58.716"	-81° 47' 26.993"	3
l_0658	185	434031.96	3164133.07	28° 36' 9.012"	-81° 40' 28.991"	3
l_0709	194	430152.54	3144436.74	28° 25' 28.282"	-81° 42' 47.516"	3
l_0816	202	455069.63	3195870.22	28° 53' 23.508"	-81° 27' 38.918"	3
l_0877	209	428359.55	3137055.52	28° 21' 28.089"	-81° 43' 51.773"	3
l_0902	210	414754.68	3179934.63	28° 44' 38.378"	-81° 52' 22.985"	3
l_0927	213	412303.94	3192373.7	28° 51' 21.937"	-81° 53' 56.802"	3
lake_ada10	214	461575.72	3159240.39	28° 33' 34.019"	-81° 23' 34.250"	3
lcfd_d_4	216	437708.15	3212737.87	29° 2' 28.950"	-81° 38' 23.273"	3
lcfd_d_9	217	425271.84	3154552.99	28° 30' 56.018"	-81° 45' 49.274"	3
lk_alfdp1	218	428986.93	3107600.29	28° 5' 31.076"	-81° 43' 22.271"	3
lk_alfdp2	219	427592.18	3116101.86	28° 10' 7.062"	-81° 44' 15.269"	3
lk_hatch	226	446249.08	3101892.15	28° 2' 28.509"	-81° 32' 48.791"	3
lk_hatchi	227	454668.7	3100797.88	28° 1' 54.080"	-81° 27' 40.256"	3
lk_oli_dp	239	436709.19	3138083.4	28° 22' 3.038"	-81° 38' 45.262"	3
lk_sawyer	248	444161.87	3148385.76	28° 27' 39.031"	-81° 34' 13.262"	3
lk_yale	250	424593.98	3180100.86	28° 44' 45.987"	-81° 46' 20.281"	3
lknowlesd	264	447763.36	3185852.73	28° 47' 57.014"	-81° 32' 7.002"	3
loomis_nur	268	512646.72	3192726.64	28° 51' 43.973"	-80° 52' 13.193"	3
loughmand	270	443052.94	3126082.25	28° 15' 34.108"	-81° 34' 50.090"	3

WELL_ID	REFERENCE_ID	X_UTMW	Y_UTMW	LATITUDE	LONGITUDE	Layer
lower_w_u	272	460418.03	3194233.96	28° 52' 30.976"	-81° 24' 21.243"	3
lower_wekf	273	461563.63	3204693.39	28° 58' 10.961"	-81° 23' 40.238"	3
m_0013	276	413951.37	3217409.65	29° 4' 55.751"	-81° 53' 2.909"	3
m_0046	277	423684.2	3206666.99	28° 59' 8.957"	-81° 47' 0.289"	3
m_0445	278	408566.01	3214992.5	29° 3' 35.867"	-81° 56' 21.377"	3
m_0467	279	404192.32	3208169.14	28° 59' 53.028"	-81° 59' 1.001"	3
m_0483	281	418579.85	3207691.61	28° 59' 41.111"	-81° 50' 9.173"	3
mascotted	283	410636.37	3156778.59	28° 32' 5.009"	-81° 54' 48.288"	3
melb_e49	287	544357.02	3102732.71	28° 2' 57.075"	-80° 32' 55.184"	3
melb_etp	288	541918.01	3097554.43	28° 0' 9.080"	-80° 34' 25.188"	3
merr_isl	289	528777.34	3144164.62	28° 25' 25.022"	-80° 42' 22.188"	3
merr_isle	290	528120.64	3168504.18	28° 38' 35.996"	-80° 42' 44.181"	3
midgard_fl	291	452587.25	3085358.97	27° 53' 32.095"	-81° 28' 54.257"	3
mobil_uf_5	292	425449.5	3060718.71	27° 40' 6.912"	-81° 45' 21.292"	3
mobil_uf_9	293	421516.92	3062658.09	27° 41' 9.132"	-81° 47' 45.287"	3
moore	296	509492.53	3206818.39	28° 59' 21.965"	-80° 54' 9.193"	3
mosspk_d	297	481296.96	3139128.67	28° 22' 42.032"	-81° 11' 27.222"	3
naranatha	301	458385.44	3043918.22	27° 31' 6.017"	-81° 25' 16.995"	3
neuman_we	302	445241.22	3058991.92	27° 39' 14.212"	-81° 33' 18.593"	3
o0174	303	458113.17	3155897.97	28° 31' 45.022"	-81° 25' 41.250"	3
obs_sem257	306	478253.4	3185569.99	28° 47' 50.985"	-81° 13' 22.227"	3
ok0001	309	519267.64	3045221.3	27° 31' 50.173"	-80° 48' 17.562"	3
okf_34	310	497662.7	3046067.05	27° 32' 18.146"	-81° 1' 25.228"	3
onfalex_sp	312	450638.48	3213167.59	29° 2' 44.954"	-81° 30' 25.255"	3
or0003	314	497358.49	3150375.27	28° 28' 47.976"	-81° 1' 37.161"	3
or0007	315	491000.14	3157857.44	28° 32' 51.013"	-81° 5' 31.222"	3
or0025	317	490614.86	3143670.83	28° 25' 9.996"	-81° 5' 44.985"	3
or0029	318	505292.12	3141255.46	28° 23' 51.588"	-80° 56' 45.525"	3
or0068	319	456284.24	3181016.14	28° 45' 21.001"	-81° 26' 52.007"	3
or0106	320	443234.25	3175809.84	28° 42' 30.000"	-81° 34' 52.265"	3
or0265	321	490659.66	3148295.96	28° 27' 40.296"	-81° 5' 43.473"	3
or0468	323	463388.68	3159456.58	28° 33' 41.232"	-81° 22' 27.548"	3
or0548	326	454520.28	3176076.11	28° 42' 40.261"	-81° 27' 56.339"	3
or0662	337	457153.6	3183259.74	28° 46' 34.009"	-81° 26' 20.256"	3
or0669	339	498397.7	3140860	28° 23' 38.772"	-81° 0' 58.893"	3
or0796	348	450315.12	3171180.83	28° 40' 0.637"	-81° 30' 30.562"	3
os0004	366	504953.84	3099720.02	28° 1' 21.805"	-80° 56' 58.591"	3
os0016	367	504639.89	3105726.16	28° 4' 36.996"	-80° 57' 10.004"	3
os0017	368	506796.39	3105974.23	28° 4' 45.025"	-80° 55' 50.984"	3
os0018	369	505105.39	3101634.29	28° 2' 24.013"	-80° 56' 53.011"	3
os0019	370	505261.14	3098354.29	28° 0' 37.417"	-80° 56' 47.359"	3
os0031	375	499263.78	3110249.4	28° 7' 4.020"	-81° 0' 26.996"	3

WELL_ID	REFERENCE_ID	X_UTMW	Y_UTMW	LATITUDE	LONGITUDE	Layer
os0069	376	503853.52	3112859.91	28° 8' 28.836"	-80° 57' 38.732"	3
os0231	380	504022.24	3078256.1	27° 49' 44.268"	-80° 57' 32.971"	3
os0238	382	505668.98	3123451.03	28° 14' 12.996"	-80° 56' 31.988"	3
os0254	383	452468.02	3124069.77	28° 14' 30.057"	-81° 29' 4.252"	3
osf_101	384	456028.39	3129468.5	28° 17' 25.940"	-81° 26' 54.337"	3
osf_102	385	458340.02	3114444.01	28° 9' 17.970"	-81° 25' 27.541"	3
osf_11	386	455810.11	3114086.82	28° 9' 6.067"	-81° 27' 0.253"	3
osf_4	388	478158.74	3090147.12	27° 56' 10.090"	-81° 13' 19.239"	3
osf_42	389	502650.33	3066066.32	27° 43' 8.121"	-80° 58' 23.221"	3
osf_52	391	480469.81	3075401.43	27° 48' 11.003"	-81° 11' 53.798"	3
osf_60a	392	510238.59	3063612.9	27° 41' 48.255"	-80° 53' 46.174"	3
osf_62	393	495585.25	3086202.76	27° 54' 2.521"	-81° 2' 41.505"	3
osf_64	394	472526.44	3105254.08	28° 4' 20.659"	-81° 16' 46.604"	3
osf_68	396	487096.17	3116412.09	28° 10' 24.067"	-81° 7' 53.233"	3
osf_70	397	467806.68	3125201.94	28° 15' 8.521"	-81° 19' 41.504"	3
osf_93	400	495553.69	3127698.73	28° 16' 31.051"	-81° 2' 43.225"	3
ouc_no_4	414	455485.51	3143813.86	28° 25' 12.035"	-81° 27' 16.252"	3
ouc_wr_uf1	415	452400.67	3168044.5	28° 38' 19.008"	-81° 29' 13.255"	3
palm_lake	417	450370.51	3150235.11	28° 28' 40.029"	-81° 30' 25.256"	3
paul_shokl	418	446057.82	3205278.77	28° 58' 27.962"	-81° 33' 13.262"	3
perry_flor	420	443081.33	3092969.9	27° 57' 38.090"	-81° 34' 43.264"	3
pine_lakes	422	456999.34	3200062.56	28° 55' 39.968"	-81° 26' 28.247"	3
pinecastle	423	464366.44	3147691.77	28° 27' 19.030"	-81° 21' 50.248"	3
pof_22	428	460737.33	3102622.36	28° 2' 54.067"	-81° 23' 58.218"	3
polk_landf	431	416867.91	3098761.02	28° 0' 41.309"	-81° 50' 44.086"	3
rcid_no_1	435	448592.01	3141472.36	28° 23' 55.036"	-81° 31' 29.256"	3
river_ranr	457	480533.01	3071158.34	27° 45' 53.110"	-81° 11' 51.239"	3
rock_sprdp	466	450908.8	3181283.61	28° 45' 28.995"	-81° 30' 10.259"	3
rodeo_fld	467	509455.48	3117701.08	28° 11' 6.061"	-80° 54' 13.211"	3
romp_44_fl	470	441105.3	3077895.61	27° 49' 27.912"	-81° 35' 52.891"	3
romp_45_su	473	422539.25	3071334.93	27° 45' 51.312"	-81° 47' 9.988"	3
romp_57_fl	476	438739.77	3086683.51	27° 54' 13.110"	-81° 37' 20.990"	3
romp_57a_o	480	444271.84	3085872.01	27° 53' 47.611"	-81° 33' 58.490"	3
romp_58_oc	481	441558.75	3088463.47	27° 55' 11.408"	-81° 35' 38.188"	3
romp_60_fl	484	403301.71	3085503.36	27° 53' 27.213"	-81° 58' 56.887"	3
romp_60x_f	485	406555.7	3092915.94	27° 57' 28.913"	-81° 56' 59.986"	3
romp_70_fl	486	406118.34	3105490.98	28° 4' 17.411"	-81° 57' 19.596"	3
romp_73_fl	487	428120.52	3099725.3	28° 1' 15.007"	-81° 43' 52.287"	3
romp_76a	492	418494.41	3117730.13	28° 10' 58.061"	-81° 49' 49.274"	3
romp_88	493	410666.05	3131942.62	28° 18' 38.043"	-81° 54' 40.278"	3
romp_cl_2i	494	449666.75	3070336.46	27° 45' 23.512"	-81° 30' 38.792"	3
romp_cl_2w	496	449666.75	3070336.46	27° 45' 23.512"	-81° 30' 38.792"	3

WELL_ID	REFERENCE_ID	X_UTMW	Y_UTMW	LATITUDE	LONGITUDE	Layer
romp_cl_3f	497	443519.1	3071034.3	27° 45' 45.310"	-81° 34' 23.489"	3
romp_wr_3f	500	401327.32	3201151.62	28° 56' 4.252"	-82° 0' 44.657"	3
ross_w_onl	502	444505.41	3152015.32	28° 29' 37.024"	-81° 34' 1.260"	3
s_0001	506	488392.64	3176286.65	28° 42' 49.800"	-81° 7' 7.857"	3
s_0028	507	485812.51	3177281.05	28° 43' 22.019"	-81° 8' 43.005"	3
s_0034	508	491148.44	3179672.1	28° 44' 39.888"	-81° 5' 26.373"	3
s_0086	509	491426.32	3184442.41	28° 47' 14.904"	-81° 5' 16.258"	3
s_0097	510	460399.64	3189685.16	28° 50' 3.168"	-81° 24' 21.348"	3
s_0122	511	460429.98	3185992.39	28° 48' 3.180"	-81° 24' 19.763"	3
s_0123	512	468440.67	3185869.23	28° 47' 59.976"	-81° 19' 24.238"	3
s_0243	514	467186.88	3189401.38	28° 49' 54.636"	-81° 20' 10.859"	3
s_0829	516	469974.67	3177133.87	28° 43' 16.260"	-81° 18' 26.817"	3
s_1014	517	465278.04	3172850.56	28° 40' 56.652"	-81° 21' 19.474"	3
s_1056	523	473196.68	3170397.88	28° 39' 37.632"	-81° 16' 27.477"	3
s_1193	526	479500.21	3170277.64	28° 39' 34.140"	-81° 12' 35.241"	3
s_1201	527	488783.77	3172712.29	28° 40' 53.664"	-81° 6' 53.313"	3
s_1230	530	461238.79	3188561.12	28° 49' 26.736"	-81° 23' 50.243"	3
s_1253	531	488585.53	3178779.17	28° 44' 10.800"	-81° 7' 0.837"	3
s_1397	552	469126.69	3188794.45	28° 49' 35.088"	-81° 18' 59.218"	3
s_1408	556	464351.21	3178706.33	28° 44' 6.840"	-81° 21' 54.286"	3
sea_world	565	453467.72	3142683.03	28° 24' 35.035"	-81° 28' 30.255"	3
seminol125	566	464149.34	3174434.2	28° 41' 48.001"	-81° 22' 1.244"	3
shingle_cr	567	457328.69	3126820.8	28° 16' 0.055"	-81° 26' 6.251"	3
skylake_g	568	462277.89	3146503.7	28° 26' 40.212"	-81° 23' 6.902"	3
smith_no_2	569	406888.55	3197926.23	28° 54' 20.963"	-81° 57' 18.307"	3
south_egl	571	477685.27	3129226.75	28° 17' 20.052"	-81° 13' 39.241"	3
spread_rdp	572	429251.4	3124523.69	28° 14' 41.051"	-81° 43' 16.265"	3
st_francis	574	459397.23	3212025.41	29° 2' 8.956"	-81° 25' 1.241"	3
ten_mile_r	585	514589.96	3088259.31	27° 55' 9.096"	-80° 51' 6.209"	3
tenoroc_fl	586	414747.7	3108585.8	28° 6' 0.074"	-81° 52' 4.278"	3
th_10	590	494967.87	3095143.93	27° 58' 53.089"	-81° 3' 4.226"	3
th_3	591	501383.7	3127697.95	28° 16' 31.050"	-80° 59' 9.218"	3
thornhilsf	592	423453.96	3095910.02	27° 59' 10.090"	-81° 46' 42.275"	3
tillery_rd	594	411151.84	3091040.35	27° 56' 29.099"	-81° 54' 11.282"	3
tosohatchg	613	508586.62	3150410.19	28° 28' 49.019"	-80° 54' 44.207"	3
tower_b_dp	614	430477.31	3220165.82	29° 6' 28.941"	-81° 42' 52.284"	3
usgs_ow_7	617	492344.11	3217126.52	29° 4' 56.955"	-81° 4' 43.205"	3
usgs_owala	620	490819.59	3203863.73	28° 57' 45.966"	-81° 5' 39.206"	3
usgs_owha	623	439309	3140777.89	28° 23' 31.037"	-81° 37' 10.261"	3
v_0082	626	466741.88	3199202.13	28° 55' 13.056"	-81° 20' 28.319"	3
v_0101	628	490807.32	3202605.71	28° 57' 5.088"	-81° 5' 39.623"	3
v_0110	629	493024.06	3207197.56	28° 59' 34.344"	-81° 4' 17.831"	3

WELL_ID	REFERENCE_ID	X_UTMW	Y_UTMW	LATITUDE	LONGITUDE	Layer
v_0117	631	493442.01	3212475.44	29° 2' 25.848"	-81° 4' 2.495"	3
v_0118	632	479568.1	3212582.56	29° 2' 28.800"	-81° 12' 35.494"	3
v_0156	633	465013.26	3217679.86	29° 5' 13.284"	-81° 21' 34.237"	3
v_0164	634	505374.89	3209942.13	29° 1' 3.553"	-80° 56' 41.315"	3
v_0165	635	489654.48	3190537.23	28° 50' 32.904"	-81° 6' 21.814"	3
v_0196	637	470348.75	3198151.97	28° 54' 39.252"	-81° 18' 15.010"	3
v_0198	638	493265.84	3197538.68	28° 54' 20.496"	-81° 4' 8.686"	3
v_0240	640	476106.34	3193022.32	28° 51' 53.004"	-81° 14' 41.997"	3
v_0435	641	504380.43	3205308.41	28° 58' 33.001"	-80° 57' 18.143"	3
v_0508	642	507577.69	3209974.39	29° 1' 4.561"	-80° 55' 19.883"	3
v_0521	643	507635.93	3198508.67	28° 54' 51.997"	-80° 55' 18.011"	3
v_0772	646	477853.94	3200106.12	28° 55' 43.296"	-81° 13' 37.990"	3
v_0777	649	476660.48	3204698.56	28° 58' 12.443"	-81° 14' 22.414"	3
v_0808	651	473369.59	3218816.65	29° 5' 50.950"	-81° 16' 25.221"	3
v_0818	655	480161.67	3186843.69	28° 48' 32.484"	-81° 12' 11.913"	3
v_0840	659	515859.04	3188080.64	28° 49' 12.876"	-80° 50' 14.854"	3
v_0867	661	469021.61	3208181.06	29° 0' 5.016"	-81° 19' 5.016"	3
v_1091	677	466750.65	3199201	28° 55' 13.020"	-81° 20' 27.995"	3
w_b_geiger	683	426522.58	3050576	27° 34' 37.514"	-81° 44' 39.894"	3
w815149233	685	419097.45	3126188.81	28° 15' 33.050"	-81° 49' 29.271"	3
w82513801	686	436419.2	3144885.93	28° 25' 44.031"	-81° 38' 57.263"	3
w82912802	687	453584.46	3151575.97	28° 29' 24.026"	-81° 28' 27.253"	3
w83012801	688	453290.23	3152808.05	28° 30' 4.024"	-81° 28' 38.255"	3
west_ast	692	427633.72	3176019.27	28° 42' 33.995"	-81° 44' 27.277"	3
whitehurst	693	423103.14	3057909.17	27° 38' 35.136"	-81° 46' 46.286"	3
willaway12	694	509322.15	3042716.74	27° 30' 29.151"	-80° 54' 20.218"	3
withlacoo	695	403829.97	3148738.19	28° 27' 42.019"	-81° 58' 56.291"	3
wolf_sink	696	440947.09	3184930.52	28° 47' 25.987"	-81° 36' 18.268"	3
ashton_for	4	476995.01	3124427.81	28° 14' 44.059"	-81° 14' 4.240"	4
bonnet_lk	16	456065.61	3047249.41	27° 32' 54.016"	-81° 26' 41.994"	4
l_0704	193	444177.97	3190795.64	28° 50' 37.081"	-81° 34' 20.138"	4
lrosal_nw	275	458401.42	3090599.21	27° 56' 23.089"	-81° 25' 22.256"	4
osf_18	387	473133.45	3115912.22	28° 10' 7.065"	-81° 16' 25.244"	4
romp_45_ap	472	422539.29	3071341.14	27° 45' 51.514"	-81° 47' 9.988"	4
canoe_crk	40	473915.16	3111725.71	28° 7' 51.071"	-81° 15' 56.242"	5
cecil_whal	44	465206.97	3119009.87	28° 11' 47.062"	-81° 21' 16.246"	5
cfind_lf_1	45	403901.22	3050351.53	27° 34' 25.117"	-81° 58' 24.796"	5
city_wel_r	51	425163.17	3158831.38	28° 33' 15.013"	-81° 45' 54.276"	5
cocoa_11	61	490715.05	3141056.3	28° 23' 45.036"	-81° 5' 41.226"	5
cocoa_12a	62	492212.31	3141916.72	28° 24' 13.032"	-81° 4' 46.224"	5
cocoa_b	70	487072.31	3144383.08	28° 25' 33.033"	-81° 7' 55.229"	5
cresent_dp	82	405244.18	3107445.94	28° 5' 20.711"	-81° 57' 52.187"	5

WELL_ID	REFERENCE_ID	X_UTMW	Y_UTMW	LATITUDE	LONGITUDE	Layer
east_lk	86	458316.48	3081830.07	27° 51' 38.101"	-81° 25' 24.254"	5
hif_3	123	474181.83	3044893.97	27° 31' 39.143"	-81° 15' 41.247"	5
l_0677	186	429815.39	3144891.88	28° 25' 43.006"	-81° 43' 0.008"	5
l_0730	199	430629.23	3144055.02	28° 25' 15.970"	-81° 42' 29.912"	5
lk_joel	236	484494.97	3129061.98	28° 17' 15.050"	-81° 9' 29.232"	5
lk_poinse	247	513549.57	3137983.14	28° 22' 5.036"	-80° 51' 42.202"	5
lkland_st	263	406473.79	3105528.19	28° 4' 18.711"	-81° 57' 6.586"	5
n_floridaa	300	405946.87	3104128.93	28° 3' 33.110"	-81° 57' 25.486"	5
or_47	313	453446.92	3158038.96	28° 32' 54.021"	-81° 28' 33.254"	5
or0563	327	470561.71	3156260.13	28° 31' 58.020"	-81° 18' 3.242"	5
or0617	330	488993.37	3155598.02	28° 31' 37.536"	-81° 6' 44.997"	5
or0652	335	457153.6	3183259.74	28° 46' 34.009"	-81° 26' 20.256"	5
or0673	340	498397.7	3140860	28° 23' 38.772"	-81° 0' 58.893"	5
or0678	342	480883.46	3152884.51	28° 30' 9.021"	-81° 11' 43.236"	5
or0827	350	463797.29	3154619.5	28° 31' 4.092"	-81° 22' 11.960"	5
orleans_st	357	406022.82	3099198.13	28° 0' 52.910"	-81° 57' 21.287"	5
os0022	371	499284.39	3110056.65	28° 6' 57.756"	-81° 0' 26.240"	5
osf_44	390	471763.85	3124839.11	28° 14' 57.058"	-81° 17' 16.246"	5
osf_66	395	481347.73	3100234.31	28° 1' 38.080"	-81° 11' 23.120"	5
osf_82u	399	467820.22	3125093.89	28° 15' 5.011"	-81° 19' 40.996"	5
osf_99	402	450583.5	3125656.57	28° 15' 21.371"	-81° 30' 13.646"	5
pof20r397f	429	486706.08	3059365.79	27° 39' 30.129"	-81° 8' 5.235"	5
romp_43xxf	469	452625.98	3053483.93	27° 36' 16.215"	-81° 28' 48.292"	5
romp_55_fl	474	444803.76	3074250.21	27° 47' 30.012"	-81° 33' 37.092"	5
romp_59_ap	482	414943.63	3084646.13	27° 53' 2.210"	-81° 51' 50.888"	5
romp_74x_u	490	444506.64	3114698.52	28° 9' 24.409"	-81° 33' 54.790"	5
romp_dp101	499	409426.9	3147955.18	28° 27' 18.021"	-81° 55' 30.286"	5
s_1017	520	465278.04	3172850.56	28° 40' 56.652"	-81° 21' 19.474"	5
s_1189	525	479500.21	3170277.64	28° 39' 34.140"	-81° 12' 35.241"	5
s_1224	529	488585.53	3178779.17	28° 44' 10.800"	-81° 7' 0.837"	5
s_1398	553	469126.69	3188794.45	28° 49' 35.088"	-81° 18' 59.218"	5
s_1407	555	464351.21	3178706.33	28° 44' 6.840"	-81° 21' 54.286"	5
sanlon_ran	561	409244.22	3097569.95	28° 0' 0.810"	-81° 55' 22.887"	5
tely	584	460360.91	3137334.3	28° 21' 42.043"	-81° 24' 16.249"	5
usaf_ap#1	615	465279.14	3058854.18	27° 39' 12.128"	-81° 21' 7.250"	5
usgs_ip	616	418494.62	3117760.93	28° 10' 59.062"	-81° 49' 49.274"	5
usgs_ow10	618	493040.96	3207216.63	28° 59' 34.964"	-81° 4' 17.206"	5
v_0083	627	466688.08	3201841.36	28° 56' 38.808"	-81° 20' 30.588"	5
v_0115	630	466703.98	3211051.54	29° 1' 38.075"	-81° 20' 30.984"	5
v_0742	644	469933.94	3219594.84	29° 6' 15.960"	-81° 18' 32.400"	5
v_0776	648	476660.48	3204698.56	28° 58' 12.443"	-81° 14' 22.414"	5
v_0801	650	480161.67	3186843.69	28° 48' 32.484"	-81° 12' 11.913"	5

WELL_ID	REFERENCE_ID	X_UTMW	Y_UTMW	LATITUDE	LONGITUDE	Layer
v_0810	652	478494.06	3193686.81	28° 52' 14.748"	-81° 13' 13.905"	5
v_1098	679	486768.11	3219463.35	29° 6' 12.720"	-81° 8' 9.563"	5
w_5110	682	450894.43	3158480.11	28° 33' 8.018"	-81° 30' 7.256"	5
w84512005	689	466177.54	3181382.99	28° 45' 33.993"	-81° 20' 47.242"	5
or0547	325	454520.28	3176076.11	28° 42' 40.261"	-81° 27' 56.339"	6
or0615	329	488545.04	3144303.01	28° 25' 30.480"	-81° 7' 1.089"	6
or0675	341	498397.7	3140860	28° 23' 38.772"	-81° 0' 58.893"	6
s_1016	519	465278.04	3172850.56	28° 40' 56.652"	-81° 21' 19.474"	6
s_1257	532	473196.68	3170397.88	28° 39' 37.632"	-81° 16' 27.477"	6
v_0081	625	478285.63	3218649.75	29° 5' 45.864"	-81° 13' 23.339"	6
cocoa_c_z4	71	486365.05	3144414.57	28° 25' 34.030"	-81° 8' 21.228"	7
cocoa_r	77	484348.32	3141740.02	28° 24' 7.036"	-81° 9' 35.232"	7
l_0599	183	422897.79	3197123.61	28° 53' 58.716"	-81° 47' 26.993"	7
l_0729	198	430629.23	3144055.02	28° 25' 15.970"	-81° 42' 29.912"	7
l_0817	203	455069.63	3195870.22	28° 53' 23.508"	-81° 27' 38.918"	7
or0009	316	461559	3159265.24	28° 33' 34.824"	-81° 23' 34.868"	7
or0467	322	463388.68	3159456.58	28° 33' 41.232"	-81° 22' 27.548"	7
or0614	328	488545.04	3144303.01	28° 25' 30.480"	-81° 7' 1.089"	7
or0618	331	488993.37	3155598.02	28° 31' 37.536"	-81° 6' 44.997"	7
or0794	347	443265.97	3175811.95	28° 42' 30.073"	-81° 34' 51.096"	7
or0829	351	463797.29	3154619.5	28° 31' 4.092"	-81° 22' 11.960"	7
orf_60	355	442415.27	3139305.7	28° 22' 43.705"	-81° 35' 15.854"	7
os0025	373	499284.39	3110056.65	28° 6' 57.756"	-81° 0' 26.240"	7
osf_82l	398	467820.22	3125093.89	28° 15' 5.011"	-81° 19' 40.996"	7
osf_98	401	450583.5	3125656.57	28° 15' 21.371"	-81° 30' 13.646"	7
romp_74x_l	488	444503.79	3114676.93	28° 9' 23.707"	-81° 33' 54.891"	7
s_1024	522	465278.04	3172850.56	28° 40' 56.652"	-81° 21' 19.474"	7
s_1078	524	479500.21	3170277.64	28° 39' 34.140"	-81° 12' 35.241"	7
s_1329	548	473196.68	3170397.88	28° 39' 37.632"	-81° 16' 27.477"	7
s_1406	554	464351.21	3178706.33	28° 44' 6.840"	-81° 21' 54.286"	7
v_0012	624	478285.63	3218649.75	29° 5' 45.864"	-81° 13' 23.339"	7
v_0774	647	477853.94	3200106.12	28° 55' 43.296"	-81° 13' 37.990"	7